IJOER
RESEARCH JOURNAL

International Journal of Engineering Research & Science

ISSN
2395-6992

www.ijoer.com
www.adpublications.org

Preface

We would like to present, with great pleasure, the inaugural volume-4, Issue-5, May 2018, of a scholarly journal, *International Journal of Engineering Research & Science*. This journal is part of the AD Publications series *in the field of Engineering, Mathematics, Physics, Chemistry and science Research Development*, and is devoted to the gamut of Engineering and Science issues, from theoretical aspects to application-dependent studies and the validation of emerging technologies.

This journal was envisioned and founded to represent the growing needs of Engineering and Science as an emerging and increasingly vital field, now widely recognized as an integral part of scientific and technical investigations. Its mission is to become a voice of the Engineering and Science community, addressing researchers and practitioners in below areas

Chemical Engineering	
Biomolecular Engineering	Materials Engineering
Molecular Engineering	Process Engineering
Corrosion Engineering	
Civil Engineering	
Environmental Engineering	Geotechnical Engineering
Structural Engineering	Mining Engineering
Transport Engineering	Water resources Engineering
Electrical Engineering	
Power System Engineering	Optical Engineering
Mechanical Engineering	
Acoustical Engineering	Manufacturing Engineering
Optomechanical Engineering	Thermal Engineering
Power plant Engineering	Energy Engineering
Sports Engineering	Vehicle Engineering
Software Engineering	
Computer-aided Engineering	Cryptographic Engineering
Teletraffic Engineering	Web Engineering
System Engineering	
Mathematics	
Arithmetic	Algebra
Number theory	Field theory and polynomials
Analysis	Combinatorics
Geometry and topology	Topology
Probability and Statistics	Computational Science
Physical Science	Operational Research
Physics	
Nuclear and particle physics	Atomic, molecular, and optical physics
Condensed matter physics	Astrophysics
Applied Physics	Modern physics
Philosophy	Core theories

Chemistry	
Analytical chemistry	Biochemistry
Inorganic chemistry	Materials chemistry
Neurochemistry	Nuclear chemistry
Organic chemistry	Physical chemistry
Other Engineering Areas	
Aerospace Engineering	Agricultural Engineering
Applied Engineering	Biomedical Engineering
Biological Engineering	Building services Engineering
Energy Engineering	Railway Engineering
Industrial Engineering	Mechatronics Engineering
Management Engineering	Military Engineering
Petroleum Engineering	Nuclear Engineering
Textile Engineering	Nano Engineering
Algorithm and Computational Complexity	Artificial Intelligence
Electronics & Communication Engineering	Image Processing
Information Retrieval	Low Power VLSI Design
Neural Networks	Plastic Engineering

Each article in this issue provides an example of a concrete industrial application or a case study of the presented methodology to amplify the impact of the contribution. We are very thankful to everybody within that community who supported the idea of creating a new Research with IJOER. We are certain that this issue will be followed by many others, reporting new developments in the Engineering and Science field. This issue would not have been possible without the great support of the Reviewer, Editorial Board members and also with our Advisory Board Members, and we would like to express our sincere thanks to all of them. We would also like to express our gratitude to the editorial staff of AD Publications, who supported us at every stage of the project. It is our hope that this fine collection of articles will be a valuable resource for *IJOER* readers and will stimulate further research into the vibrant area of Engineering and Science Research.

Mukesh Arora

(Chief Editor)

Board Members

Dr. S.R.Boselin Prabhu

Ph.D, Wireless Sensor Networks, M.E. Network Engineering, Excellent Professional Achievement Award Winner from Society of Professional Engineers Biography Included in Marquis Who's Who in the World (Academic Year 2015 and 2016). Currently Serving as Assistant Professor in the department of ECE in SVS College of Engineering, Coimbatore.

Dr. Maheshwar Shrestha

Postdoctoral Research Fellow in DEPT. OF ELE ENGG & COMP SCI, SDSU, Brookings, SD Ph.D, M.Sc. in Electrical Engineering from SOUTH DAKOTA STATE UNIVERSITY, Brookings, SD.

Zairi Ismael Rizman

Senior Lecturer, Faculty of Electrical Engineering, Universiti Teknologi MARA (UiTM) (Terengganu) Malaysia Master (Science) in Microelectronics (2005), Universiti Kebangsaan Malaysia (UKM), Malaysia. Bachelor (Hons.) and Diploma in Electrical Engineering (Communication) (2002), UiTM Shah Alam, Malaysia

Dr. D. Amaranatha Reddy

Ph.D.(Postdocteral Fellow,Pusan National University, South Korea), M.Sc., B.Sc. : Physics.

Dr. Dibya Prakash Rai

Post Doctoral Fellow (PDF), M.Sc.,B.Sc., Working as Assistant Professor in Department of Physics in Pachhuncga University College, Mizoram, India.

Dr. Pankaj Kumar Pal

Ph.D R/S, ECE Deptt., IIT-Roorkee.

Dr. P. Thangam

BE(Computer Hardware & Software), ME(CSE), PhD in Information & Communication Engineering, currently serving as Associate Professor in the Department of Computer Science and Engineering of Coimbatore Institute of Engineering and Technology.

Dr. Pradeep K. Sharma

PhD., M.Phil, M.Sc, B.Sc, in Physics, MBA in System Management, Presently working as Provost and Associate Professor & Head of Department for Physics in University of Engineering & Management, Jaipur.

Dr. R. Devi Priya

Ph.D (CSE),Anna University Chennai in 2013, M.E, B.E (CSE) from Kongu Engineering College, currently working in the Department of Computer Science and Engineering in Kongu Engineering College, Tamil Nadu, India.

Dr. Sandeep

Post-doctoral fellow, Principal Investigator, Young Scientist Scheme Project (DST-SERB), Department of Physics, Mizoram University, Aizawl Mizoram, India- 796001.

Mr. Abilash

MTech in VLSI, BTech in Electronics & Telecommunication engineering through A.M.I.E.T.E from Central Electronics Engineering Research Institute (C.E.E.R.I) Pilani, Industrial Electronics from ATI-EPI Hyderabad, IEEE course in Mechatronics, CSHAM from Birla Institute Of Professional Studies.

Mr. Varun Shukla

M.Tech in ECE from RGPV (Awarded with silver Medal By President of India), Assistant Professor, Dept. of ECE, PSIT, Kanpur.

Mr. Shrikant Harle

Presently working as a Assistant Professor in Civil Engineering field of Prof. Ram Meghe College of Engineering and Management, Amravati. He was Senior Design Engineer (Larsen & Toubro Limited, India).

Table of Contents

Analysis on the junction point's stress located at considering fluid-solid coupling effects for support arm under different wall thickness

Zhi-jin Zhou[1], Zhi Yang[2], Ai-jun Liu[3]

[1,3]School of Mechanical Engineering;Guizhou Institute of Technology; Guiyang Guizhou 550003, China;
[2]Hunan Provincial Key Laboratory of Health Maintenance for Mechanical Equipment; Hunan University of Science and Technology; Xiangtan 411201, China

Abstract— *Fluid-structure interaction has a significant effect on stresses in the hinge point because of the impact of ocean currents to the pipeline. Aimed to support arms for deep-sea mining, numerical analysis method and the finite element software ADINA were adopted to analyze the pipeline structure - external fluid mutual coupling effect on stress at the hinge point. The results were shown that: (1) In the case of different wall thickness, the stress changes of the entire pipeline is relatively small, stress located mainly these places close to the junction in the pipelines, the maximum stress exists at the upper connection; (2) With wall thickness of the support pipe increasing, the maximum stress decreases, and when wall thicknesses changed from 9.5mm to 28.7mm interval 2.4mm ,the maximum stress value decreased 19.3%, 15.9%, 13.5%, 11.7%, 10.3%, 9.2%, 8.3%, 7.6% ;(3) With wall thickness increasing, the minimum stress value also reduced, and a minimum stress values decreased 19.9%, 14.0%, 5%, 14.6%, 28.7%, 15.9%, 8.6%, 2.7%,respectively.*

Keywords— Support arm, Fluid–structure interaction, Different wall thickness, Stress.

I. INTRODUCTION

Fluid-structure interaction problems and general multi-physics problems are often too complex and difficult to analyze and solve, so they would be completed by experimental or numerical simulation method. Because of the Computational Fluid Dynamics and computational structural dynamics field study obtain great progress, these achievements make the fluid-structure interaction numerical simulation is completed.

At the same time, the way of Newton-Raphson and Fixed point iteration can be used to solve the problem which is involve in Fluid-structure interaction. In view of Newton-Raphson iteration method the monolithic [1] [2] [3] and partition [4] [5] method has been widely used. We can use the Newton-Raphson method to solve the nonlinear fluid equations and structural equation. The problem of the system lacking the knowledge of Jacobi matrix iteration method can be solved by the iterative linear equations within the Newton- Raphson. Besides it can use the product finite difference of vector Jacobi to approximate.

As we all know, Newton-Raphson method can not only work out the state flow and structural problems in the whole liquid and solid domain, but also may be applied to the FSI device problem of multi-degree freedom system on the situation of interface location unknown. This domain decomposes and condenses into subspace FSI problem error [6]. Therefore, the FSI problem with the unknown location of the interface can be transformed into the problem of finding roots or fixed point.

Using the Newton-Raphson iterative interface Newton - Raphson method may be able to find the answers, such as the Jacobi approximation linear physical model [7] [8].In the coupling iteration process, using the least squares model coupling the black boxes and the Newton Falla comparable to reverse approach for solving the domain of fluid and structure [9].This technique is based on the interface of quasi Newton least square model, and re- expresses FSI problem as the Jacobian matrix approximation technique of an unknown equation which is in the condition of system interface location and interface stress distribution. The system solves the Gauss - Seidel type and the fluid and structure solving the Jacobian matrix block quasi-Newton iterative approximation least squares model [10] .The fixed point problem can be solved by fixed point iteration which is also known as the Gauss - Seidel iteration [6].It means that the fluid and structural issues have been resolved, until the change is less than the convergence criterion. However, the convergence speed is slow, especially in times of the interaction between the fluid and structural strong, such as High density fluid, Structure proportion or incompressible fluid. It adapt to the fixed point iteration convergence based on previously iteration, which can be stabilized and accelerated by the fastest descent relaxation factors and Aitken relaxation.

If the interaction between the fluid and the structure is weak, it only needs fixed point iteration in each time step. This was so-called staggered or loosely coupled method does not enforce the balance of the fluid structure interface within a time step,

but they apply to the structure simulation with the structure of the heavy and fairly rigid .Doing some part of research analysis the stability of the interaction segmentation algorithm used to simulate the fluid-structure stability [11] [12].

Putting forward the Pivot arm - outrigger composite collection agencies, as shown in figure 1.The collection agency was mainly consisted of the outrigger, pivot arm， holder, buoyancy wheel and cylinder. Pivot arm rotating around the outrigger, double lower end of the Cantilever using hinge to connect, the upper using the cylinder support and adjustment. The wheel worked as the support and enhances the buoyancy effect. The mining head was derived by the screw on Pivot arm.

During the Bracket walls (hollow tube) rotating around outrigger, it was a elastomer and affected by the internal and external fluids. The role of the fluid caused the pipe wall deformation or movement, which would change the morphology of the flow field in turn, thus changing the state of the fluid flow, and so affect the movement and deformation of the pipe. Under the support of the different constraints, this interaction between the pipe and fluid would produce a variety of different patterns of fluid-structure interaction phenomena [3], that is the strongly nonlinear coupling between the pipe and the fluid .Scholars in the past mostly payed more attention on the level of transmission, fixed support, elastic support (multi-point) pipeline studies [4-7], negligence the study on one end of the pipe vibration, not to mention the research on the dynamic characteristics of the pipeline in the fluid-structure interaction effect of the transport process with the heave compensation device hinged support case [13] [14].

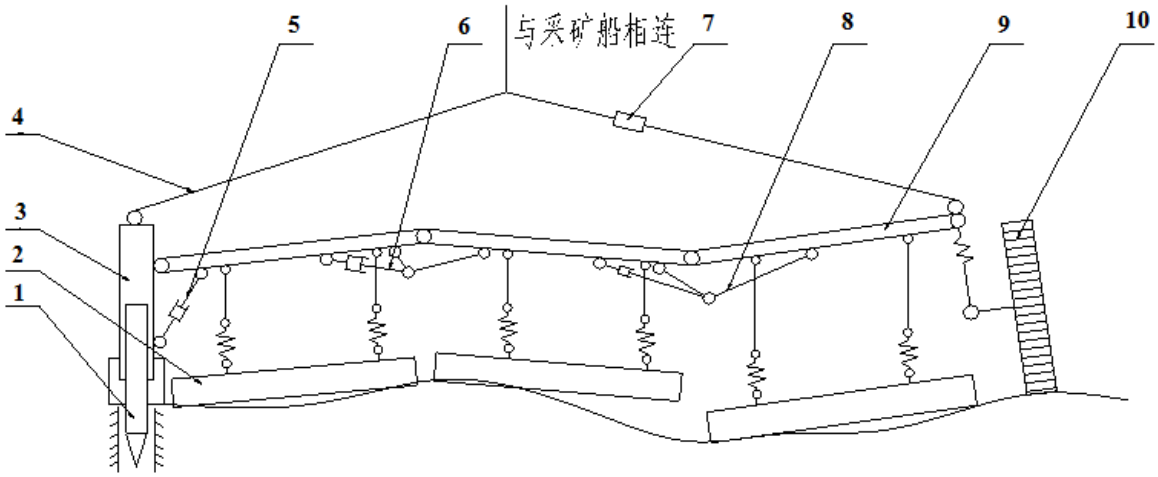

FIG.1 CANTILEVER - OUTRIGGER COMPOSITE MINING MECHANISM

II. STRESS ANALYSIS IN THE CONNECTION POINTS

When bracket piping around the legs rotate, as in the marine environment, the support pipe will inevitably be affected by the role of the waves and currents. Besides, it would also bear its own gravity, buoyancy and internal pulp. There is no really ideal fluid in nature. For the viscosity coefficient μ (coefficient of dynamic viscosity and was also known as a first coefficient of viscosity) of the fluid, its basic equation:

The Mass conservation equation:

$$\frac{\partial \rho}{\partial t} + div(\rho u) = 0 \tag{1}$$

The Momentum conservation equation:

$$\frac{\partial}{\partial t}(\rho u) + div(\rho u \otimes u - P) = \rho F \tag{2}$$

Among of them $P = \{p_{ij}\}$

$$p_{ij} = -p\delta_{ij} + \mu(\frac{\partial u_i}{\partial x_i} - \frac{2}{3} divu\delta_{ij}) + \mu' divu\delta_{ij} \tag{3}$$

Among of them $\mu' = \lambda + \frac{2}{3}\mu$ It is called the Expansion viscosity coefficient or the Second viscosity coefficient.

The Energy conservation equation:

$$\frac{\partial}{\partial t}\left(\rho e + \frac{1}{2}\rho u^2\right) + div\left(\left(\rho e + \frac{1}{2}\rho u^2\right)u - pu\right) = div(kgradT) + \rho F \cdot u \tag{4}$$

k is the Thermal conductivity coefficient. Above of the equations constitute a viscous hydrodynamic equations. Density is constant for viscous incompressible viscous fluid, take $\rho \equiv 1000 Kg/m^3$

Therefore

$$divu = 0 \tag{5}$$

Momentum conservation equation can be changed to the following equation.

$$\frac{\partial u_i}{\partial t} + \sum_{k=1}^{3} u_k \frac{\partial u_i}{\partial x_k} - \mu \Delta u_i + \frac{\partial p}{\partial x_i} = F_i \tag{6}$$

The above conservation of energy and momentum conservation equations are the three-dimensional Navier-Stokes equations of incompressible viscous fluid, which is short as the NS equations.

Considering the seawater is non-ideal fluid and the relative speed of the lifting system cannot be ignored, seawater are taken as a viscous fluid in the calculation .We get knowledge from the fluid mechanics that viscous fluid will generate the flow around detached phenomenon of the boundary layer separation when the viscous fluid flow around is not streamlined objects. Obviously, when the shape of Support pipe was a cylinder, it was adverse streamlined objects. The flow around phenomenon of the viscous fluid is different when it flows around the adverse streamlined objects at the different Reynolds. We can get the following form fluid dynamics.

$$\mathrm{Re} = \frac{\rho v d}{\eta} \tag{7}$$

Among of them : ρ ——the density of seawater; v ——the flow rate of seawater; d ——the viscosity coefficient of seawater (It have some relationship with seawater temperature).

Seawater flow rate in the deep-sea mining process will change; small changes in other parameters can be ignored. When the support pipe work in seawater, the relative velocity of the currents and Support pipe work as the following.

$$V = V_c + V_h \tag{8}$$

Among of them : V_c ——the speed of the mining ship; V_h ——at a depth of ocean currents speed; the solving formula for ocean current speed:

$$V_h = (V_a - V_b)e^{(-hH)} + V_b \tag{9}$$

Among of them : e —natural constants; V_h ——the flow rate of the water depth h; V_a —the speed of the sea currents; V_b — the speed of the deep ocean currents; h — the calculated depth of Pipeline; H ——water depth.

The main resistance of the support pipe flow around is composed by the frictional resistance and the pressure drag [16].

$$F_D = F_f + F_p \tag{10}$$

$$F_f = \int_A \tau_0 \sin\theta dA \tag{11}$$

$$F_p = \int_A p \sin\theta dA \tag{12}$$

Among of them: A-the total surface area of the object; θ -The normals of the object surface differential area dA and the direction of flow's angle.

Frictional resistance and pressure drag can be expressed as the kinetic energy of the flow in the unit volume with a particular area of the product, coupled with a drag coefficient.

$$F_f = C_f \frac{\rho U_0^2}{2} A_f \tag{13}$$

$$F_f = C_p \frac{\rho U_0^2}{2} A_p \tag{14}$$

Among of them : C_f —the frictional resistance coefficient; C_p —the pressure drag coefficient; A_f —the Shear stress area; A_p —the facing the flow projected area of the Support pipe perpendicular to flow velocity.

In the working process of the lifting system, not only will the ocean currents and the mining ship towage produce drag force, but also the waves will produce drag force. This force is closely related to the density of seawater, the geometry of wave size and shape and the Support pipe. Here is the formula.

$$f = \frac{1}{2}\rho_w C_D D|u - y'|(u - y') + \rho_w C_M \frac{\pi D^2}{4} a_y - \rho_w (C_M - 1)\frac{\pi D^2}{4} y'' \tag{15}$$

Among of them : u — the horizontal velocity of the water points; C_D — drag coefficient; a_y — the horizontal acceleration of the water points; C_M —inertial force coefficient; D —Support pipe diameter; y —Support pipe lateral offset; ρ_w ——the density of seawater.

III. STRESS ANALYSIS AT THE HINGE

Pipe with different wall thickness, the junction points of pipeline generate different stress values in the same flow impact speed. Although we can find the foreign pipeline wall thickness range data， we need to analyze it to find its own rules. After information search, we can get the date that the abroad pipeline wall thickness selected range of 9.2mm-28.7mm, the simulation analysis of pipe wall thickness in the range. Selecting a wall thickness of 9.5mm, 11.9mm, 14.3mm, 16.7mm, 19.1mm, 21.5mm, 23.9mm, 26.3mm, 28.7 mm to analyze the stress changes, the velocity in the external flow field is 1.8 m / s, the speed in the internal flow field is 2m / s, in the case of different wall thicknesses obtained effects such as stress cloud shown in Figures 2 and 3.

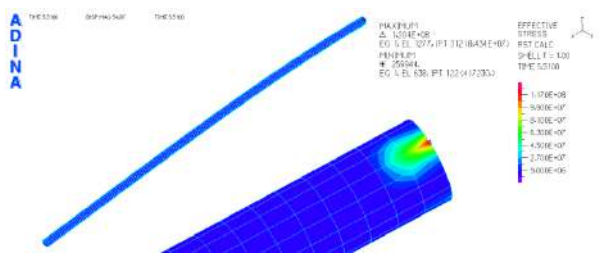

FIG.2 WALL THICKNESS IS 9.5MM EQUIVALENT STRESS

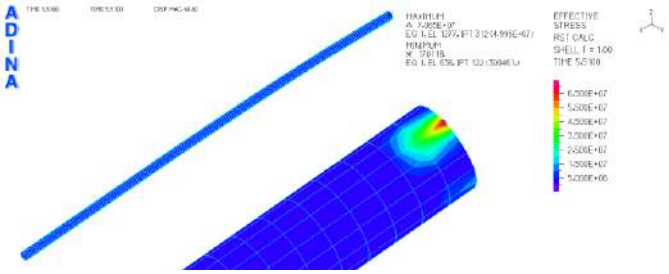

FIG.3 WALL THICKNESS IS 16.9MM EQUIVALENT STRESS

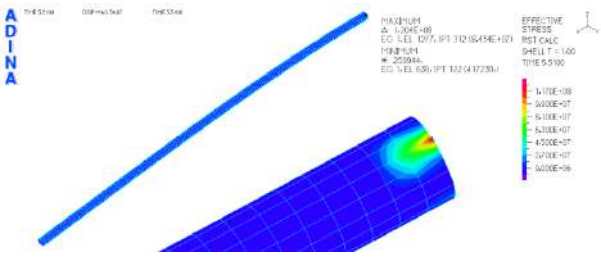

FIG.4 WALL THICKNESS IS 16.9MM EQUIVALENT STRESS

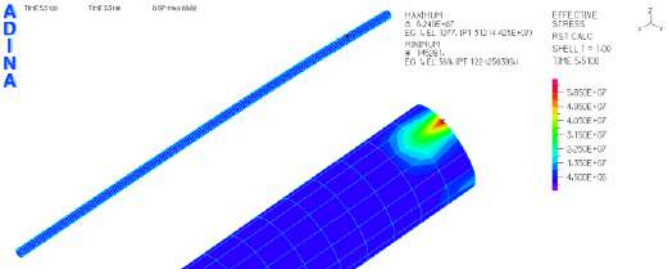

FIG.5 WALL THICKNESS IS 28.7MM EQUIVALENT STRESS

We can see from Figure 2 to Figure 5, in the case of different thickness, the stress changes of the entire pipe are relatively small, the stress changes mainly in the pipeline near the junction, the upper end of the pipe connection at the maximum stress occurs.

Fitting the different thickness of the point of maximum stress, as the corresponding curve shown in Figure 3.The law of maximum stress value with thickness variation as follow.

$$y = 2.111\times10^{11}x^2 - 1.18\times10^{10}x + 2\times10^8 \tag{16}$$

We can see from the curves shown in Figure 6, with the Support pipe wall thickness increases, the maximum stress decreases. From the diagram ,we can calculate each increase the thickness of 2.4mm, the maximum stress value decreased 19.3%, 15.9%,13.5%, 11.7%, 10.3%, 9.2%, 8.3%, 7.6%, and the thickness of 28.7mm reduced 64.2% than 9.5mm. From these data, the stress reducing effect can be found by increasing the wall thickness so that increasingly smaller.

Fitting the different thickness of the point of minimum stress, as the corresponding curve shown in Figure 5.The law of minimum stress value with thickness variation as follow.

$$y = 33282\times10^4x^2 - 22208\times10^3x + 435540 \tag{17}$$

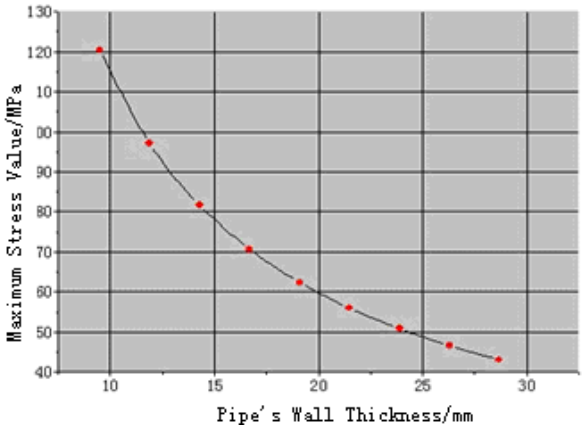

FIG.6 MAXIMUM STRESS OF DIFFERENT WALL THICKNESS

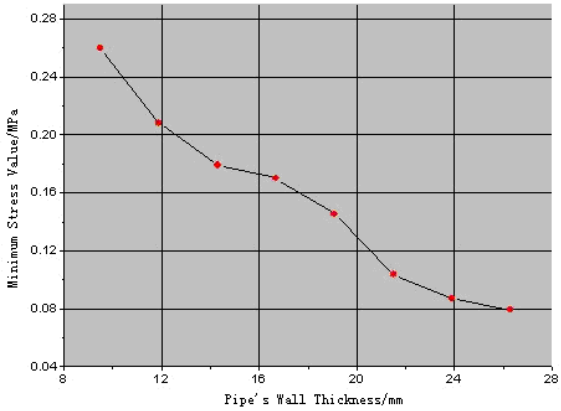

FIG.7 MINIMUM STRESS OF DIFFERENT WALL THICKNESS

We can see from the curves shown in Figure 7, with the pipe wall thickness increases, the minimum stress decreases. From the diagram, we can calculate each increase the thickness of 2.4mm, the minimum stress value decreased 19.9%, 14.0%,5%, 14.6%, 28.7%, 15.9%, 8.6%, 2.7%, and the thickness of 28.7mm reduced 70.2% than 9.5mm. From these data, the stress reducing effect can be found by increasing the wall thickness so that increasingly smaller.

IV. CONCLUSION

By studying mining institutions with the bracket connected , the pipeline was impacted by the external flow velocity of 1.8m / s, the internal conveying speed is 2 m / s, We obtained the law of effects such as stress and some meaningful conclusions as the follows.

(1) In the case of different thickness, the stress changes of the entire pipeline is relatively small, it is mainly in the pipes close to the junction, the maximum stress occurs at the upper end of the pipe connection.

(2)With the Support pipe wall thickness increases, the maximum stress decreases. From the diagram, we can calculate each increases the thickness of 2.4mm, the maximum stress value decreased 19.3%, 15.9%, 13.5%, 11.7%, 10.3%, 9.2%, 8.3%, 7.6%, and the thickness of 28.7mm reduced 64.2% than 9.5mm.From these data, the stress reducing effect can be found by increasing the wall thickness so that increasingly smaller.

(3)With the support pipe wall thickness increases, the minimum stress value decreases。From the diagram， we can calculate each increases the thickness of 2.4mm, the minimum stress value decreased 19.9%, 14.0%, 5%, 14.6%, 28.7%, 15.9%, 8.6%, 2.7%, and the thickness of 28.7mm reduced 64.2% than 9.5mm. From these data, the stress reducing effect can be found by increasing the wall thickness so that increasingly smaller.

ACKNOWLEDGEMENTS

This work is supported by Major Program of National Natural Science Foundation of China under the grant number 51174087 and the Guizhou provincial science and technology cooperation project under the grant number LH [2015]7087. The authors wish to express their deep appreciation and profound gratitude to Mr.Ning Yang, Professor of Institute of Deep-sea Science and Engineering and to Mr.Yimin Xia, Professor of Central SouthUniversity ,for their great assistance during this study and the modification of this paper.

REFERENCES

[1] M. Heil (2004). "An efficient solver for the fully coupled solution of large- displacement fluid-structure interaction problems". Computer Methods in Applied Mechanics and Engineering 193: 1–23.

[2] K.-J. Bathe; H. Zhang (2004). "Finite element developments for general fluid flows with structural interactions". International Journal for Numerical Methods in Engineering 60: 213–232.

[3] J. Hron, S. Turek (2006). A monolithic FEM/multigrid solver for ALE formulation of fluid-structure interaction with application in biomechanics. Lecture Notes in Computational Science and Engineering. Fluid–Structure Interaction – Modelling, Simulation, Optimisation. Springer-Verlag. pp. 146–170.

[4] J. Degroote, K.-J. Bathe, J. Vierendeels (2009). "Performance of a new partitioned procedure versus a monolithic procedure in fluid–structure interaction". Computers and Structures 87: 793.

[5] J. Vierendeels, L. Lanoye, J. Degroote, P. Verdonck (2007). "Implicit coupling of partitioned fluid-structure interaction problems with reduced order models". Computers and Structures 85 (11–14): 970–976.

[6] U. Küttler, W. Wall (2008). "Fixed-point fluid-structure interaction solvers with dynamic relaxation". Computational Mechanics 43 (1): 61–72.

[7] J. Degroote, P. Bruggeman, R. Haelterman, J. Vierendeels (2008). "Stability of a coupling technique for partitioned solvers in FSI applications". Computers and Structures 86 (23–24): 2224–2234.

[8] R. Jaiman, X. Jiao, P. Geubelle, E. Loth (2006). "Conservative load transfer along curved fluid-solid interface with non-matching meshes". Journal of Computational Physics 218 (1): 372–397.

[9] J. Vierendeels, K. Dumont, E. Dick, P. Verdonck (2005). "Analysis and stabilization of fluid-structure interaction algorithm for rigid-body motion". AIAA Journal 43 (12): 2549–2557.

[10] J. Vierendeels, L. Lanoye, J. Degroote, P. Verdonck (2007). "Implicit coupling of partitioned fluid-structure interaction problems with reduced order models". Computers and Structures 85 (11–14): 970–976.

[11] U. Küttler, W. Wall (2008). "Fixed-point fluid-structure interaction solvers with dynamic relaxation". Computational Mechanics 43 (1): 61–72.

[12] J. Degroote, P. Bruggeman, R. Haelterman, J. Vierendeels (2008). "Stability of a coupling technique for partitioned solvers in FSI applications". Computers and Structures 86 (23–24): 2224–2234.

[13] ZHANG Zhi-ping, HUANG Wei-ping, LI Hua-jun, The nonlinear dynamic analysis of offshore platform structure in case of considering the fluid-structure interaction [J] ,Periodical of Ocean University of China， 2005,35（5）：823-826

[14] Mr Yang, Fan Shi-Juan， Pipes for Fluid coupled vibration numerical analysis[J]. Vibration and Shock， 2009,28(6):2148-2157.

Integrated Process Planning and Scheduling of Mechanical Manufacturing

Daschievici Luiza[1], Ghelase Daniela[2]

Department of SIM, Dunarea de Jos University, Galati, Romania

Abstract— *This paper presents a product time and cost estimation method taking account the market dynamics and manufacturing system competitiveness. The method is based on the behavioral modeling using on-line unsupervised learning. On one hand, it is modeled the interaction between task and manufacturing system, and on the other hand the interaction between task and market, finally resulting behavioral modeling of the market-manufacturing system relationship to substantiate the strategic component of the competitive management thus ensuring extension in time of the high performance.*

Keywords— Behavioral modeling, Cost estimation, Manufacturing system, Product time.

I. INTRODUCTION

The cost estimation is used in price determination. If the price estimation is less than product cost then can be financial losses for the enterprise. On the other hand, if the price estimation is much higher than the product cost it is possible that the client to place his order with another company that offers a better price. The product time estimation is used to determine the date of the delivery. The classification of the different methods and estimation models used to obtain a reliable quotation is presented in [1] as follows: *1) qualitative estimation methods; 2) quantitative estimation methods.*

Qualitative estimation methods include: a) Intuitive methods- based on the use of previous experience. Of them, can be observed case-based methodology and decision support systems, b) Analogical methods- based on the similarity between the new product and past cases. These methods can be classified as regression analysis and artificial neural networks.

Qualitative estimation methods include:

a) Parametric methods- derived from the application of statistical methods to define the cost as a function of different product variables. These methods provide fast estimation; b) Analytical methods- based on the breakdown of the product into elements. Product cost is calculated as a sum of all of the components. Of these methods that are amongst the most reliable can be cited the following: operation-based, breakdown-based, tolerance-based, based on the product feature, ABC method (activity-based-costing).

II. BEHAVIORAL MODELING

By competitive management adaptation takes place of the manufacturing system for the purpose of profit maximization. To achieve adaptation, it is necessary to achieve modeling of the interaction between all elements of manufacturing system - market assembly, which shall be called behavioral modeling from now on. The term of behavioral modeling is introduced by the authors of this paper and, for presenting this notion, we shall consider two elements H1 and H2, which interact with each other (Fig. 1 a).

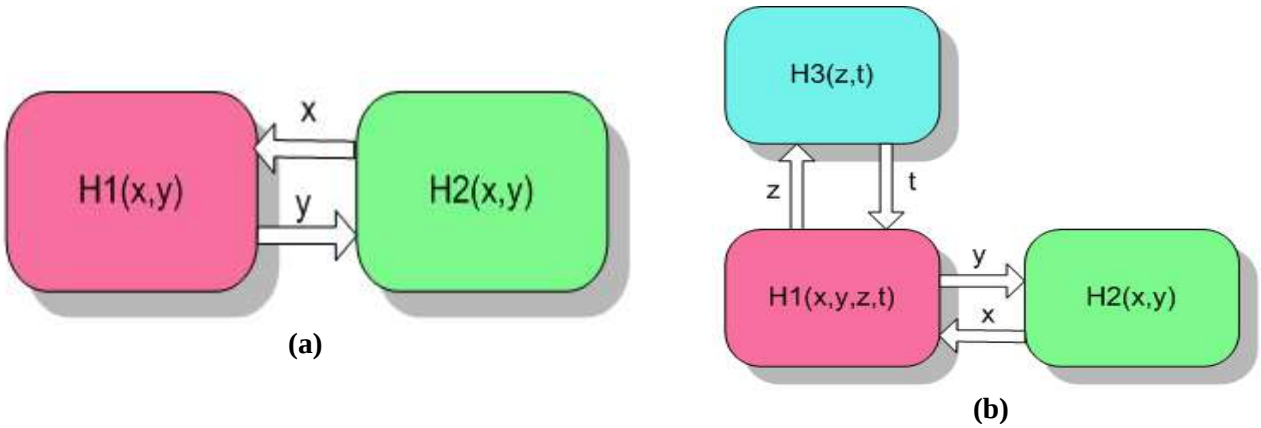

FIG. 1. BEHAVIORAL MODELING

Model H1 of the first element establishes a connection between the input x and output y. If x and y are at the same time input and output of another element, whose model is H2, then the two elements interact with each other. Modeling their interaction (behavioral modeling) means setting the pairs of values (x, y) which satisfy the transfer functions H1 and H2. The multitude of solutions which satisfy both transfer functions H1 and H2 represent the behavioral model because they describe the behavior of the elements during their interaction. For instance, under the theme concerned, H1 could stand for the manufacturing system while H2, for the market. Behavioral modeling becomes increasingly complex as the number of interacting elements is growing too. For example, in case of Fig. 1.b, three elements interact and behavioral model represents the relationship between the values of x, y, z and t for which the three elements can interact. Considering elements H1 and H2 with the following transfer functions:

$$\begin{cases} H1(x, y) = 0 \\ H2(x, y) = 0 \end{cases} \quad (1)$$

then, the solutions of the system (1) represent the behavior model of H1-H2 assembly. If the solution is unique, then the behavioral model is reduced at one operational point. Considering H1(x,y) and H2(x,y) as being two lines, then the solution of the system is the intersection point H0 (Fig. 2).

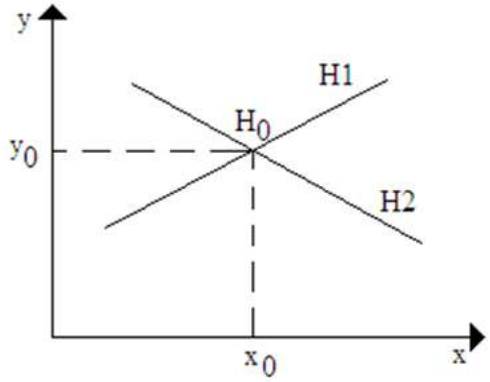

FIG. 2. BEHAVIORAL MODEL WITH UNIQUE SOLUTION

If there is a values string x_0 and y_0 as solutions of the system (1), then the behavioral model includes all these points (Fig. 3): (x_0', y_0'), (x_0'', y_0''), (x_0''', y_0''').

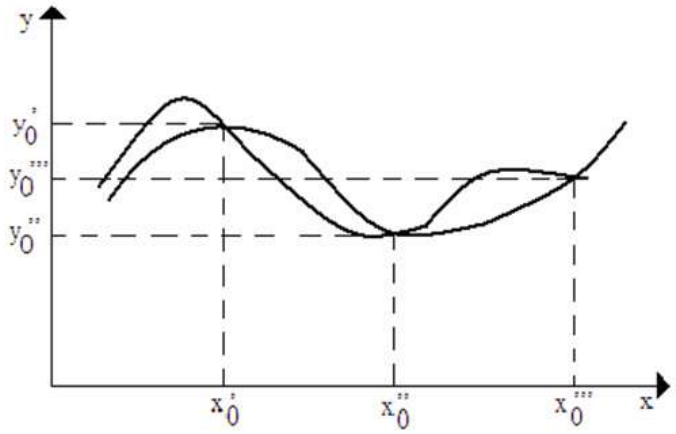

FIG. 3. BEHAVIORAL MODEL WITH MULTIPLE SOLUTION

If the system (1) is incompatible, then there isn't any behavioral model that meets H1 and H2 assembly. In the case of Fig.1.b, the case of the interaction of three elements H1, H2, H3, the behavioral model is given by (x_0, y_0, z_0, t_0), the system solution:

$$\begin{cases} H1(x, y, z, t) = 0 \\ H2(x, y) = 0 \\ H3(z, t) = 0 \end{cases} \quad (2)$$

As the number of variables is more than equations, we expect the system (2) is indeterminate. The model will include a infinite points number. The behavioral modeling method of the manufacturing system-market assembly is developed on these assumptions: elements H1 (manufacturing system) and H2 (market) operate and are monitored on-line; during operation, elements H1 and H2 pass through different states**,** that means they operate with various values of the state parameters. For example, H1, the manufacturing system, processes various products with various machining parameters and with various time, materials consumptions. Element H2, market, operate similarly, selling various products with various prices in various supply conditions.

- elements H1 and H2 interact, but not throughout their operation (the manufacturing system can interacts with another markets).

The algorithm used for modeling is based on states clustering and consists of following steps:

Step 1: clustering of variables based on the causal relationships;

Step 2: states clustering;

Step 3: building of the mathematical model corresponding to the states cluster and variables cluster set.

Then the causality relationships between parameters are identified. Based on these relationships, clusters of independent variables are established. Further, based on the dataset to be used for the model fitting, a cluster of neighbouring states is made up, at the centre of which is the state to which the respective input data are related. Finally, a linear model whose variables are the variables of one of the clusters of identified variables is fitted on the manufacturing system states cluster. These input data are the ones which have been previously considered in the procedure of enclosing the manufacturing system states cluster. It can be noted that, according to the proposed method, the model construction and its operation are accomplished within an integrated algorithm which is run through upon each interrogation of the manufacturing system model. At the operational level, the variable clustering is based on the "*best NN model*" facility which is offered by the neural networks technique applied to a data set recently obtained from monitoring the manufacturing system. The states cluster construction, the linear model is fitted to, first implies the use of the 2^{nd} rank Minkowski distance for the classification of states, in the increasing order of their distance to the state to be used for model interrogation. That is why only the variables representing these input data will be considered in the calculation of Minkowski distance.

The states cluster is to be obtained either by restricting the value of the distance or by restricting the number, *k*, of retained states or using both conditions. The construction of the mathematical model is made by linear regression. It can be noted that this is a local model, as it is valid only in the vicinity of the state for which the model is interrogated. This model is meant to be used just once was, after the interrogation, it is given up. In conclusion, the aim of the proposed method is to develop cost estimation for the required product in terms of time required by the customer. To be sure winning the product auction, the manager must to apply an attractive price. In determining the price of the product is necessary to know the product cost. Thus, for a specific task required and in imposed time conditions, through modeling are obtained the relations as: Cost = f(task) ; Time = f(task). At the same time, the manager must have a model of the product markets by monitoring the auctions.

Auctions provides data on market price quotation. By modeling of market data it obtained a relationship of dependency as: Market = f(task). The method proposed for achievement of the three models (fig.4) consists of monitoring and recording the relevant state variables of the manufacturing system in a database.

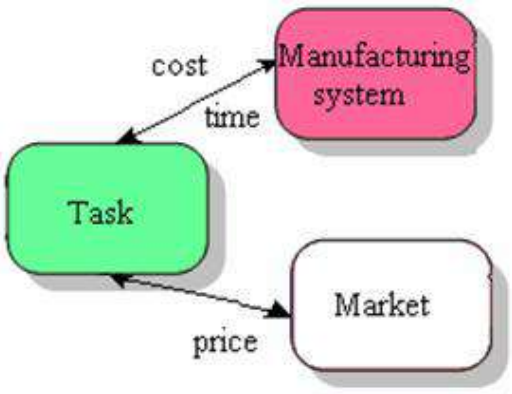

FIG. 4. THE INTERACTION BETWEEN TASK-MANUFACTURING SYSTEM AND BETWEEN MARKET-TASK

III. STUDY CASE

During the experiment data have been collected with regard to the manufacturing machines that had been used for manufacturing some important parts in the construction of dump truck bins, namely the attachment plate of the supplementary chassis of the dump truck bin (fig. 5).

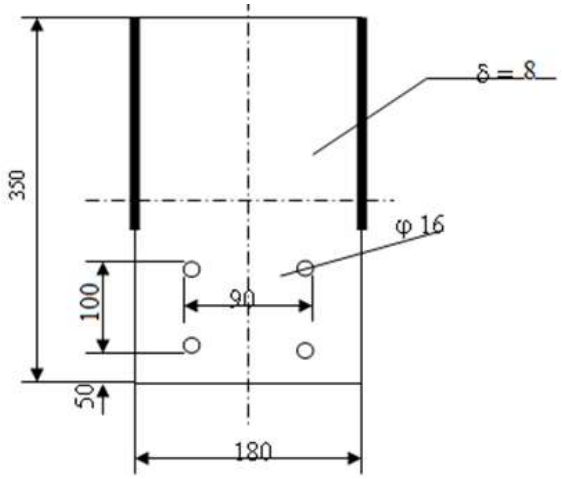

FIG. 5. ATTACHMENT PLATE OF THE SUPPLEMENTARY CHASSIS OF THE DUMP TRUCK BIN

Data regarding the actual work times, data referring to the modes of operation, data regarding the amounts of resulted wastes, data regarding all types of consumption, as well as data regarding the orders for delivered products were collected. We use the database of a cutting process that has the following parameters: type of the material, length of cutting, cutting width, cutting speed, the feed rate, number of pieces, machining time, energy consumption, cost of operation and waste quantity, Table 1. Measuring and monitoring of the cutting process were made, whose results are summarized in the Table 1.

TABLE 1
EXAMPLE OF EXPERIMENTAL DATA REGARDING THE PROCESS VARIABLES COLLECTED FOR THE CUTTING OFF PROCESS

Item nr.	Type of material	Length of cutting (mm)	Cutting off width (mm)	Cutting off speed (mm/s)	Feed rate (mm/s)	Number of pieces	Machining time (s)	Energy consumption (kwh)	Cost of operation (Euro)	Waste quantity (Kg)
-	V_1	V_2	V_3	V_4	V_5	V_6	V_7	V_8	V_9	V_{10}
1	OL 52	350,1	180,15	3,1	0,5	50	1200	14,74	1781,3	26,51
2	OL 52	253,1	184,15	4,1	1,5	75	2254	18,24	2186,2	32,78
3	OL 37	257,15	172,1	5,1	2,5	100	2011	24,84	2861,6	42,91
4	OL 42	462,05	268,1	5,15	2	45	3201	18,45	2190,4	32,86

Clustering technique is based on algorithms from the neural networks.

A. Clustering variables

Clustering variables consists in grouping variables which are variables in dependence. Thus using "best NN model", the choice of many consecutive columns and determination of the best links with the 1, 2 or i variable we determine the cluster of variables which are in the best relationship of dependency. For example, in table 1, considering the cutting process variables that denote the V_1, V_2, ..., V_{10} and using the "best NN model" facility, results the column V_7 - time of cutting, as the most influential variable in determining the time of operation. There are the best relationships with dependent columns V_2 and V_4.

B. Clustering states

Suppose that the manufacturing system is required to execute an operation that $V_2 = 150$, and $V_4 = 3$, where you don't find in our experiment. Clustering states consists in identifying groups of related records that can be points of departure for further

exploration of relationships. In the process of grouping elements is necessary to estimate the minimum distance between those elements with the function:

$$d = \sqrt{\left(V_2 - 150\right)^2 + \left(V_4 - 3\right)^2} \tag{6}$$

C. The mathematical model

Mathematically can write a linear relationship:

$$V_7 = a \cdot V_2 + b \cdot V_4 \tag{7}$$

Retaining the first 2 states, so for k = 2 according to k-NN algorithm can be written:

$$\begin{cases} a \cdot 158,25 + b \cdot 1,2 = 8201 \\ a \cdot 158,25 + b \cdot 9,25 = 8835 \end{cases} \tag{8}$$

which represents a system of two equations with two unknowns. Finding system solutions are obtained the values for *a* and respectively *b* which are replaced in the relationship (7) resulting relationship (9).

$$V_7 = 51,225 \cdot V_2 + 78,75 \cdot V_5 \tag{9}$$

Linear model so determined will be used in modeling task-time relationship. This is a local model that is only valid in the vicinity of the state in connection with which it is interrogated and ephemeral because after the query is dropped. Taking the reasoning again we modeled the relationship between task and cost. In this case we found that the influence variable is variable V_8, using "best NN model". Similarly on determine:

$$V_8 = 0,05 \cdot V_2 - 1,08 \cdot V_4 \tag{10}$$

Returning to the example above, the $V_2 = 150$ and $V_4 = 3$, it follows the same steps as in modeling of relationships: task-time and task-cost and obtain a mathematical relationship for model task-market model, taking V_9 as the influence variable.

$$V_9 = 5,78 \cdot V_2 - 116,52 \cdot V_4 \tag{11}$$

In conclusion, if we introduce variations of the process parameters and a variable restriction we can get a table of solutions that will help to find common solutions through negotiation between the customer's requirements and possibilities of economic and technical producer.

IV. CONCLUSION

Note that we propose to give managers a model so that they can interact with the economic environment (market). Practically, this happens before the actual work of manufacturing system, so we have to do with a function of anticipation. The proposed method has the advantage of being applicable to any manufacturing system, regardless the physical nature of the process and the product features. The method provides the extended modeling of the relationship between manufacturing system- market. The level of extension is only limited by the number of the monitored state variables. The level of the modeling accuracy satisfies both the requirements specific to a contract negotiation and the ones specific to the operational management. The developed method allows the identification of the variables of one model that represents the relation between the output and the input model. The proposed method develops cost estimation for the required product in terms of time required by the customer.

REFERENCES

[1] Garcia-Crespo A., Ruiz-Mezcua B., „A review of conventional and knowledge based systems for machining price quotion", J Intell Manuf, Springer, 2009.

[2] H'nida F., Martin P., Vernadat F., „Cost estimation in mechanical production:The Cost Entity approach applied to integrated product engineering", International Journal of Production Economics, 103, 2006, pp.17-35.

[3] Lerch F.J., Harter D.E., „Cognitive support for real-time dynamic decision making", Information System Research, 12(1), 2001, pp.63-82.

An Intelligent Knowledge Management for Machining System

Ghelase Daniela[1], Daschievici Luiza[2]

Department of SIM, Dunarea de Jos University, Galati, Romania

Abstract— *Today, information has become more important. Even data, information and knowledge are often used as if they have same meaning. This problem raises difficulties in engineering. It is necessary to exist a knowledge management system to avoid increased costs, waste of time and increased errors. Knowledge management is a comprehensive process of knowledge creation, knowledge validation, knowledge presentation, knowledge distribution and knowledge application. In this paper, knowledge management has been explained in general. Then as an example for this study, machining system has been considered, and an application of Knowledge Management in engineering has been attempted to explain. The paper proposes a knowledge management to achieve a competitive control of the machining systems. The model can be used by the manager for the choosing of competitive orders.*

Keywords— Competitive control, Information technology, Knowledge management, Machining system, Marketing knowledge.

I. INTRODUCTION

A general definition has been 'getting the right information to the right people at the right time' in order for them to make better decisions.

Due to technology facilitates the rapid exchange of information, the pace of acquisition is growing exponentially in both large and small enterprises. The vast amounts of knowledge possessed by the enterprises are spread across countless structured and unstructured sources.

To improve processes and bring new products to the market faster and more cheaply, the enterprises have to identify, make available and apply this knowledge.

It is necessary to exist a knowledge management system and coordination between disciplines to avoid increased costs, waste of time and increased errors. Thus, information must be understood, organized and transformed for problems solving.

Consequently, information transformed in product is knowledge and coordination of this kind of knowledge is made by means of knowledge management.

The manufacturing industry faces the challenge of responding quickly to the ever-changing requirements of customers. It is necessary that in these high competitive environments, enterprises to control production system dynamics of such as:

- change in the product types and variants;

- change in the production quantities.

Enterprises have to develop and implement more responsive and flexible manufacturing systems based on knowledge. By this way, they can respond to outgoing and difficult to predict change in production requirements and make products with high quality, low cost and fast delivery.

The market dynamics is further passed to the mode of operation and management. In a knowledge-based society and economy, operations such as determining the relevant information and aggregating them into pieces of knowledge must be automated, because in such a complex and unpredictable environment, they are indispensable tools for creating, searching and structuring knowledge. The interaction between the economic environment and the manufacturing system is a major source of knowledge about the economic environment and the manufacturing system themselves [3].

II. KNOWLEDGE MANAGEMENT IN ENGINEERING

Information is becoming ever more important in engineering. It is not suitable to use data, information and knowledge conventionally. That is there is conceptual confusion. Also, today's technological products need interaction between different disciplines. So the confusion increases more. At the multidisciplinary engineering system, any discipline contains some information peculiar to system. However, most of the information mean essentially same even if they are expressed in

different terms in different disciplines. Therefore, the available information must be evaluated, simplified and transformed into usable form that is knowledge.

Next, the knowledge is coordinated and connected with the system. So, a kind of know-how is acquired for the technological product. This case is generally based on a model, while it has special characteristics. An example of machining system has been analyzed in the following section. The model produced by technical knowledge which is acquired by the interaction of data, information and knowledge, by the coordination and the application of them on engineering system. KM model is presented in Fig. 1.

KM is a comprehensive process of knowledge creation, knowledge validation, knowledge presentation, knowledge distribution and knowledge application [2]. When KM model is applied by the enterprise into its production process it is obtained increasing competitiveness of the product in the market. That is KM model can be used for every stage of the engineering works such us design, manufacture, maintenance and repair.

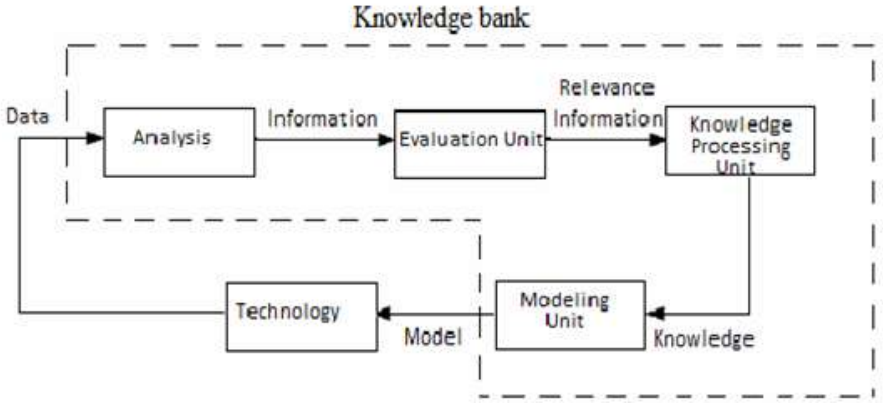

FIG. 1: KM MODEL

III. APPLICATION OF THE KNOWLEDGE MANAGEMENT ON MACHINING SYSTEM

By manufacturing system we understand all the technological systems that are used to produce a specific product.

Each of these technological systems is composed of machine-tool, tools, devices, parts, operator and carries out one of the operations of the technological process of making that product.

The machining system performance depends on how it is run. In more specialized papers [1] reference is made to the relationships between the parameters of the processing regimes and the technical performance of the machining system (purely technical aspects), while in others, equally numerous [4], [5] references are made to the relationship between the product made by the machining system and the market (economic relations).

In the literature no attempt to approach the whole machining system – market assembly is reported; therefore, there are significant resources to improve performance which are not used because the technical and economic aspects are dealt with separately.

Also, it is not known an algorithm for the management of the machining system – market assembly, but only algorithms for the technical control of the technological systems [5] and tools of economic management of the relationship between the technological system as a whole and the market [6].

Nowadays, the machining systems are controlled by means of numerically programmed machine tools which are part of the system [7]. The control is exclusively technical because there is no economic variable, although this is actually the ultimate goal of any processing process.

The dynamic changes and the overall progress of society are reflected at company level by many orders in number, small in volume, very diverse, obtained through frequent auctions with short- term response, which leaves no time for a relevant analysis of said orders.

As a result, a long-term management is no longer possible. A sort of fluctuating (just like the market) on-line, fast responsive, prompt and rapid, however, ephemeral management is called for [4]. For these goals we propose knowledge management model of machining system.

The architecture of KM model of machining system is presented in Fig. 2. The system showed in Fig. 2 consists of KM model, CNC Machining System, Marketing Knowledge.

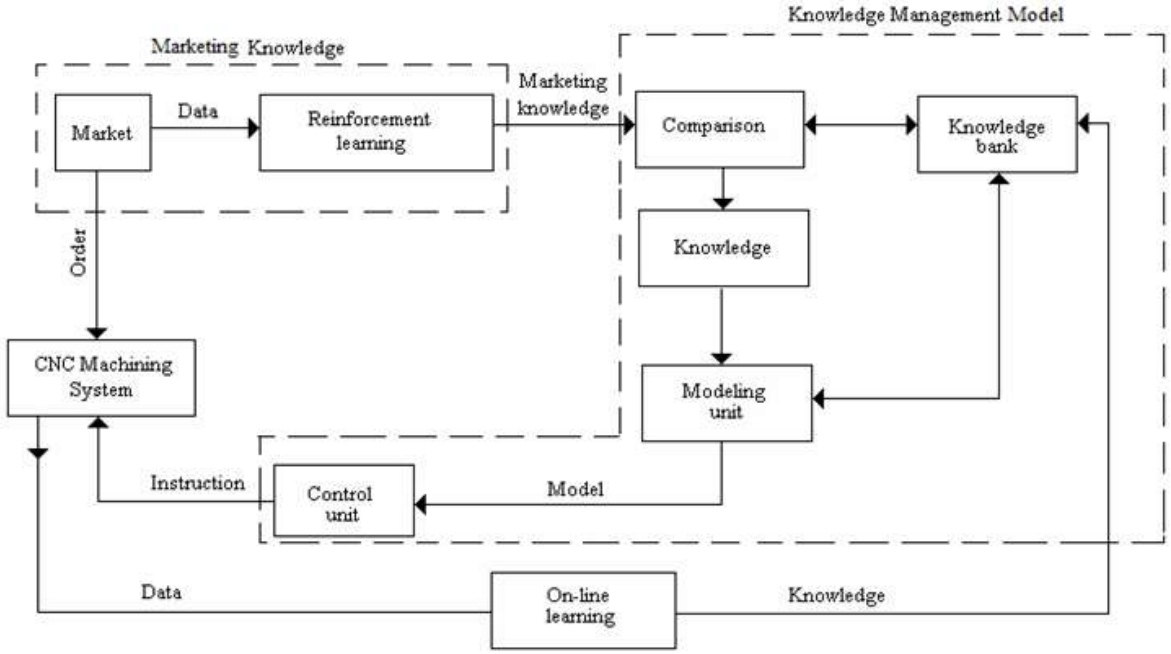

FIG. 2. KNOWLEDGE MANAGEMENT ARCHITECTURE OF THE MACHINING SYSTEM

KM model contains very important features of the system.

KM model consists of knowledge bank, compare, modeling and control units. The knowledge bank is formed according to the characteristics of the system.

It is very important that information which concerns with subject, correct, update, concordant must be converted knowledge and they must be stored in this unit. It is necessary that this unit becomes a flexible structure because it can be updated depending on the market dynamics and technical characteristics of the new manufacturing products.

The information coming from the Marketing Knowledge-unit are diagnosed by the comparison unit. Also the comparison unit has information-receive ability from knowledge bank. The essential function of the comparison unit is to compare the information and knowledge with each other. The output information from the comparison units is a new knowledge. This new knowledge has been sent to modeling unit.

Not only does the modeling unit receive information from the comparison unit, it also interacts with the knowledge bank. The output of the modeling unit is the model which is analyzed in control unit. This unit sends the manufacturing instruction for to the CNC Machining System. Through on-line learning, the output information from CNC Machining System unit becomes the new knowledge and has been sent to knowledge bank.

On the other hand, after assessing competitiveness, the management system should enable to develop competitive offer for the tenders. To achieve these two objectives, the competitive control uses the reinforcement learning to get to know the market and the non supervised on-line learning technique to get to know the machining system.

IV. STUDY CASE

Let us assume that in market there are more offers quotations for a certain product. Using reinforcement learning, the information from market becomes marketing knowledge and they are compared with the ones from knowledge bank.

After the comparison, knowledge unit send the technical-economic parameters to the modeling unit. Also, modeling unit interacts with the knowledge bank to achieve the machining model.

On basis of generated model, simulations are made and analyzed in control unit. This unit sends to the CNC machining system the manufacturing instructions that satisfy the customer demands in the competitive conditions of the enterprise.

For example, from the simulations (Fig. 3.a) it can see that the minimum cost is obtained for the cutting speed v'_{op}=84m/min. The control unit sends to the CNC machining system the manufacturing parameters: cutting speed v'_{op}, feed rate *s*, depth of cut *t*.

Also, corresponding to this cutting speed, it can be read the necessary time τ for 1 cm^2 surface area machining (Fig. 3.b), the profit rate *r* (Fig. 3.c) and the environmental impact *I* (Fig. 3.d). On basis of these simulations the manager can decide if the order is accepted or rejected.

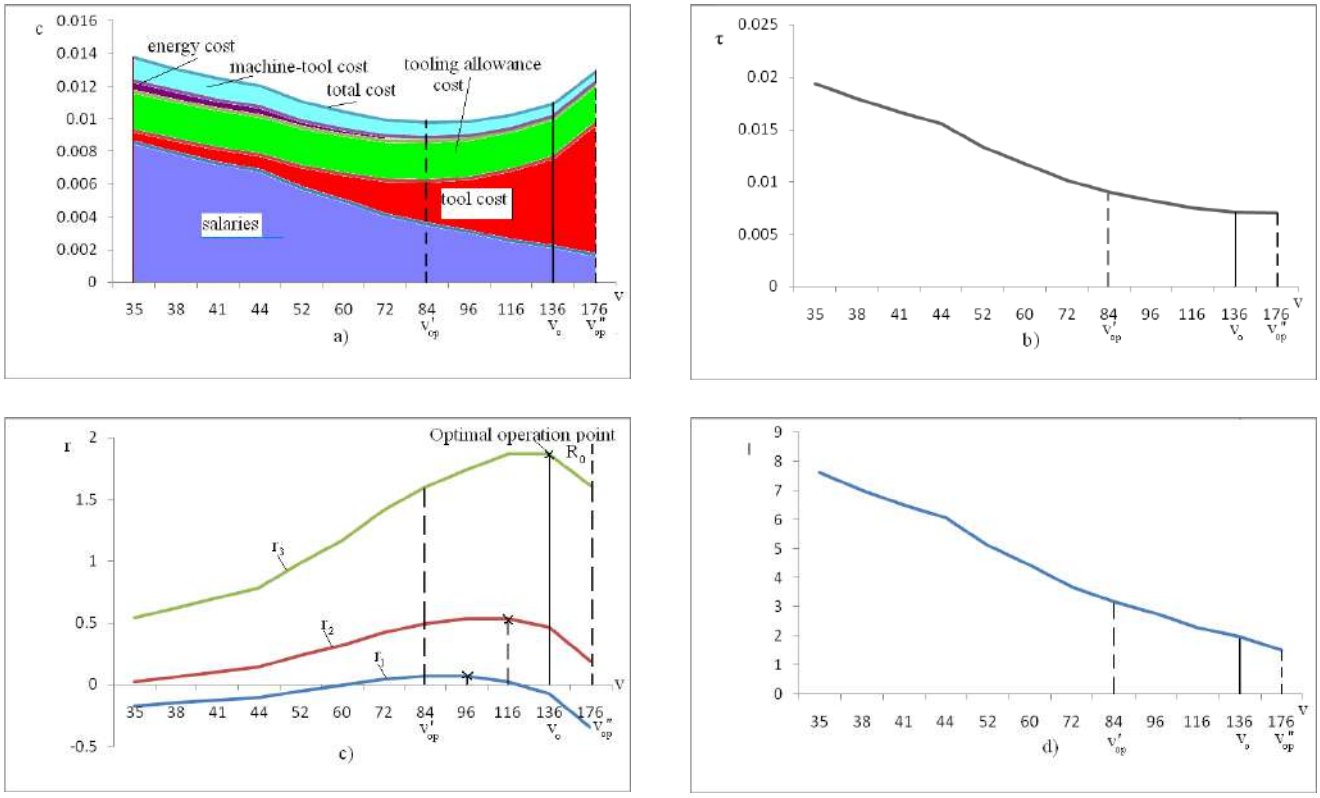

FIG. 3. SIMULATIONS FOR A TURNING PROCESS AND SYSTEM: a) **STRUCTURE OF THE COST** *c*; b) **TIME** τ; c) **PROFIT RATE** *r*; d) **ENVIRONMENTAL IMPACT** *I*

V. CONCLUSION

In this paper the architecture of the knowledge management of the machining system was achieved.

Using and comparing marketing knowledge with stored and updated ones the machining model is carried out, analyzed and on its basis are generated instructions regarding the progress of the machining process in order to obtain maximum competitiveness.

By modeling and simulations, the manager can decide if the order is accepted and control the machining system to satisfy the customer demands.

To achieve these objectives, the competitive control uses the reinforcement learning to get to know the market and the unsupervised on-line learning technique to get to know the machining system.

Note that we propose to give managers a knowledge management model, so that they can interact with the economic environment (market).

This knowledge management model represents a technical-economic model that can be used for competitive control of the manufacturing process without requesting experiments and based on the extraction of the knowledge from the previous experience.

REFERENCES

[1] Cios K., Pedrycz W., Siniarski R.,Kurgan L., „Data Mining- A knowledge Discovery Approach", Springer, 2007.

[2] Christoph H. L., Chick S. and Huchzermeier A., „Can European Manufacturing Companies Compete?: Industrial Competitiveness Employment and Growth in Europe", European Management Journal, Volume 25, Issue 4, August, 2007, pp.251-265.

[3] H'nida F., Martin P., Vernadat F., „Cost estimation in mechanical production, The Cost Entity approach applied to integrated product engineering", International Journal of Production Economics, 103, 2006, pp.17-35.

[4] Hoda A. EIMaraghy, „Flexible and reconfigurable manufacturing systems paradigms", Spriger Science+Business Media, LLC, 2006, pp.261-276.

[5] Karayel D., Ozkan S., Keles R., „General framework for distributed knowledge management in mechatronic systems", Journal of intelligent manufacturing, 2004, pp.511-515.

[6] Lerch F.J., Harter D.E., „Cognitive support for real-time dynamic decision making", Information System Research, 12(1), 2001, pp.63-82.

[7] Toly C., „Evaluating the mid-term competitiveness of a product in a semiconductor fabrication factory with a systematic procedure", Computers & Industrial Engineering, Volume 53, Issue 3, October, 2007, pp.499-513.

Performance Analysis of Manufacturing System at the Operational Level

Daschievici Luiza[1], Ghelase Daniela[2]

Department of SIM, Dunarea de Jos University, Galati, Romania

Abstract— *In this paper, we propose a method to control of make-to-order (MTO) manufacturing system for the operation level. Control achieved with the proposed method is based on modeling the relationship between cost and time, two very important elements of manufacturing process performance evaluation. In order to better represent the specified goal of manufacturing process we propose (as a novelty) as a criteria the Earning Power (EP). It is both synthetic (because it reflects the essential motivation of manufacturing process) as compliant with the most important five performance aspects, namely: profitability, conformance to specifications, customer satisfaction, return on investment and materials/overhead cost, selected by researchers in order of importance.*

Keywords— Control, Earning power, Manufacturing operation, Manufacturing system, Simulation.

I. INTRODUCTION

By definition, Earning Power is an operating income divided by total assets. Here, operating income is an income resulting from a firm's primary business operations, excluding extraordinary income and expenses. It gives a more accurate picture of a firm's profitability than gross income. Asset is something that an entity has acquired or purchased, and that has money value (its cost, book value, market value, or residual value). An asset can be: something physical, such as cash, machinery, inventory, land and building; an enforceable claim against others, such as accounts receivable; right, such as copyright, patent, trademark or an assumption, such as goodwill. For determination of EP it must be estimated: cost, time, asset, and price. Current methods for estimating the cost and time are based on breakdown of the product into elements, cost estimation of each element and summing of other costs [1,2]. As an element, we can consider one product component, one manufacturing component or one activity component. To estimate the cost for each element there are used element's different features that are closely related to cost. With few exceptions, estimation methods lead to cost estimation without a mathematic model describing relation between cost and element's different features. As a plus, those methods have a slight adaptation capacity to different specific situations because the information that is provided in order to estimate is general and does not adapt to specific case. Therefore, in this paper, cost and time will be estimated by techniques that are based on analytical modeling, neuronal modeling, or k-nearest neighbor regression. Each of these techniques cover a range of specific cases, namely: analytical technique covers process cases with all known regularities. The technique based on neuronal modeling covers cases when a large number of similar products are manufactured, slightly different. Moreover, k-NN regression technique covers cases when there is little data to produce a model (production is diverse and manufactured series are few).

It is not difficult to estimate the asset because in the balance sheet there are quite accurate and updated data. Price estimation goes from costs and represents the company mission in relation to the market.

II. OPERATION MODELING

We consider that we have to manufacture the part from Fig. 1. The technological process needed to process the part consists of the following operations: turning, drilling and welding. In order to evaluate the order EP we have to calculate job EP and operation EP. To do this, the order will be divided in job 1 (rod 1, Fig. 1) and job 2 (plate 2, Fig. 1). To perform job 1 it is necessary to use the turning operation. For job 2 we need drilling and welding operations.

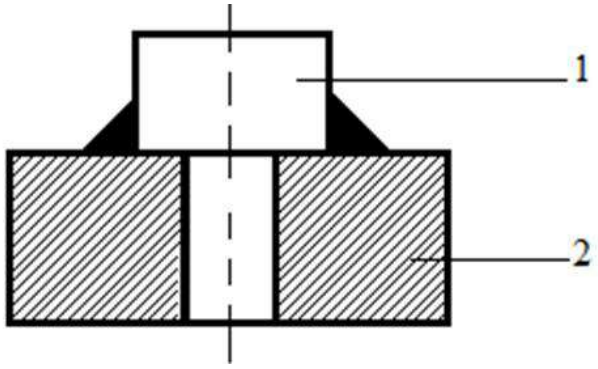

FIG. 1. MANUFACTURING PART: 1 - ROD, 2- PLATE

Taking the case of a cutting process for an order *i* with *j* jobs and *k* operations we can define EP_{ijk} for operation level as:

$$EP_{ijk} = \frac{P_{ijk} - c_{ijk}(p_{jkn})}{A_{ijk} \cdot t_{ijk}(p_{jkn})} \qquad \left[\frac{\text{Euro}}{\text{Euro} \cdot \text{min}}\right] \tag{1}$$

where: P_{ijk} is the minimum market price for operation *k* and for job *j* in order *i* [Euro]; $c_{ijk}(p_{jkn})$ expenses necessary to achieve job *j* depending on parameters *n* for operation *i* [Euro]; A_{ijk} – is the operation asset *k* from job *j* in order *i* [Euro]; $t_{ijk}(p_{jkn})$ – time for workstation's process when make the operation *k* from job *j* [min].

In order to determine EP we must estimate: cost, time, asset, and price. In this paper, cost and time will be estimated by some techniques based on analytical modeling, neuronal modeling, or modeling by k-nearest neighbour regression.

2.1 Analitical Model

The operation of turning will be analytically modeled on the base of the relation:

$$c_{ijk} = C_{amijk} + C_{pijk} + c \cdot S_{ijk} \cdot N_{ijk} \tag{2}$$

where: C_{amijk} is cost for auxiliary labor for carrying out the operation *k* from job *j* [Euro]:

$$C_{amijk} = \frac{C_{mijk} \cdot N_{ijk}}{4} \tag{3}$$

C_{mijk} - cost for labor of operation *k* from job *j*. For turning operation that is part from job 1,

C_{mijk} = 2.75 Euro; N_{ijk} - number of pieces to be processed; C_{pijk} - cost to prepare the operation *k* from job *j* [Euro]. For turning operation, C_{pijk} = 2.7 Euro.

$$c = \frac{c_\tau}{10vs} + \frac{\tau_{sr}c_\tau + c_s}{10Tvs} + \frac{t \cdot c_{mat}}{10} + \frac{K_e c_e}{10000vs} + \frac{C_M}{10K_M} v^{\alpha-1} s^{\beta-1} t^{\gamma} \text{ [Euro/cm}^2\text{]}, \tag{4}$$

where: c_τ is cost for one minute to use the job place, 0.45 Euro/min; τ_{sr} – time to change and sharpening the tool [min], 10 min; c_s – tool cost between two consecutive re-sharpening processes, 20 Euro; c_{mat} – cost to remove one cm^3 of additional material, 0.008/cm^3; c_e – cost for one KWh of electric power, 0.23 Euro/KWh; K_e – energy coefficient [Wh/min], 15 Wh/min; K_M – machine tool coefficient, $5.4 \cdot 10^6$;

C_M – cost of machine tool [Euro], 100000 Euro; v – cutting speed [m/min]; s – feed rate [mm/rev], 0.15 mm/rev; t – cutting depth[mm], 3mm; $\alpha = \beta = \gamma = 0.5$;

T – tool durability

$$T = \left[\frac{470}{v}\right]^{2.5} \text{[min]}; \tag{5}$$

S_{ijk} – processed surface [cm^2]; 281.34 cm^2.

For cutting process, loading time modeling for a workstation to perform operation *k* of job *j* of order *i* is:

$$t_{ijk} = t_{pijk} + t_{aijk} \cdot N_{ijk} + \tau \cdot S_{ijk} \cdot N_{ijk} \quad [\text{min}] \tag{6}$$

where: t_{pijk} – time to prepare the operation, 60 min; t_{aikj} – operation auxiliary time, 4.4 min

$$t_{aijk} = 0{,}2 \cdot t_{uijk} \quad [\text{min}] \tag{7}$$

t_{uijk} - unitary time to perform the operation, 22 min; τ - specific time necessary to remove one cm^2 of material.

$$\tau = \frac{T + \tau_{sr}}{10 \cdot T \cdot v \cdot s} \ [\text{min/cm}^2] \tag{8}$$

It can be observed that EP by cost and time depends on several parameters p_{jkn}.

The optimal control operation is controlled so that the maximum EP be provided that restrictions on the accuracy, surface quality, stability and product ecology are respected. We ask the question: which are the parameters that must perform the operation for EP to be up?

We can observe that cost c_{ijk}, and time t_{ijk} are dependent by a series of variables named by the us parameters p_{jkn}: c_τ, τ_{sr}, c_s, c_{mat}, c_e, K_e, K_M, C_M, v, s, t, α, β, γ

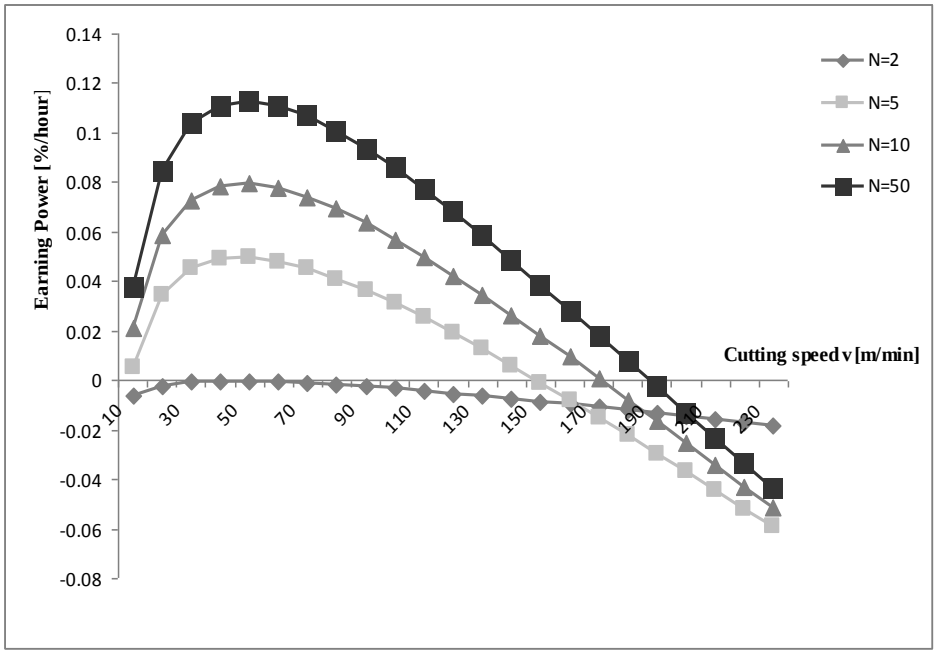

FIG. 2. THE VARIATION OF THE EARNING POWER DEPENDING ON CUTTING SPEED

Part of these variables depends by the workstation (K_M, C_M), others by the tool (τ_{sr}, c_s), others by the process (v, s, t). By these variables, we can control the process, i.e. they can influence the value of EP so that it becomes maximal. Taking into consideration all restrictions imposed by the process, we will have to choose the variables by which we can control the process. For example, for cutting process, the control variable can be cutting speed *v* or/and tool material and then we'll need to know the value for these control variables so that EP becomes maximum. Feed rate *s* could influence EP, but it is determined depending on surface roughness and it cannot be changed during the cutting process to achieve maximum EP.

The cutting depth *t* is restricted because it is considered that the addition of the entire processing must be removed in a single pass. It cannot be taken as control variable. Note that the control variable for the cutting process is cutting speed, *v*. When graphically representing the EP of turning operation according to cutting speed we can see there is a maximum value for EP for a specific optimal value of cutting speed (Fig. 2). For example, for a number of pieces *N=2*, maximum value of EP is -0.0002898 %/hour when *v=40* m/min*; N = 5*, maximum value of *EP=0.0496663* %/hour for a cutting speed *v=50* m/min; for *N=10*, maximum value of *EP* = 0.079419 %/hour for *v=50* m/min and when *N=50*, maximum value of *EP*=0.112742971

%/hour for v= 50m/min. It can be noted that depending on the number of pieces of processed product *N*, choosing the optimal cutting speed can be obtained a maximum EP, i.e. can realize an optimal control of the turning operation.

2.2 Neural Network Modeling

Welding operation for job 2 is modeled by a Neural Network technique. "Best NN model" or the best model provided by a neuronal network is a practical modality to find out causality relations between variables in order to be able to determine the variable clusters. Using neuronal network to compare variables (each by each) we obtain sets/clusters of variables that are in causal relationship. Procuring clusters is a computer application, training the network with all its database values and determining those variables that have causality relations. From database of welding operation variables (Table 1) which we note with *v1*, *v2*,…,*v12*, we'll take into consideration column 12 containing values of variable *v11*- cost of welding operation. By a neuronal network, are determined the best relationships with the other columns.

TABLE 1
SEQUENCE FROM THE TABLE OF WELDING OPERATION VARIABLE

Item Nr.	Material type	Welding type	Length of welding seam [mm]	Nr. of passes	Current intensity [A]	Rate of welding [mm/s]	Quantity of welded wire [m]	Nr. of pieces	Welding time [s]	Energy consumption [KW/h]	Operation cost [Euro]	Waste quantity [Kg]
-	v1	v2	v3	v4	v5	v6	v7	v8	v9	v10	v11	v12
1	OL 52	corner	501	3	200	10.2	4.2	63	1375	10.521	78.9	15.781
21	OL 37	corner	503.5	9	204	5.1	4.85	103	6758	52.898	388.9	77.791
40	OL 52	corner	490	4	197	8.2	4.60	59	11243	12.656	96.3	19.273
52	OL 42	corner	515	10	188	9.2	5.20	52	2459	27.970	223.1	44.633
64	OL 52	corner	521	11	191	8.15	4.1	92	6066	55.947	439.3	87.875

It is determined the best dependence relationships with the columns *v3*– length of welding seam, *v4* – number of passes, *v6* – rate of welding and *v8* – number of pieces. The result will be a cluster of variables (*v3*, *v4*, *v6*, *v8*). Using the data from cluster of variables database a neuronal network is trained. The trained network is a search model and by interrogation, we can find out the value for variable that interest us to know, *v1*– operation cost. Then, the same steps will be followed but comparing the column 10 that has values for variable *v9* – time of welding operation with the other columns. It will result a cluster of variables, which becomes the pair (*v3*, *v4*, *v6*). Trained network is a search model and by interrogation, we can find out the value for variable that interest us to know, *v1*– operation time. Knowing the cost, time, asset and price gained through negotiation with the client for welding operation, is calculated the Earning Power for welding operation with relation (1). Asset's estimation is not difficult because in the balance sheet there is enough accurate and updated information. We obtained a curve of EP variation depending on rate of welding considered as control parameter for welding process (Fig. 3).

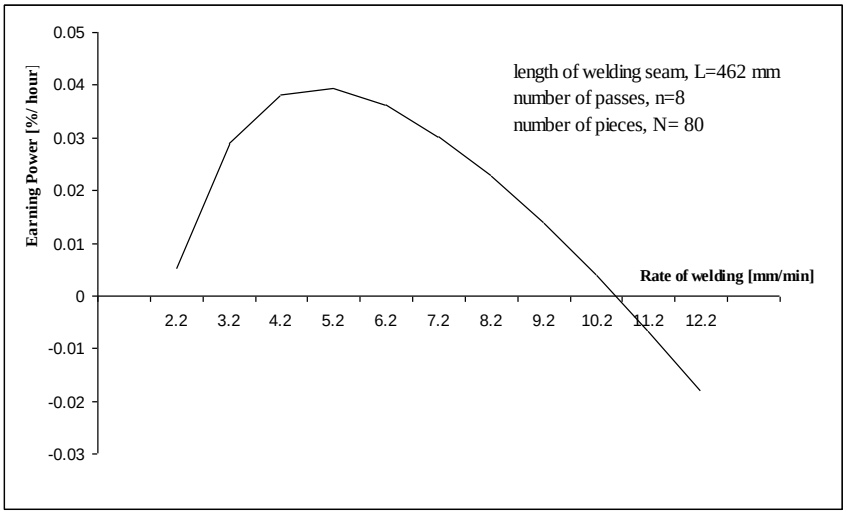

FIG. 3. THE VARIATION OF THE EARNING POWER DEPENDING ON RATE OF WELDING

After analyzing the diagram from Fig. 3, we can emphasize that there is a maximum value for EP for a certain rate of welding, optimal rate of welding. Therefore, when we are welding, the rate of welding can be adjusted so that the efficiency of operation becomes maximum and the economical effect on company will be maximum too. It is made a control of welding operation.

2.3 Data mining technique

Drilling operation for job 2 will be modeled by data mining technique. We will be using a computer program named Visual FoxPro and C++ that needs the mathematical library called MatLab. For start we'll take a random sequence from drilling operation database (Table 2), where we can find the notations *vi*, with *i=1,...,10*.

TABLE 2
SEQUENCE FROM TABLE WITH DRILLING OPERATION VARIABLES

Item Nr.	Material type	Hole diameter [mm]	Nr. of holes	Drilling speed [mm/s]	Drilling feed[mm/s]	Nr. of pieces	Drilling time [s]	Energy consumption [KW/h]	Operation cost [Euro]	Waste quantity [Kg]
-	v1	v2	v3	v4	v5	v6	v7	v8	v9	v10
6	OL 37	17.55	8	3.2	0.75	77	2459	13.17	158.10	75.89
14	OL 37	28.6	6	3.2	0.45	65	2410	29.53	265.8	127.60
31	OL 37	32.6	7	5.1	0.2	70	4011	41.32	433.9	208.30

Consider that customer's requirements are: v1=OL 37; v2=21; v3=6; v6=82. At the operational level, the variables clustering is based on facility "best model" provided by the technique of neuronal networks applied on experimental data set. After using the software, our variables, time and cost: v7 and v9, necessary to calculate the EP for drilling operation are dependent on the following variables: v7=(v2, v4, v5) ; v9=(v2, v3, v4).

For the state clustering those lines for which the common distance will be minimal will be chosen from the database. A set of data will be selected, data that are close to customer's demands and thus, the mathematical model will be linear, resulting mathematical models for time and cost during drilling operation:

$$\begin{aligned} v7 &= a_0 + a_1 v2 + a_2 v4 + a_3 v5 \\ v9 &= b_0 + b_1 v2 + b_2 v3 + b_3 v4 \end{aligned} \tag{9}$$

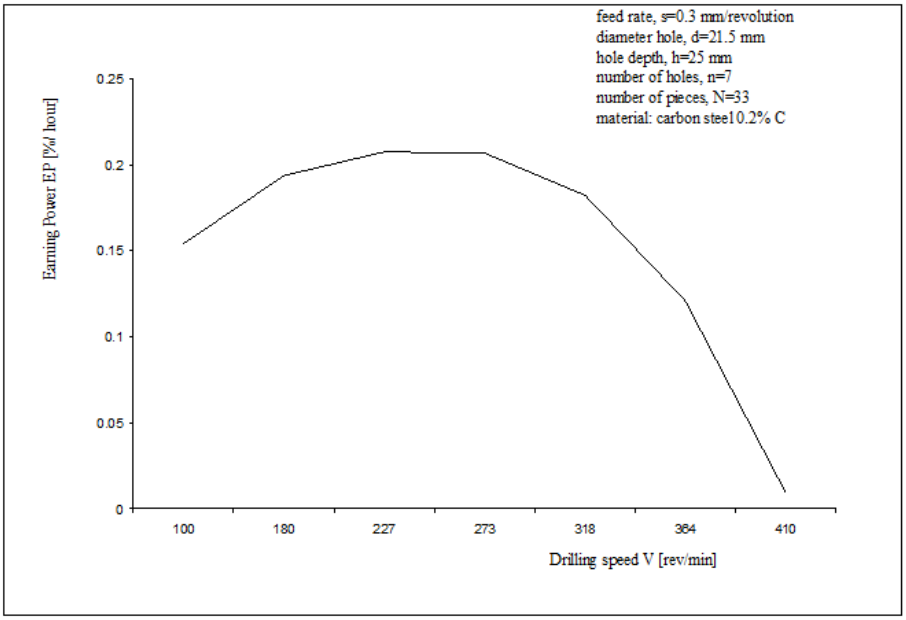

FIG. 4. THE VARIATION OF THE EARNING POWER DEPENDING ON DRILLING SPEED

Having the first four states, k=4, according to algorithm k-NN (Near Neighbour) will be obtained a system mathematic for cost and time. Solving the systems solutions will be obtained for determining the coefficient of the mathematical model. Linear models obtained for the cost and time are local models because they are valid only near the state are queried. They are also ephemeral because after interrogation they are abandoned. The method is very efficient because a mathematical model is built for each input series. Moreover, after practical checking the solution resulted during negotiations with customer, this model will be added in the table with initial experimental data, enriching the database by one new experience.

Taking the drilling speed, *v*, as a control parameter for the entire process, we represented the EP variation graphically depending on *v* (Fig. 4).It can be noted that when turning and welding operations as well as for the drilling operation, EP has a maximum value for a certain speed value, i.e. for optimal speed. In case of drilling operation, optimal speed is *v=227 rev/min*.

III. CONCLUSION

The three operations comprising the order were modeled by means of different techniques: turning by analytical method, drilling by data mining technique, and welding by neural network technique. By the three methods there was determined the value of a maximal EP resulting the optimal value of the process parameter, i.e. speed. Thus, for turning operation EP decreases by 34%, for a number of 5 pieces, if *v=100* m/min to the case when we work with $v=v_{optimal}$=50m/min. For drilling operation, if work speed is *v=100* rev/min EP decreases by 1.3 times to the case when the optimal work speed is, *v=227* rev/min. For welding operation, if the process is performed at the speed *v=2.2* mm/s then the value of EP will decrease 78 times to the case when $v=v_{optimal}$ =5.2mm/s. It follows that, for an operation, the optimal operation control can be made by knowing the maximal EP.

Depending on the maximum value of the order EP, the manager can decide whether to perform all operations to accomplish the job within the company or not. The manager can choose to outsource those operations that EP does not have a positive effect.

REFERENCES

[1] Niazi, A., Dai, J., Balabani, S., & Seneviratne, L., "Product cost estimation: Technique classification and methodology review", Journal of Manufacturing Science Engineering,128(2), 2006, pp.563–575.

[2] E. Shehab and H. Abdalla, "An Intelligent Knowledge-Based System for Product Cost Modelling", Int J Adv Manuf Technol 19, 2002, pp.49–65.

Analysis of Scheduling Models Applicable in Referral Health Systems

Joshua Agola[1], George Raburu[2]

Department of Computer science and Software Engineering, Jaramogi Oginga Odinga University of Science and Technology, P.O. Box 210 Bondo 40601 Kenya

Abstract— *Scheduling patient referrals is one of the most important administrative responsibilities performed in the medical office. A referral scheduling algorithm can be a useful tool in the hands of a primary provider. Primary providers are lacking knowledge regarding the care and treatment of chronic diseases and are not familiar with the current status of available resources (consultant doctors) for patient referrals. During patient referral there is a need to know of the availability of the consultant doctor and his/her status in terms of the patient workload. Referring a patient to a doctor with many patients on the waiting queue might delay the treatment. This can results in "added healing time, pain, and even death. This paper investigates the scheduling models applicable in referral health systems and hence proposes a suitable scheduling optimization model.*

Keywords— Dynamic, Static, Scheduling, Referral, Model.

I. INTRODUCTION

The main objective of scheduling is an efficient allocation of shared resources over time to competing activities. Emphasis has been on investigating machine scheduling problems where jobs represent activities and machines represent resources. The problem is not only NP-hard, but also has a well-earned reputation of being one of the most computationally difficult combinatorial optimization problems considered to date. This intractability is one of the reasons why the problem has been so widely studied.

The problem of scheduling is concerned with searching for optimal (or near-optimal) schedules subject to a number of constraints. A variety of approaches have been developed to solve the problem of scheduling

Scheduling patient referrals is one of the most important administrative responsibilities performed in the medical office. A referral scheduling algorithm can be a useful tool in the hands of a primary provider.

Primary providers are lacking knowledge regarding the care and treatment of chronic diseases and are not familiar with the current status of available resources (consultant doctors) for patient referrals. During patient referral there is a need to know of the availability of the consultant doctor and his/her status in terms of the patient workload. Referring a patient to a doctor with many patients on the waiting queue might delay the treatment. This can results in "added healing time, pain, and even death (Arntson, 2011).

According to a Baseline Study on the Functionality of the Health Referral System conducted between June and July 2013 in eight counties: Garissa, Kakamega, Kilifi, Kirinyaga, Machakos, Nairobi, Nakuru, and Siaya, indicates that the health referral system in Kenya is less than optimal by 60% and the system needs immediate strengthening. (MoH – Kenya, 2014).

II. LITERATURE REVIEW

2.1 Health referral systems

According to (Mehrotra, Christopher, & Caroline, 2011), the current state of the specialty-referral process in the United States provides substantial opportunities for improvement, as there are break downs and inefficiencies in all its components. Despite the frequency of referrals and the importance of the specialty-referral process, the process itself has been a long-standing source of frustration among both primary care physicians (PCPs) and specialists

In England, the implementation of the NHS e- Referral is still undergoing. According to (A Vision for new patient electronic referral service, 2013, June 12) there is a need for a new, re invigorated Vision for an NHS e-Referral Service, which supports a paperless NHS.

The current healthcare system in Scotland does not manage referrals from Primary to Secondary care in the best way possible. There is a need for a framework to help plan and deliver this change. (Patient Pathway management & Referral Facilitation, (2007, March 19))

The current state of health information systems in Phillippines: The national and local health information systems are poorly integrated and are weakly governed (Alberto et al., 2011). These negative conditions create information gaps at the national and local levels.

Armenia's overall healthcare referral system is not well structured: it does not clearly delineate functions, reporting or referral patterns nor does it address instances where the patient should be referred with certain conditions. Providers in Armenia are frustrated with the lack of communication between referral facilities, mainly in regards to the lack of referral and counter referral systems. (Gohar & Karina, 2009).

The Johns Hopkins University and the Basic Support for Institutionalizing Child Survival (BASICS II) Project conducted a study in Imbabura, Ecuador from September 1999 to April 2000 looking at barriers and constraints to referral in a province with 100% IMCI (Integrated Management of childhood illness) coverage. They looked at demographics and socio economic status, family dynamics, caregivers' perceived problems, access, and health system-caretaker interaction. This study found that health worker behavior, namely providing a written referral slip and counseling the caretaker to "immediately seek referral care," was the most important factor in predicting accessed referral. In addition, risk factors of needing to stay overnight and particularly with a child less than two months of age, interaction with each other were important constraints to compliance with referral. Transportation costs and households in which the mother was not the decision-maker were also important factors (Kalter, Salgado, Moulton, Nieto, Contreras, Egas, & Black, 2003)

A referral assessment in Eritrea found that only 38% of referrals found through record review made it to the next level of care (Cervantes, Salgado, Choi, &Kalter, 2003). Very little is known about what happens to severely ill children who do not comply with referral. Among a sample of 81 caretakers in Nepal who were told to seek care at the nearest health facility, but who chose not to do so, 77 sought care at alternative sources, primarily medical shops (75%) and hospitals (22%). The majority (53%) felt that better care was available elsewhere, and 65% felt the recommended facility was too far, closed, or would not have medicine available.

In South Africa, the Government has developed a framework to unify fragmented health services at all levels into a comprehensive and integrated National Health Services (NHS). To achieve the goal, there is a need to reorganize the health care system based on primary health care services, with effective referral systems at the primary, secondary and tertiary care levels (Ministry of Health, South Africa, 2009)

(Atkinson, Ngwengwe, Ngulube, Harpham, & O'Connell,(1999)) study results revealed that in urban Zambia, where people sought care at hospital facilities, not for perceived improved quality services, but because they thought they were less costly and better stocked with drugs

A referral assessment in Ghana showed that with only one out of 34 (3%) caretakers interviewed in the referral sites having been referred. Of the children admitted into the inpatient ward, only 11% had been referred to the hospital (BASICS II and the Ghana Health Service, 2003).

A study in Tanzania where Integrated Management of Childhood Illness (IMCI) strategy was being implemented showed that 91% of sick children and 75% of admissions at the referral hospital came from within a 10-kilometer radius. Only 235 out of the 7,989 children (3%) had been referred to the hospital and the referrals that arrived at the hospital, almost half (48%) delayed by two or more days (Font, Quinto, Masanja, Nathan, Ascaso, Menendez, Tanner, Schellenberg, & Alonso, 2002).

A study in Uganda showed that while health workers perceived that a majority (64%) of children referred complied, the reality was that only 28% actually accessed referral care. Health workers also perceived cost and the availability of transport as the main barriers, although in reality the cost of medical care at the referral hospital was the principal constraint for caretaker's not accessing referral (Ministry of Health Uganda, 2012.).

According to Malgo (2015) research carried out in Uganda on the understanding of the relationship between the state of the referral system and the final delivery of quality care found that the functionality of the referral system changes the level of quality care in the same direction; if the functionality is improved, the quality of care will improve as well.

Baseline Study on the Functionality of the Health Referral System conducted between June and July 2013 in eight counties: Garissa, Kakamega, Kilifi, Kirinyaga, Machakos, Nairobi, Nakuru, and Siaya, indicates that the health referral system in Kenya is less than optimal and the system needs immediate strengthening. (The Kenya Health Policy 2012–2030)

2.2 Scheduling models

Previous studies have used analytical and simulation models to explore in detail the scheduling of appointments for outpatient services (Cayirli &Veral, 2003). Applications of the simulation approach have included assessing the impact of alternative appointment schedules on waiting times in a specialty department (Harper & Gamlin, 2003), examining the capacity needed to reduce access times in outpatient departments (Elkhuizen, Das, Bakker, & Hontelez, 2007), evaluating scheduling rules in terms of physicians' idle time when the type of patient requesting an appointment at a later time is unknown (Klassen & Rohleder, 2004), comparing appointment systems for patients with different needs in a multi-facility internal medicine department (Wijewickrama & Takakuwa, 2008), and assessing the impact of operating conditions on the performance of rules for scheduling appointments (Ho & Lau, 1999). Other authors have described the use of computer simulation to support decision-making in outpatient clinics (Erdem et al., 2002), to improve utilization of resources, and to reduce physicians' overtime.

Other investigators have established that the length of time a patient has to wait between referral and consultation depends not only on the method for scheduling appointments and the number and type of referrals, but also on the availability of surgeons for appointments, as these physicians may have administrative, educational, or research commitments in addition to their clinical practices (Harper & Gamlin, 2003).

(Hadwan, Ayob, Sabar, & Qu, 2013) investigated how to minimize the penalty cost of a nurse schedule. (Aickelin and Dowsland, 2004) applied a genetic algorithm to solve the nurse shift schedule problem in hospitals with the aim to minimize the penalty cost for not fulfilling the preferences of the nursing staff. (Maenhout and Vanhoucke, 2013) studied the penalty costs with multiple constraints (including the nursing staff's preferences and some certain combinations of work shifts and days off). (Topaloglu and Selim ,2010) considered a variety of uncertain factors in nurse schedule to propose a fuzzy multi-objective integer programming model which takes into consideration the fuzziness of the objective and the nursing staff's preferences.

Ouelhadj & Petrovic (2009) did a survey research of dynamic scheduling in manufacturing systems. They found that a vast majority of the literature dealing with production scheduling has primarily been focused on finding optimal or near-optimal predictive (static) schedules for simple scheduling models with respect to various criteria assuming that all problem characteristics are known. Such predictive schedules are often produced in advance in order to direct production operations and to support other planning activities. Unfortunately, most manufacturing systems operate in dynamic environments subject to various real-time events, which may render the predictive optimal schedule neither feasible nor optimal. Therefore, dynamic scheduling is of great importance for the successful implementation of real-world scheduling systems.

Apurva, Ketan, & Dipti (2010) developed and simulated Dynamic scheduling for real-time distributed systems using ant colony optimization and found that the proposed algorithm is equally efficient during under-loaded conditions. The performance of Earliest Deadline First decreases as the load increases, but the proposed algorithm works well in overloaded conditions also. Because of this type of property, the proposed algorithm is more suitable for the situation when future workload of the system is unpredictable.

The study by (Liu et al., 2010) focuses on scheduling appointments within the same hospital and not outside. It does not consider expanding the supply to meet the demand

More specifically, the objective of this study is to develop dynamic scheduling algorithm model that explores a wider search space for specialist doctors hence increasing the supply to meet the demand in assigning an appointment date to each patient depending on the clinic's appointment schedule at the time of the patient's need and preferences during referral

Algorithms are used in many health care areas to help clarify treatment guidelines, promote best practices and as an attempt to help non-specialists to properly manage patients with wounds and make appropriate referrals when needed (Alsbjörn, Gilbert, Hartmann, Kaźmierski, Monstrey, Palao, Roberto,Van, & Voinchet, 2007). Wound care algorithms have been used extensively by the Agency for Healthcare and Quality, especially related to guidelines in the treatment of pressure ulcers.

The Veterans Administration podiatry service in Cleveland, Ohio, developed an algorithm to connect the elderly diabetic veteran population with podiatry services and medicine department to facilitate appropriate referral, admission, and management of diabetic foot ulcers (Robbins, Nicklas, & Sarah, 2006).

Whiting and Parnell, (2007) used a referral flowchart to visually describe how referrals are made to the wound care clinic. The referral flow, or algorithm, starts with the ambulant patient with wound acute/chronic/complex being directed to the wound clinic and being examined by wound care experts.

Gottrup (2003) describes the organization of a wound healing center in Denmark, where a multidisciplinary team treats patients with all types of wounds. He describes how referrals are made to the center and the possible treatment course with visual schematics of decision-making trees, or algorithms. This format clearly defines which possibilities the patient with a wound may see for treatment: private practitioner, which in turn refers to the multidisciplinary wound healing team; the multidisciplinary wound healing team directly; or the wound healing center

The use of a referral algorithm is one way to help ensure proper management of patients with wounds, including appropriate referral guidelines (Arntson, 2011)

From the literature, most of the algorithms used in referrals are just mere referral guideline steps in the form of flowcharts. These guideline steps are not able to deal with the emerging issues of constrained resources as well as resources that require mutual exclusion utilization.

2.3 The referral models

2.3.1 The Three Delays framework

The Three Delays framework (Thaddeus and Maine, 1994) is one of the most consulted model in respect of maternal and child health care. The framework is still useful today due to the unfortunate fact that emergency obstetric complications are still one of the largest causes for maternal and neonatal deaths. The framework explains maternal mortality in the context of emergency obstetric complications. This being a major cause for maternal deaths, the author tries to understand what happens in the time span before the eventual complication or death occurs. If a patient receives care on time, the outcome is mostly satisfactory. Therefore Thaddeus and Maine (1994) conclude that a delay in being treated is the biggest reason for maternal deaths. They identify three phases in the decision-making process which can all three lead to a delay in receiving the necessary care as shown in Fig 2.1.

Phase 1 Delay: Decision to seek care

Phase 2 Delay: Arriving at health facility

Phase 3 Delay: Provision of adequate care

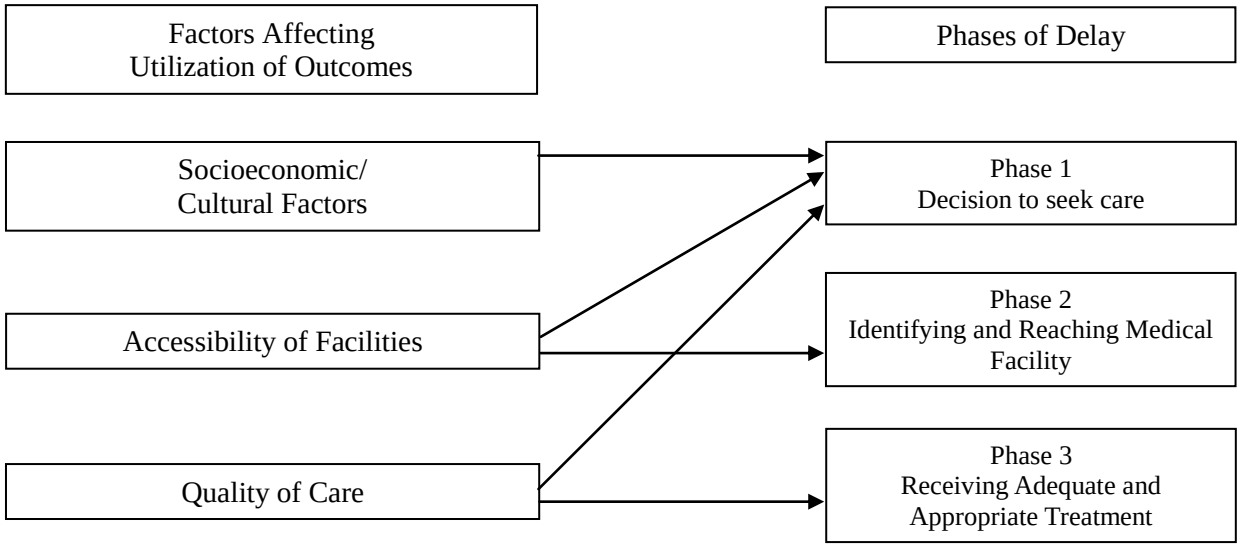

FIGURE 2.1: THREE DELAYS FRAMEWORK
Source: Thaddeus and Maine (1994:1093)

2.3.2 The Access model

(Peters, Garg, Bloom, Walker, Brieger,& Rahman, 2008) designed a conceptual model to assess the access to quality care along four dimensions (Fig. 2.2):

1. Geographic Accessibility (physical distance and possibilities to bridge that distance)

2. Availability (necessary care is present – (human) resources, location, time)

3. Acceptability (relation between social and cultural values of users and of providers)

4. Financial Accessibility (prices of services and the possibility/willingness of users to pay)

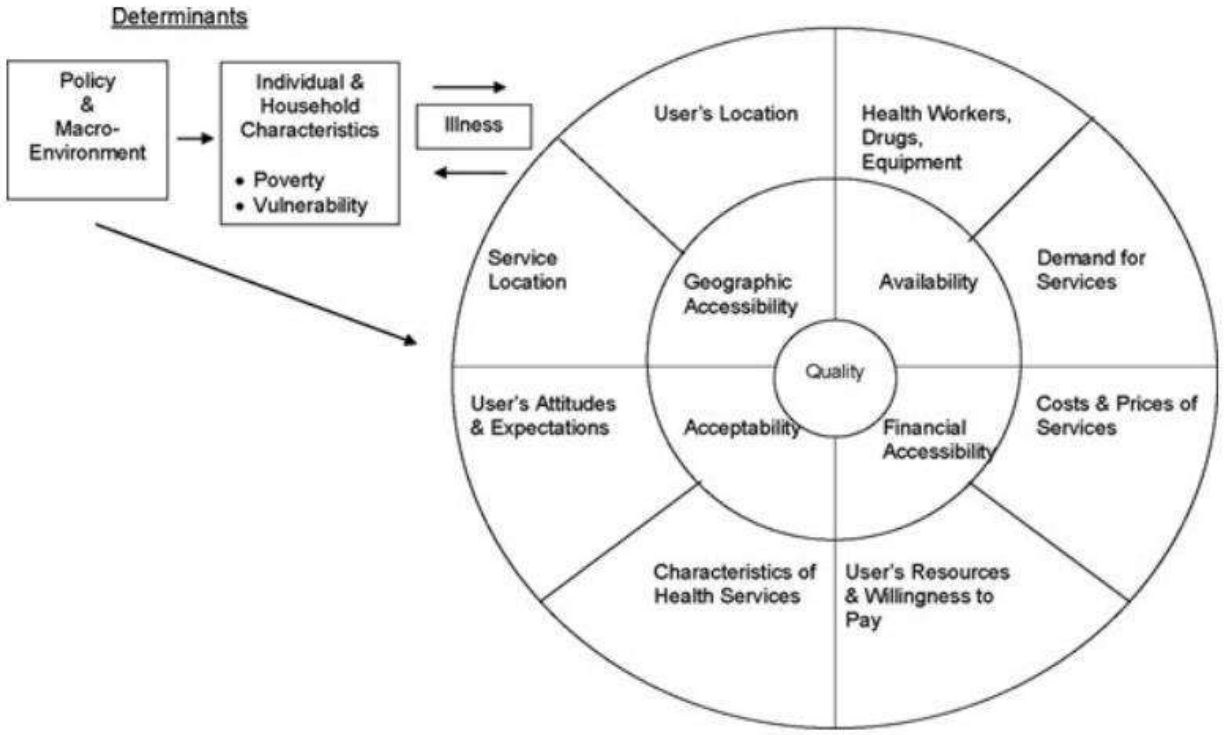

FIGURE 2.2: ACCESS MODEL
Source: Peters et al. (2008:162)

All four dimensions are individually influenced by a factor from the demand side and a factor from the supply side. The policy and macro environmental level and the individual and household level both influence the access to health services and the eventual delivery of overall quality care (Peters et al., 2008). Furthermore it is explained that the poverty level of an individual is an important determinant in establishing that person's health needs, which they describe as 'illnesses. So the level of illness interacts with the level of poverty.

The Access Model is developed in a similar line of thought as the Three Delays Model (Thaddeus and Maine, 1994) so they have some common ground. They both discuss if quality care is within reach for the care seeker and how this influences their decision-making and the eventual care delivery. The Access Model is however applicable to a wider variety of health contexts and does not only focus on maternal health. Also, the Access model tries to explain the relationship between poverty and access to health care, while the Three Delays Model tries to relate the high mortality rates to delays in receiving care.

III. DISCUSSION

Health referral systems are using static scheduling techniques to schedule patients to consultant doctors. Vast majority of the literature dealing with scheduling models have primarily focused on finding optimal or near-optimal predictive (static) schedules for simple scheduling models with respect to various criteria assuming that all problem characteristics are known. Such predictive schedules are often produced in advance in order to direct production operations and to support other planning activities. Unfortunately, most health referral systems operate in dynamic environments subject to various real-time events, which may render the predictive optimal schedule neither feasible nor optimal.

Though the two models (the three delay model and the access model) are both extensively used for analysis and cited in other researches. The models concentrate only on the external influencing factors to access of quality health care but not on how to balance the available resources towards quality health care access. The two models have not considered optimization of available resources which is a very important influencing factor in the referral system as a mean to quality health care access. For the referral system to be successful in delivering quality health care the available resources should be optimized besides influencing factors in the access. Therefore optimization of available resources is a requirement in quality health care delivery.

IV. CONCLUSION

The research proposes a dynamic scheduling optimization model for patient referral system. The model should take into account the influencing factors in the access model.

REFERENCES

[1] L. Arntson. Wound care referral algorithm. *Doctor of nursing practice systems change projects*, 2011.

[2] Ministry of Health Kenya. The Kenya Health Policy, 2014–2030: *Towards attaining the highest standard of health*, 2014.

[3] A. Mehrotra, B.F. Chritoper, and Y.Caroline, Dropping the baton: specialty referrals in the United States. *A multidisciplinary journal of population health and health policy*, 89(1), 2012, 39-68.

[4] Patient Pathway management & Referral facilitation, 2007.

[5] P. Gohar, and B. Karina. *Armenian mertanal and child health referral system study for the United States Agency for International Development, 2*009.

[6] H. D. Kalter, R.Salgado, L.H. Moulton, Nieto, A. Contreras, M.L. Egas, and R.E. Black. Factors constraining adherence to referral advice for severely ill children managed by the Integrated Management of Childhood Illness approach in Imbabura province, Ecuador. 92(1), 2003, 103–110.

[7] K. Cervantes, R. Salgado, M. Choi, and H.D. Kalter. The status of referral in Eritrea: Analysis of referral pathways in children under five. *A guide for Programme Manager*. 2003.

[8] Ministry of Health (South Africa).*White paper for the transformation of the health system in South Africa*, 2009.

[9] S. Atkinson, A. Ngwengwe, M. Macwan'gi, T. J. Ngulube, T. Harpham, and A. O'Connell. The referral process and urban health care in sub-Saharan Africa: the case of Lusaka, Zambia. *Journal of Social science and medicine*, 49(1), 1999, 27-38.

[10] Basics II and the Ghana health service. *The status of referrals in three districts in Ghana: Analysis of referral pathways for children under five years. Virginia, Arlington*, 2003.

[11] F. Font, L. Quinto, H. Masanja, R. Nathan, C. Ascaso, C. Menendez, M. Tanner, J. A. Schellenberg, and P. Alonso. Paediatric referrals in rural Tanzania: the Kilombero District Study – a case series. *Journal of BMC International Health and Human Rights*, 2(4), 2002.

[12] Ministry of Health - Uganda. *Uganda Health System Assessment 2011*, 2012.

[13] A. Malgo. *The state of the referral system and how this influences maternal healthcare in the Kabarole district, Uganda: A playground for inequality and corruption*. MSc Thesis, 2015.

[14] T. Cayirli and E. Veral. Outpatient scheduling health care: A review of literature. *The journal of Production and Operations Management.* 12(4), 2003, 519 – 549.

[15] P. R. Harper and H. M. Gamlin. Reduced outpatient waiting times with improved appointment scheduling: a simulation modelling approach. *The journal of OR Spectrum*, 25(2), 2003, 207 – 222.

[16] S. G. Elkhuizen, S. F. Das, P. J. M. Bakker, and J. A. M. Hontelez. Using computer simulation to reduce access time for outpatient departments. *Journal of Quality and safety in health care*, 16(5), 2007, 382-386.

[17] K. J. Klassen and T. R. Rohleder .Outpatient appointment scheduling with urgent clients in a dynamic, multi-period environment. *International Journal of Service Industry Management*, 15(2), 2004, 167-186.

[18] A. Wijewickrama and S.Takakuwa. *Outpatient appointment scheduling in a multifacility system*, 2008.

[19] C. Ho and H. Lau. Evaluating the impact of operating conditions on the performance of appointment scheduling rules in service systems. *European Journal of Operational Research*, 112(3), 1999, 542-553

[20] H. I. Erdem , T. Demirel and S. Onut. An efficient appointment system design for outpatient clinic using computer simulation. *The Proceedings of the 2002 Summer Computer Simulation Conference*, 299-304.

[21] P. R. Harper and H. M. Gamlin. Reduced outpatient waiting times with improved appointment scheduling: a simulation modelling approach. *The journal of OR Spectrum*, 25(2), 2003, 207 – 222.

[22] M. Hadwan, M. Ayob, N. R. Sabar and R. Qu. A harmony search algorithm for nurse rostering problems. *Journal of Information Sciences*, 233(6), 2013, 126–140.

[23] B. Maenhout and M. Vanhoucke. An integrated nurse staffing and scheduling analysis for loner-term nursing staff allocation problems. *Journal of Omega*, 40(2), 2013, 485–499.

[24] S. Topaloglu and H. Selim. *Nurse scheduling using fuzzy modeling approach. Fuzzy sets and systems*, 161(11), 2010, 1543-1563.

[25] D. Ouelhadj and S. Petrovic. Survey of dynamic scheduling in manufacturing systems. *Journal of Scheduling*, 12(4), 2009, 417-431.

[26] S. Apurva, K. Ketan and S. Dipti. Dynamic scheduling for real-time distributed systems using ant colony optimization. *International Journal of Intelligent Computing and Cybernetics*, 3(2), 2010, 279-292.

[27] N. Liu, S. Ziya and V. G. Kulkarni. Dynamic Scheduling of Outpatient Appointments Under Patient No-Shows and Cancellations. *Journal of Manufacturing & Service Operations Management*, 12, 2010, 347-364.

[28] J. Robbins, J. B. Nicklas and A. Sarah. Reducing the rate of amputations in acute diabetic foot infections. *Cleveland Clinic journal of medicine*. 73, 2006, 679-83.

[29] L. Whiting and C. Parnell. Developing wound care clinics: *Journal of Primary Healthcare*, 17(4), 2007, 26-27.

[30] F. Gottrup. Organization of wound healing services: the Danish experience and the importance of surgery. *Journal of Wound repair and regeneration*, 11(6), 2003, 452-7.

[31] L. Arntson. Wound care referral algorithm. *Doctor of nursing practice systems change projects*, 2011.

[32] S. Thaddeus and D. Maine. Too far to walk: Maternal mortality in context. *Journal of Social science and medicine,* 38(8), 1994, 1091 – 110.

[33] D. H. Peters, A. Garg, G. Bloom, D. G. Walker, W.R. Brieger and M. H. Rahman. Poverty and access to health care in developing countries. *Journal of Annals of the New York Academy of Sciences*, 1136, 2008, 161–71.

Effect of Base Isolation in Multistoried RC Regular and Irregular Building using Time History Analysis

Omkar Sonawane[1], Swapnil B. Walzade[2]

[1]PG. Student, Department of Civil engineering, Trinity College of engineering and research, yevalewadi, pune
[2]Assistant Professor, Department of Civil engineering, Trinity College of engineering and research, yevalewadi, pune.

Abstract— *Base isolation (BI) is a technique that has been used around the world to protect the building structures from the damaging effects of earthquake. The installation of isolator in building at base level considerably increases the time period of the structure, which means it reduces the possibility of resonance of the structure giving rise to better seismic performance of the building. The analysis is performed to compare the effectiveness of base isolation in regular and irregular multi-storied RC frame building. For this study, 15 storied R.C frame building has been considered and Time History analysis is carried out using ETABS software version 2013. The Lead Rubber Bearing (LRB) is designed by considering the maximum gravity load coming on the column at the base and the same has been used for analysis. The results obtained from the analysis are compared in terms of time period, base shear, story displacement and story acceleration. Time period for the base isolated structures are higher than that of the fixed base structure. Due to the presence of isolator, base shear and story acceleration are significantly reduced in each direction (X and Y direction) as compared to fixed base building. When compared to base isolated regular building the plan irregular (re-entrant corner) and vertical irregular (vertical geometric irregular) base isolated building gives better performance.*

Keywords— Base Isolation, Time History Analysis, lead rubber Bearing, UBC 97 code, ETABS 2013, Base shear.

I. INTRODUCTION

An earthquake is a sudden and transient motion of the earth's surface. According to geologists, the earth has suffered earthquakes for hundreds of millions of years, even before humans came into existence. Because of the randomness, the lack of visible causes, and their power of destructiveness, ancient civilizations believed earthquakes to be supernatural phenomena – the curse of God. In terms of the geological time scale, it is only recently (the middle of seventeenth century) that an earthquake has been viewed as a natural phenomenon driven by the processes of the earth as a planet. Thus subsequent work, especially in nineteenth century, led to tremendous progress on the instrumental side for the measurement of earthquake data. Seismological data from many earthquakes were collected and analyzed to map and understand the phenomena of earthquakes [1]. Causes of earthquakes: Movement of the tectonic plates relative to each other, both in direction and magnitude, leads to an accumulation of strain, both at the plate boundaries and inside the plates. This strain energy is the elastic energy that is stored due to the straining of rocks, as for elastic materials. When the strain reaches its limiting value along a weak region or at existing faults or at plate boundaries, a sudden movement or slip occurs releasing the accumulated strain energy. The action generates elastic waves within the rock mass, which propagate through the elastic medium, and eventually reaches the surface of the earth. Most earthquakes are produced due to slips at the faults or at the plate boundaries [1]. In most earthquakes, the collapse of structures like houses, schools, hospitals, historic and public buildings results in the widespread loss of lives and damage. Earthquakes also destroy public infrastructure like roads, dams and bridges, as well as public utilities like power and water supply installations. Past earthquake shows that over 95% of the lives were lost due to the collapse of buildings that were not due to earthquake. Though there are building codes and other regulations which make it mandatory that all structures in earthquake-prone areas in the country must be built in accordance with earthquake-resistant construction techniques, new constructions often overlook strict compliance to such regulations and building codes. A large number of buildings in India have been constructed without due consideration to earthquake loads. Further, the earthquake loads are also under continual revision in successive revisions of codes. Buildings also deteriorate with time and get damaged due to earthquake, flood, fire, blast, etc. All these circumstances require evaluation and retrofitting of existing building. From the past earthquake it was observed that, during earthquake most of the buildings were collapsed due to their irregular configuration in plan and elevation. In regular building earthquake force will be transfer uniformly from bottom to top of the building but in irregular

building it distribute non-uniformly throughout the building. In traditional earthquake design it is compulsory that structure should have regular configuration. Base isolation is a recent and new earthquake resistance technology; in this system earthquake force induced to the structure is reduced at base level of the structure and avoids the transfer of load to the super structure. So that any type of building configuration can be constructed over the isolation system. For the present work regular and irregular buildings have been taken to study their performance using isolation system and without using isolation system during an earthquake.

1.1 Structural irregularities

In the past, several major earthquakes have exposed the shortcomings in buildings, which lead to damage or collapse. It has been found that regular shaped buildings perform better during earthquakes. The structural irregularities cause non-uniform load distribution in various members of a building. There are various types of irregularities in the buildings; they are divided into two groups, plan irregularities and vertical irregularities.

Plan irregularity: It comprises following types of irregularities

1. Torsion irregularity
2. Re-entrant Corners
3. Diaphragm Discontinuity
4. Non parallel Systems

Vertical irregularity: It comprises following type of irregularities

1. Stiffness Irregularity
2. Mass Irregularity
3. Vertical Geometric Irregularity
4. In Plane discontinuity in vertical elements resisting lateral force
5. Discontinuity in capacity-weak story

In this study, regular, plan irregular (Re-entrant corners) and vertical irregular (Vertical Geometric Irregularity) buildings are considered for the isolated and non-isolated buildings.

1.2 Base Isolation

The isolation technique decouples the structure from the horizontal components of the ground motion by interposing structural element with low horizontal stiffness between the structure and the foundation. This gives the structure a fundamental frequency that is much lower than its fixed base frequency of the ground motion. The first dynamic mode of isolated structure involves deformation only in the isolation system, the structure above being to all intents and purposes rigid. The higher modes that produce deformation in the structure are orthogonal to the first mode and, consequently, to the ground motion. These higher modes do not participate in the motion, so that the high energy in the ground motion at these higher frequencies cannot be transmitted into the structure [4].

1.3 Objectives of the work

1. To compare the response of the building such as base shear, time period, displacement and acceleration with and without base isolation. Following are the different types of building for the earthquake analysis.

   a. 15 storied RC regular building.

   b. 15 storied RC plan irregular building.

   c. 15 storied RC *vertical irregular building.*

2. To find out the response of buildings with and without base isolation by considering the time history analysis using Bhuj earthquake data.

3. To design the lead rubber bearing using UBC 97 code.

II. LITERATURE REVIEW

Abrishambaf and G. Ozay [2010] [6], has briefly described the "Effects of isolation damping and stiffness on the seismic behavior of structures". In this paper his intention was to study the earthquake performance and optimization of bearing by considering 3,6, and 9 storied seismic isolated building using LRB, high damping and friction pendulum system bearing. The parameters like acceleration, maximum displacement and seismic coefficient was compared with fixed base and base isolated structure. The results concluded that LRB represents minimum seismic coefficient, acceleration and maximum displacement compared to friction pendulum and high damping rubber bearing.

Athamnia Brahim and Ounis Abdelhafid [2011] [7], has been studied "Effects of seismic isolation in the reduction of the seismic response of the Structure" by considering the 8 story plan irregular building using lead Rubber bearing. A nonlinear time history analysis was carried out using ETABS version 9.7.0 software. The results obtained concluded that lead rubber bearing minimizes the seismic response of the building

Mehmet Komur et. al. [2011] [8], for his study he was considered fixed-base and base isolated 4 and 8 storey reinforced concrete buildings. The LRB was taken as an isolation system. In base-isolated buildings large reduction is detected in base shear, acceleration values, and relative storey displacements as compared to fixed base buildings. In addition to this, the displacements and time period of isolated buildings are increased when compared with non-isolated buildings.

Shirule P.A. et. al. [2012] [9], used an 18-storey symmetrical R.C.C. building as a test model. Lead Rubber Bearing (LRB) and Friction Bearing (FB) was used as isolation system in this study. Nonlinear Time history analysis was used on both of fixed base and base isolated buildings. There are two portions; one is comparative study of performance of fixed base condition and base isolation (LRB and FB) condition and the comparative study of performance by three different time histories Bhuj, Koyana and Lacc T.H. Finally, base shear, displacement and acceleration are compared from 3 times histories analysis between fixed base condition and base isolated condition. The base shears in each direction are decreased with LRB by 46 % and with FB by 35% in base-isolated building compared to the fixed base building.

III. BASE ISOLATION

3.1 Introduction

A large proportion of the world's population lives in region of seismic hazard, at risk from earthquake of varying severity and varying frequency of occurrence. Earthquake cause significant loss of life and damage to property every year. Various a seismic construction designs and technologies have been developed over the years in attempts to mitigate the effect of earthquakes on buildings, bridges and potentially vulnerable contents. Seismic isolation is relatively recent and evolving technology of this kind. Seismic isolation consists essentially of the installation of mechanism which decouples the structure, or its contents, from potentially damaging earthquake-induced ground, or support, motions. This decoupling is achieved by increasing the flexibility of the system, together with providing appropriate damping. In many, but not all, applications the seismic isolation system is mounted beneath the structure and is referred to as "BASE ISOLATION".

Isolation may often reduce the cost of providing a given level of earthquake resistance. The New Zealand approach has been to design for some increase in earthquake resistance, together with some cost reduction, a typical target being a reduction by 5% of the structural cost.

3.2 Types of base isolators

The most common types of base isolators used in buildings are:

a. Elastomeric rubber bearing.

b. High damping rubber bearing.

c. Lead rubber bearing.

d. Friction pendulum system bearing

IV. RESULTS

4.1 Time period

Comparison of time period for different models.

TABLE 1
TIME PERIOD FOR DIFFERENT MODELS

No. of modes	Time period (sec)					
	Model 1A	Model 1B	Model 2A	Model 2B	Model 3A	Model 3B
1	3.10	3.94	3.09	3.94	2.83	3.68
2	3.03	3.87	2.97	3.82	2.49	3.38
3	2.78	3.62	2.84	3.69	1.84	2.85
4	1.01	1.25	1.00	1.25	0.95	1.18
5	0.97	1.20	0.95	1.18	0.94	1.17
6	0.91	1.13	0.92	1.16	0.82	0.97
7	0.58	0.68	0.57	0.67	0.55	0.66
8	0.54	0.65	0.52	0.64	0.54	0.65
9	0.52	0.62	0.52	0.62	0.50	0.61
10	0.40	0.46	0.39	0.45	0.40	0.44
11	0.36	0.42	0.35	0.41	0.36	0.43
12	0.35	0.41	0.34	0.41	0.36	0.41

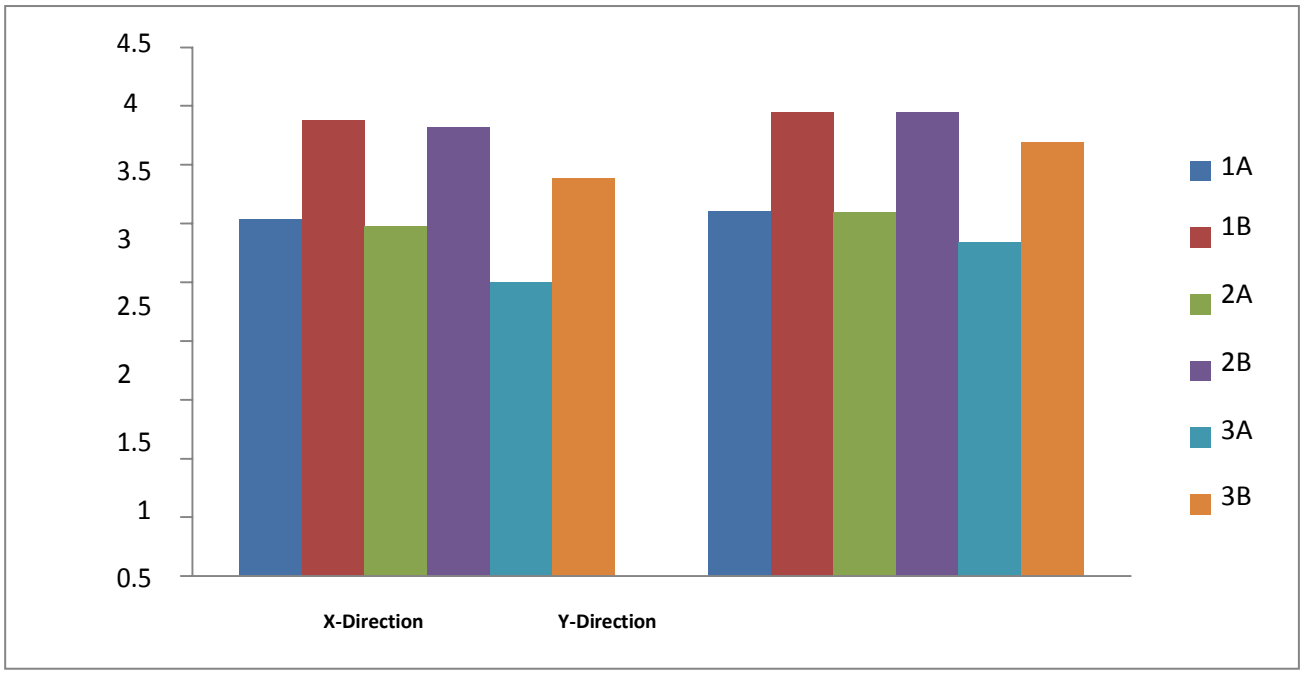

FIG. 1: TIME PERIOD FOR DIFFERENT MODELS

From the figure 1, it is observed that, time period decreases with increase in mode number. As result of the increased flexibility of the system, natural period of the structure is also increases. This shows flexibility is directly proportional to natural period.

TABLE 2
TIME PERIOD FOR DIFFERENT MODELS CONSIDERING FIRST THREE MODES

Models	Time period (sec)		
	X-X direction	Y-Y direction	Torsion
1A	3.03	3.10	2.78
1B	3.87	3.94	3.62
2A	2.97	3.09	2.84
2B	3.82	3.94	3.69
3A	2.49	2.83	1.84
3B	3.38	3.68	2.85

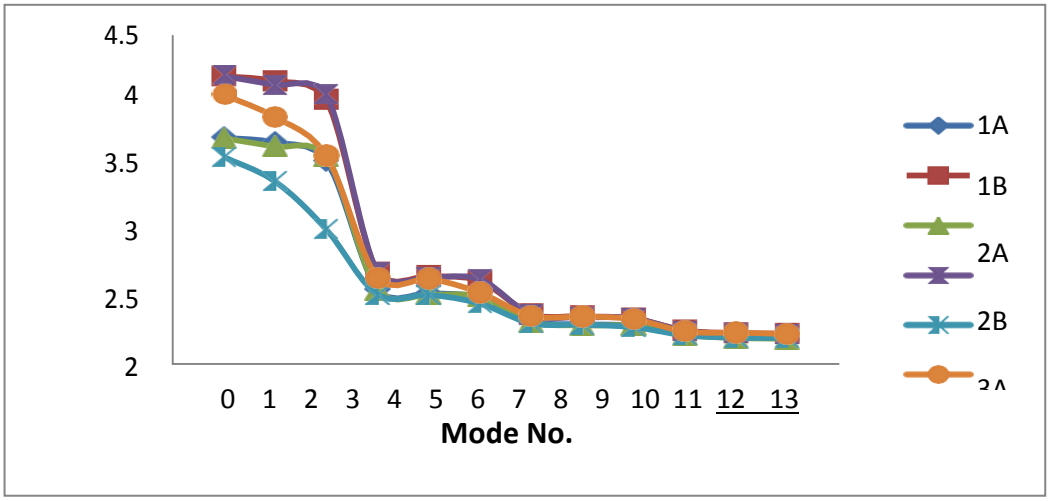

FIG. 2: TIME PERIOD FOR DIFFERENT MODELS ALONG X AND Y DIRECTION

Figure 2, shows that, in the modal analysis the time period of the structure is found to be 3.10sec, in Y-direction and the time period as 3.03sec, in X-direction for model 1A (Regular building with fixed base).

The time period of the structure is found to be 3.94sec and 3.87sec in Y and X direction respectively for model 1B (Regular building with base isolation). The time period in model 1B is 27% more than the model 1A both in Y and X direction.

The time period of the structure is found to be 3.09sec, in Y-direction and the time period as 2.97sec, in X-direction for model 2A (Plan irregular building with fixed base).

The time period of the structure is found to be 3.94sec and 3.82sec in Y and X direction respectively for model 2B (Plan irregular building with base isolation). The time period in model 2B is 27% more in Y and 28% more in X-direction than the model 2A. The time period of the structure is found to be 2.83sec, in Y-direction and the time period as 2.49sec, in X-direction for model 3A.

The time period of the structure is found to be 3.68sec and 3.38sec in Y and X- direction respectively for model 3B (Vertical irregular building with base isolation). The time period in model 3B is 30% more in Y and 36% more in X-direction than the model 3A.

4.2 Base shear

4.2.1 Comparison of base shear for different models

TABLE 3
VARIATION OF BASE SHEAR (KN) ALONG X AND Y DIRECTION FOR DIFFERENT MODELS

Models	Base shear (kN)	
	X-direction	Y-direction
1A	4810.02	3753.21
1B	2680.25	2723.46
2A	3629.20	2793.13
2B	1988.94	1921.50
3A	5739.24	3596.05
3B	2312.51	2362.89

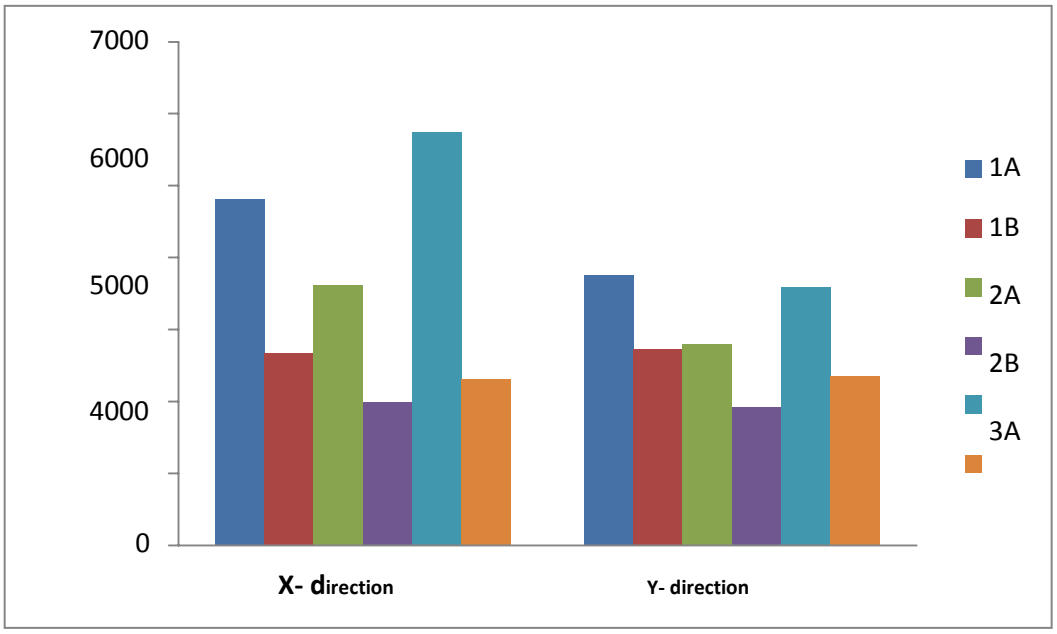

FIG. 3: BASE SHEAR (KN) ALONG X AND Y-DIRECTION

From the figure 3, it is observed that, the base shear in model 1B is decreases by 44% as compared to model 1A in X-direction.

The base shear in model 2B is decreases by 45% as compared to model 2A in X- direction. Similarly, it is decreases by 60% in model 3B as compared to model 3A in X- direction.

The base shear in Y-direction for model 1B, 2B and 3B are decreases by 27%, 31% and 35% as compared to model 1A, 2A and 3A respectively. This shows isolator gives better performance compared to fix base building.

4.2.2 Story displacement

➢ **Comparison of story displacement for different models.**

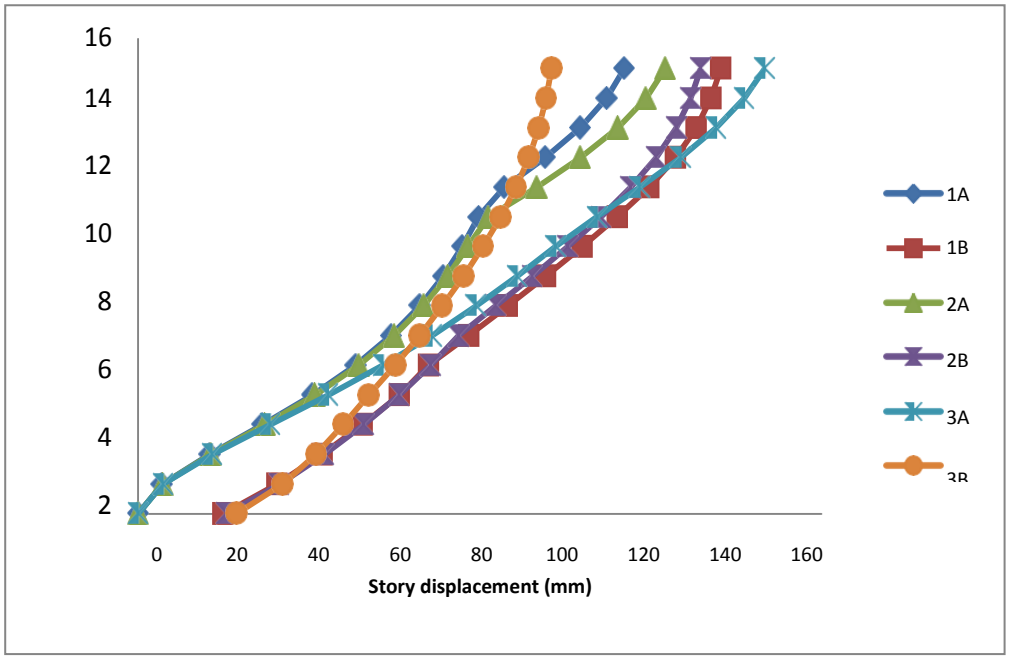

FIG. 4: STOREY DISPLACEMENT ALONG X-DIRECTION

TABLE 4
VARIATION OF STORY DISPLACEMENT (MM) ALONG X-DIRECTION FOR DIFFERENT MODELS

No. of Stories	Story displacement (mm)					
	Model 1A	Model 1B	Model 2A	Model 2B	Model 3A	Model 3B
15	113.8	136.4	123.4	131.7	146.7	96.8
14	109.7	134.1	118.9	129.4	141.9	95.5
13	103.5	130.7	112.3	126	135.3	93.8
12	95.3	125.8	103.5	121.3	127	91.5
11	85.7	119.6	93.3	115.3	117.4	88.5
10	79.7	112.2	82	108.4	107.4	84.9
9	75.9	104	77.2	100.6	97.7	80.8
8	71.4	95.4	72.4	92.3	88.7	76.2
7	65.9	86.5	66.8	83.7	79.1	71.2
6	59.2	77.4	60	75	68.8	65.9
5	50.9	68	51.6	68.5	57.3	60.2
4	40.8	61.2	41.4	61.1	44.5	54
3	29.1	52.5	29.6	52.8	30.9	48
2	16.8	43.1	17	43.6	17.4	41.7
1	5.6	32.5	5.7	33.1	5.8	33.8
0	0	19.9	0	20.6	0	23

TABLE 5
VARIATION OF STORY DISPLACEMENT (MM) ALONG Y-DIRECTION FOR DIFFERENT MODELS

No. of Stories	Story displacement (mm)					
	Model 1A	Model 1B	Model 2A	Model 2B	Model 3A	Model 3B
15	102.6	138.6	106.6	133.8	180.8	138.4
14	99.4	136.3	103	131.2	176.2	136.5
13	94	132.8	97.1	127.7	168.3	133.4
12	86.4	128	89	123	157	129.1
11	82.2	121.8	79.1	105	142.9	124.1
10	77.6	114.7	75	110.5	126.7	118.7
9	74.3	106.8	69.9	103.3	109.4	113.2
8	70.7	98.8	66.1	96	93.4	107.3
7	65.4	90.9	61.1	88.6	84.3	101.2
6	58.1	83	54.3	81	73.4	94.7
5	49.3	74.7	46	72.9	60.9	87.8
4	39.2	65.9	36.6	64.5	48.1	80.1
3	28.3	56.9	26.5	55.7	35.3	71.5
2	17.2	47.6	16.4	46.6	21.6	61.8
1	6.5	37.2	6.3	36.5	8.2	49.9
0	0	21.5	0	21	0	29.5

Figure 4 and 5 shows that, fixed base building have zero displacement at base of the building whereas in case of base isolated model appreciable amount of lateral displacement is observed at the base.

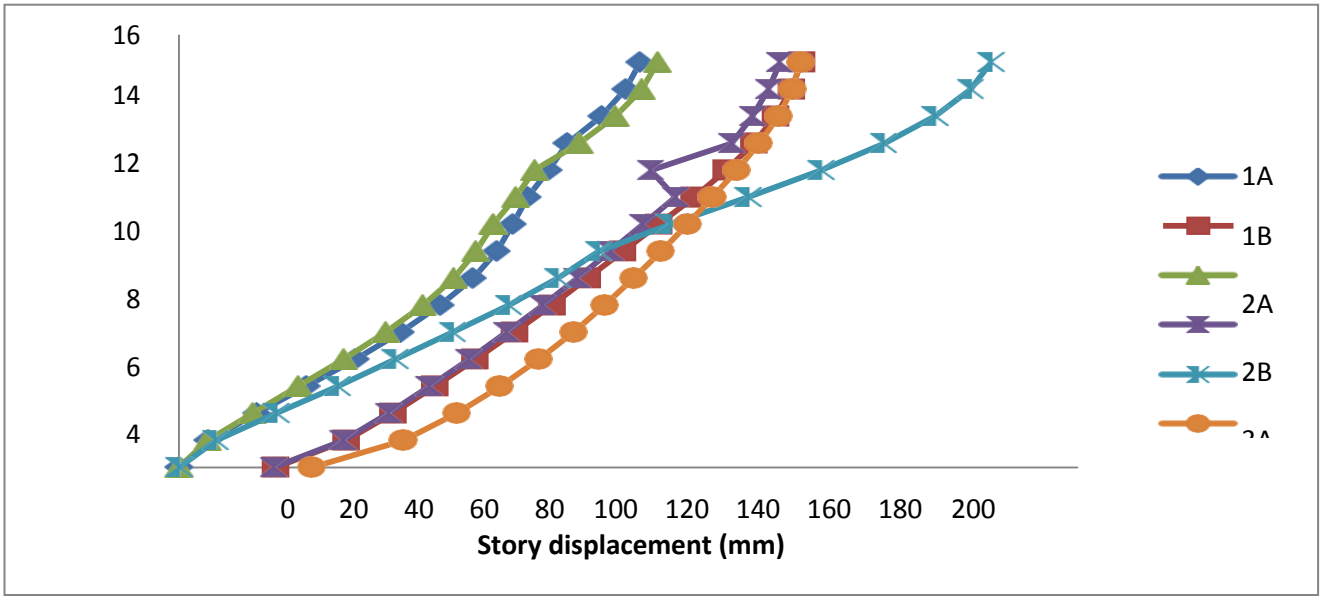

FIG. 5: STOREY DISPLACEMENT ALONG Y-DIRECTION

REFERENCES

[1] T.K. Datta (2010), "Seismic Analysis of Structures", Indian Institute of Technology Delhi, India.

[2] S.K. Sabu, H.S.Chore, S.B.Patil (2014), "Effectiveness of Lead Rubber Base Isolators, for seismic resistance of Buildings, supported on different soil stratas," ISSN (Online): 2347-2820, Volume -2.

[3] IS 1893 (part 1):2002, Criteria for earthquake resistant design of structures.

[4] Farzad Naeim and James M. Kelly (1999), "Design of seismic isolated structure", John Wiley and Sons, inc.Newyork.

[5] W.F. Chen and Charles Scawthorn (2003), "Earthquake Engineering Handbook" CRC press, Boca Raton London, New York, Washington.

[6] A. Abrishambaf and G. Ozay (2010), "Effects of isolation damping and stiffness on the seismic behaviour of structures", ISBN: 978-960-474-251-6.

[7] Athamnia Brahim and Ounis Abdelhafid (2011), "Effects of seismic isolation in the reduction of the seismic response of the structure", International Journal of Applied Engineering Research, Dindigul, Volume 2, No 2, 2011, ISSN 09764259.

[8] Mehmet Komur, Turan Karabork and Ibrahim Deneme(2011), "Nonlinear Dynamic Analysis of Isolated and Fixed-Base Reinforced Concrete Structures" Gazi University Journal of Science GU J Sci 24(3):463-475.

[9] Shirule P. A, Jagtap. L. P, Sonawane. K. R, Patil. T. D, Jadwanir. N and Sonar. S. K (2012), "Time History Analysis of Base Isolated Multi-Storyed Building", ISSN 0974-5904, Volume 05, No. 04, P.P. 809-816.

[10] Md.Arman Chowdhury, Rajib Kumar Biswas, Md.Nazmul Haq and Syeed Md. Iskander (2013), "Evaluation of Structural Implication of Incorporating Base Isolator as Earthquake Protection" , Device e-ISSN: 2278-1684,p-ISSN: 2320-334X, Volume 8, Issue 1, PP 27-30.

[11] Md. Arman Chowdhury and Wahid Hassan (2013), "Comparative study of the Dynamic Analysis of Multi-storey Irregular building with or without Base Isolator" International Journal of Scientific Engineering and Technology Volume No.2, Issue No.9, PP: 909-912.

[12] C.Prabha and Basil Sabu (2014) "Study of Base Isolation in Multi-Storeyed Buildings" ISSN: 2347 1964 (Online) 2347-1875 (Print) Vol.2, Issue 8.

[13] Syed Ahmed Kabeer K I and Sanjeev Kumar K.S (2014), "Comparison of Two Similar Buildings with and without Base Isolation", International Journal of Advance research, Ideas and Innovations in technology, volume 1, Issue 1.

[14] Ivan Skinner, R., Trevor E. Kelly and Bill Robinson, W.H. (1993) A text book on Seismic Isolation for Designers and Structural Engineers, Robinson seismic limited, Holmes consulting group.

[15] Hussein Shakeri Soleimanloo (2012), "A Survey study on design procedure of Seismic Base Isolation Systems", J. Appl. Sci. Environ. Manage. Vol. 16 (4)299 -307.

[16] Saiful Islam, A.B.M., Mohammed Jameel and Mohd Zamin Jumaat (2011), "Seismic isolation in buildings to be a practical reality',ISSN 2006-9790, Journal of Engineering and Technology Research Vol. 3(4), pp. 99-117.

[17] Fu Lin ZHOU, Zheng YANG, Wen Guang LIU and Ping TAN (2004), "New Seismic Isolation System for Irregular Structure with The Largest Isolation Building Area in The World" 13th World Conference On Earthquake Engineering Vancouver, B.C., Canada, Paper No.2349.

[18] IS 456:2000, Code of practice for plain and reinforced concrete.

[19] Trevor E Kelly, S.E. (2001), "Design Guidelines on Base Isolation of Structures", Holmes consulting group, New Zealand.

Electrophoretic Analysis of Proteins of Chemical Treated Human

Pece Sherovski[1], Natasha Ristovska[2]

Institute of Chemistry, Faculty of Natural Sciences and Mathematics, SS. Cyril and Methodius University, Skopje, Macedonia

Abstract— *Strong oxidising agents for bleaching and chemical treatments for regeneration of dry and damaged hair are most common factors that cause changes in protein structure and composition. Composition changes in fibrillar proteins - α keratins and globular proteins - KAP's (keratin-associated proteins) were investigated by protein analysis of the hair fiber using SDS-PAGE. The most significant changes in obtained electrophoregrams from SDS-PAGE analysis of bleached hair were observed in matrix protein fractions (KAP's), which contain a high concentration of cystine. Constructed electrophoregram from SDS-PAGE gel of hair treated with protein treatment indicates a new protein fraction with a molecular weight of about 2000 Da, probably due on hydrolyzed keratin as an ingredient of protein treatments.*

Keywords— bleaching, hair protein treatments, SDS-PAGE.

I. INTRODUCTION

Hair is a filamentous biomaterial composed of fibers that extend above the surface of the scalp. Human hair is comprised of approximately 80% of protein, in which two large families, the intermediate filament protein family (α-keratins) and the keratin-associated protein family (KAP's), are present. The structure of human hairs is determined by proteins as key components, which contain different amounts of disulfide bonds. For instance, the keratins are known as low-sulfur proteins consisting of at least 4—9 distinct fragments of type I acidic (40—50 kDa) and 4—6 of type II neutral/basic (55—65 kDa). On the other hand, KAP's contain high concentration of sulfur and classified into high-sulfur proteins (10—20 kDa), ultra-high-sulfur proteins (10—20 kDa), and high-glycine/tyrosine proteins (6—9 kDa) [1-3].

The main biological function of hair is protection of the body against coldness and wetness [4]. But, it also symbolizes the beauty, which is real challenge for cosmetic industry in recent decades. The development of instrumental analytical and biochemical methods effects on scientific approach for detailed study of physical and chemical properties of hair. According to the literature, the investigation of protein composition of hair fiber allows explanation of structural changes in the keratin fractions [5]. These changes are mainly caused by strong oxidizing agents for bleaching, which caused oxidative degradation of pigment melanin. The primary purpose of bleaching is to lighten the hair with hydrogen peroxide as the principal oxidizing agent and salts of persulfate as accelerators [6, 7].

On the other hand, protein treatments are used to decrease friction and detangle, minimize frizz and regenerate dry and damaged hair. There are many types of treatments with different deposition, adherence and wash out capacity which will lead to different performances of the treatment. The ideal treatment is capable of restore the hydrophobicity of the fiber and neutralizes the static electricity. Depending on the capacity of entering the fiber, they may reach the cuticle surface or the inner part of the cortex [8].

Recently, X-ray diffraction [9], IR and solid state NMR [10, 11] have been successfully applied to investigate the structural changes of protein in hair fiber. Electrophoretic analysis of hair proteins has been used for forensic identification of human hair [12], clinical investigation of genetic variability [13], and quality control of wool important for textile industry [14]. Furthermore, electrophoresis has been used to study of S-carboxymethylated low sulfur and high sulfur proteins isolated from chemical untreated hair [15].

In this study, the effects that occur in protein composition of human hair caused by various chemical treatments (bleaching and protein regeneration treatment) were investigated using SDS-PAGE. The results for chemically treated hair obtained from this method are also indicators for the quality of the hair products.

II. EXPERIMENTAL

2.1 Materials

Organic solvents, methanol, ethanol and acetic acid were supplied by Merck (Darmstadt, Germany) with purity ≥ 99.9 %. Tris–HCl (p.a), thiourea (p.a) and urea (p.a) from Merck (Darmstadt, Germany), 2-mercaptoethanol (p.a) and SDS were obtained from Sigma–Aldrich (Steinheim, Germany). Coomassie Brilliant Blue R-250 were purchased from Merck (Darmstadt, Germany). Amersham Low Molecular Weight (LMW) calibration proteins were used as a standard. In all cases double deionized water (ddH_2O) was used.

2.2 Preparation of hair samples

Human hair samples were collected from one woman to minimize the experimental variations that may be caused by age or gender. The hair samples were washed with ethanol (75 %) prior to extraction to remove any surface contaminants. External lipids were then removed by using a mixture of chloroform/methanol (2:1 v/v) for 24 h. Hair samples were exposed to the influence of bleaching reagent (bleach by Revlon with 12% H_2O_2) for 45 min, washed with ddH_2O and air drayed. After bleaching, hair was treated by protein treatments (Fiberplex and Fiberforce by Schwarzkopf and Keratin treatment by Revlon) during 30 minutes.

2.3 Extraction of Hair Proteins

Hair was cut into small pieces with a length of approximately 1-2 mm, and 5 mg hair was mixed with 1 mL solution containing 25 mM Tris–HCl, pH 8.5, 2.6 M thiourea, 5 M urea and 600 mM 2-mercaptoethanol (2-ME) at 50°C for 72 h. After protein extraction procedure, the mixture was centrifuged at 12000×**g** for 15 min at room temperature. The obtained supernatant was used as a hair protein fraction for determination of total proteins and electrophoretic analysis.

2.4 SDS-PAGE analysis

Extracted hair proteins have been analyzed by SDS-PAGE electrophoresis. For analyses 0.9 ml of obtained supernatant was mixed with 0.1 ml 10 % SDS solution and boiled for 3 min. Then 12 µL of this mixture was applied. Electrophoresis was performed on 4-22 % gradient gel at 260 V for 2 h in 0.025 M Tris, 0.2 M glycine containing 0.1% (w/v) SDS. Gels were stained with 0.1% Coomassie Brilliant Blue R-250, and distained with a mixture of acetic acid and methanol (20:80, v/v). Obtained gels were analyzed by Gel Pro software.

III. RESULTS AND DISCUSSION

Analysis of the obtained SDS-PAGE gel from chemical untreated hair indicated appearing of intense protein bands with molecular weight in the range of 40 - 45 kDa (Fig. 1 A1 and A2). This protein band corresponded to the theoretical molecular weight of keratin of type I acid proteins. In the area around 50 kDa another fraction was identified, that was consistent with the molecular weight of keratin type II neutral/base proteins.

In the obtained gel, less intense low molecular weight protein bands in the range of about 30 kDa and 10-20 kDa were also observed (Fig 1). These two distinct groups of proteins correspond to UHS (ultra high sulfur proteins) and HS (high sulfur proteins), but there was no evidence of HTP (high tyrosine proteins) [15].

The low intensity of protein fractions with a molecular weight below 30 kDa is probably due to the exposure of hair on UV irradiation and high temperature drying and styling. These factors can cause significant changes in low molecular weight fractions especially when hair is exposed for a long period (2 to 3 years) and when the samples are taken from the tips of the hair. On the other hand, low intensity may simply be due to low concentration of these proteins.

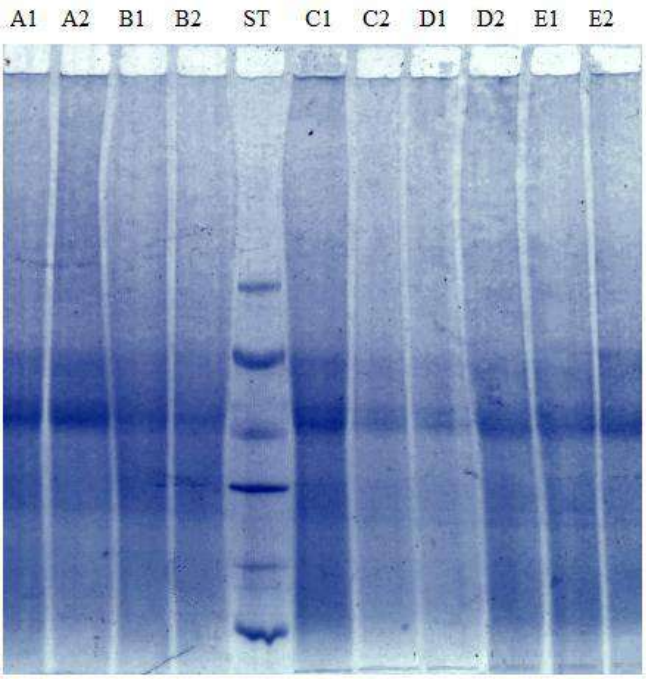

FIGURE 1. SDS-PAGE of extracted human hair protein from: A - chemical untreated hair, B - bleached hair, C - hair treated with Fiberplex by Schwarzkopf, D - hair treated with Fiberforce by Schwarzkopf and E - hair treated with Keratin treatment by Revlon (lanes 1 and 2, duplicate samples of the same hair type)

The bands of components with higher molecular weights (65-75 kDa) were also shown in electropherogram (Fig. 2). These components may represent dimeric forms of the low-sulphur proteins, that possibly obtained in incomplete reduction of the low-sulphur proteins during extraction or alternatively limited re-oxidation prior to or during electrophoresis

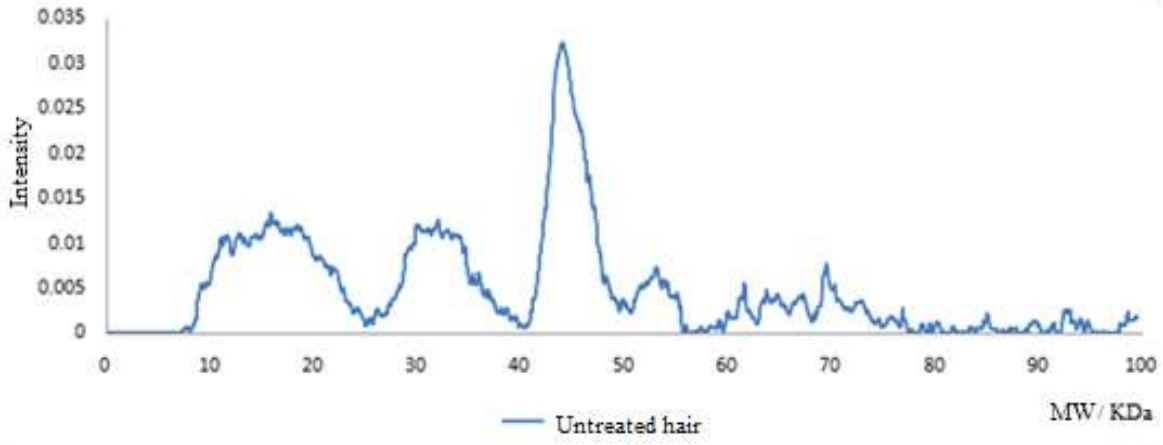

FIGURE 2. SDS-PAGE electropherograms of proteins extracted from chemically untreated hair

During bleaching, hydrogen peroxide primarily reacts with melanin and initiates a destruction of the chromophore. However, hair fiber primarily contains a large percentage of oxidizable groups (e.g., disulfide bonds of the cortical matrix and of the cuticle) and degradation of hair proteins also occur. Determination of the isolated proteins from bleached hair was achieved by SDS-PAGE analysis at the same experimental conditions. The results obtained from electropherogram (Fig. 3) exhibit that all protein fractions undergo changes, which are mostly expressed in proteins with lower molecular weight (KAP's). These changes are due to the structure of the proteins and their composition, especially the content of cystine. The cysteic acid is the final product of the oxidative cleavage of the disulfide bond during the bleaching of human hair, identified by HPLC [16]. This oxidation occurs via intermediate oxidation products (disulfide dioxides, disulfide tetroxide, cystine monoxide and cystine dioxide), extremely sensitive to alkaline hydrolysis.

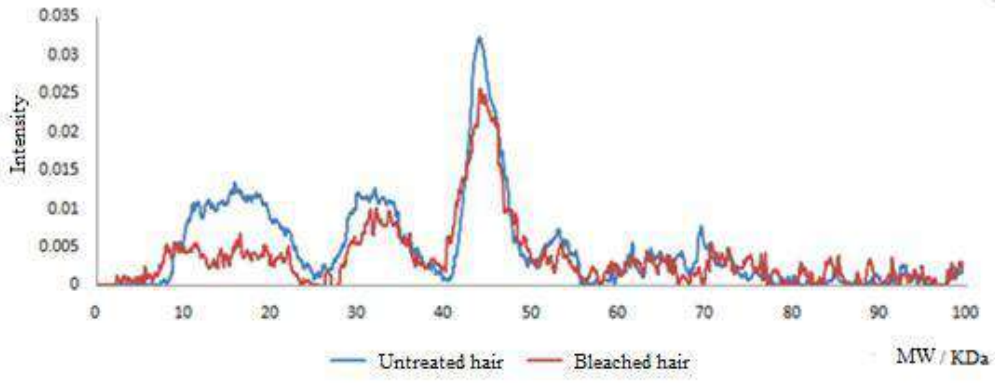

FIGURE 3. SDS-PAGE electropherograms of proteins extracted from chemically untreated and bleached hair

The results obtained from the SDS-PAGE analysis of hair treated with protein treatments by Schwarzkopf (Fiberplex and Fiberforce) and Revlon, (Keratin treatment) shown in Fig. 4 indicate a new protein fraction with average molecular weight of about 2000 Da. This protein fraction is due to the main component of chemical treatments which is hydrolyzed keratin, product of alkaline or enzymatic hydrolysis of keratin isolated from sheep or goat wool. Depending on the molecular weight, hydrolyzed proteins cannot diffuse into deeper layers, so they may only sorption on the surface of the hair shaft.

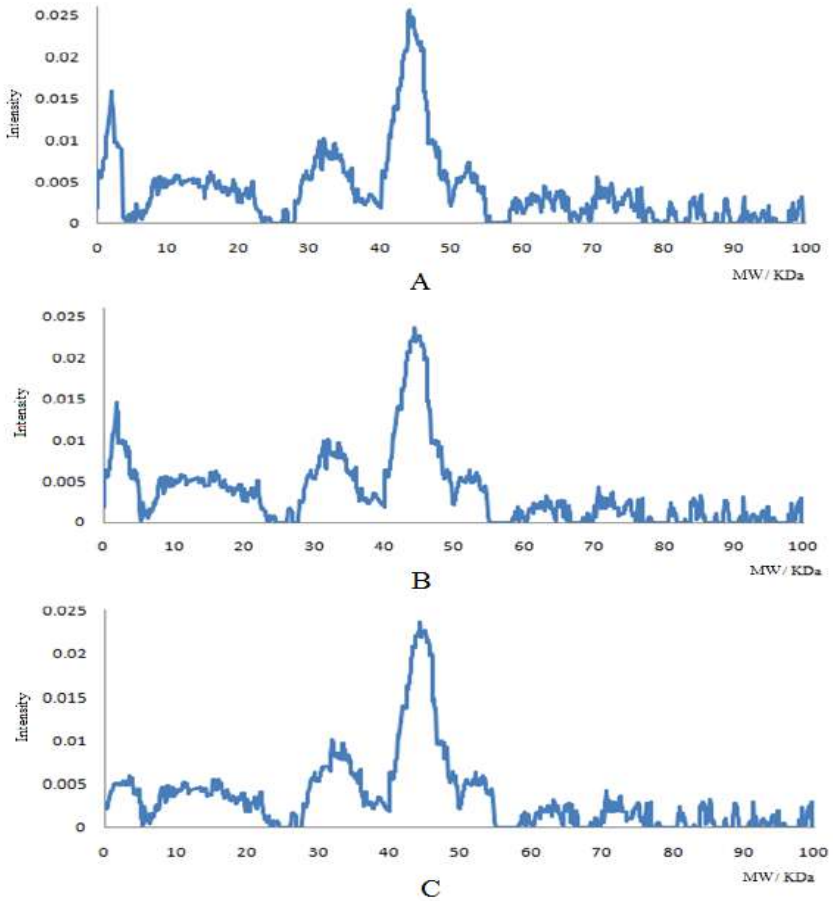

FIGURE 4. SDS-PAGE electropherograms of proteins extracted from A - hair treated with Fiberplex by Schwarzkopf, B - hair treated with Fiber force by Schwarzkopf and C - hair treated with Keratin treatment by Revlon

To provide better results, treatment is performed in several steps. In the first step, the hair is washed with high pH shampoo which affect on cuticle opening. In the next step, hydrolyzed keratin is applied and penetrates to the surface layers of the fiber through the open cuticle. The rest of the keratin that has not penetrated because of its ability to form colloids gives

a shiny and healthy look of the fiber. The final step involves washing the hair with a shampoo with pH below 5, which provides closure of the cuticle and lock in place the hydrolyzed keratin in the fiber.

IV. CONCLUSION

In this study effects of bleaching agents and protein treatments on protein composition of hair were investigated. Bleaching of human hair involved oxidative degradation of melanin and side reactions with the hair proteins as result of reaction conditions. The most significant changes in obtained electrophoregrams from SDS-PAGE analysis of bleached hair were observed in low molecular weight proteins, which contain a high concentration of cystine. These changes are probably due to oxidation of cystine to its final product - cysteic acid. On the other hand, hydrolyzed keratin is main intergradient of protein treatments and its fraction was detected on constructed electrophoregram from SDS-PAGE gel, with a molecular weight at about 2000 Da. The intensity of this band depended of the quality of cosmetic products and their efficiency for repairing dry and damaged hair.

REFERENCES

[1] N.H. Leon, "Structural aspects of keratin fibres," J. Soc. Cosmet. Chem, vol. 23, pp. 427–445, 1972.

[2] M.A. Rogers, L. Langbein, S. Praetzel-Wunder, H. Winter, and J. Schweizer, "Human hair keratin-associated proteins (KAPs)," Int. Rev. Cytol., vol. 251, pp. 209–263, 2006.

[3] D.A.D. Parry, T.A. Smith, M.A. Rogers, and J. Schweizer, "Human hair keratin-associated proteins: Sequence regularities and structural implications," J. Struct. Biol, vol. 155, pp. 361–369, 2006.

[4] G.E. Rogers, P.J. Reis, K.A. Ward, and R.C. Marshall**,** The biology of wool and hair, 1st ed, Chapman and Hall, London, New York 1989.

[5] N. Nishikawa, Y. Tanizawa, S. Tanaka, Y. Horiguchi, and T. Asakura, "Structural change of keratin protein in human hair by permanent waving treatment," Polymer (Guildf), vol. 39, pp. 3835–3840, 1998.

[6] L.J. Wolfram, D. Ph, K. Hall, B. Sc, and I. Hui, "The Mechanism of Hair Bleaching," J. Soc. Cosmet. Chem, vol. 900, pp. 875–900, 1970.

[7] C.R. Robbins, "Chemical Aspects of Bleaching Human Hair," J Soc Cosmet. Chem, vol. 22, pp. 339–348, 1971. [8]

[8] G. Dias, and M. F. Reis, "Hair cosmetics: An overview," Int J Trichol, vol. 7, pp. 2-15, 2015.

[9] R. D. B Fraser, and T. P. MacRae , "Conformation in Fibrous Proteins and Related Syntetic Poripeptides," Academic Press, pp. 469–525, 1973.

[10] H. Saitô, "Conformation-dependent 13C chemical shifts: A new means of conformational characterization as obtained by high-resolution solid-state 13C NMR," Magnetic Resonance in Chemistry, vol. 24, pp. 835-852, 1986.

[11] H. Saitô, and I. Ando, "High-resolution solid-state NMR studies of synthetic and biological macromolecules," Annual reports on NMR spectroscopy, vol. 21, pp. 209-290, 1989.

[12] R.C. Marshall, J.M. Gillespie, and V. Klement, "Methods and Future Prospects for Forensic Identification of Hairs by Electrophoresis," J. Forensic Sci, vol. 25, pp. 57-66, 1985.

[13] R.C. Marshall, and J.M. Gillespie, "Comparison of samples of human hair by two-dimensional electrophoresis," J. Forensic Sci. Soc, vol. 22, pp. 377–85, 1982.

[14] R.C. Marshall, H. Zahn, and G. Blankenburg, "Possible Identification of Specialty Fibers by Electrophoresis," Textile Research Journal, vol. 54, pp. 126- 134, 1984.

[15] R.C. Marshall, "Characterization of the proteins of human hair and nail by electrophoresis," J Invest Dermatol, vol. 80, pp. 519–524, 1983.

[16] C.R. Robbins, and C. Kelly, "Amino acid analysis of cosmetically allerted hair," J. Soc. Cosmet. Chem, vol. 20, pp. 555–564, 1969.

Microwave-assisted Synthesis of Some N-alkylisatin-β-thiocarbohydrazones

Natasha Ristovska[1], Frosa Anastasova[2]

Institute of Chemistry, Faculty of Natural Sciences and Mathematics, SS. Cyril and Methodius University, Arhimedova 5, 1000 Skopje, Macedonia

Abstract— *The effectiveness of microwave-assisted preparation of N-alkylisatin-β-thiocarbohydrazones, where alkyl group is methyl and ethyl, was evaluated. The corresponding N-alkylisatin-β-thiocarbohydrazones were predominantly obtained by TCH and N-alkyl substituted isatin in molar ratio 3:1. Reactions of carbonyl-amine condensation were performed in water acidified to pH 1.5 as a solvent system. Reaction mixtures were exposed to microwave irradiation under 300W and pressure 200 psi, for a specified incubation period of 5-15 min. The yield of products obtained by microwave assisted reaction was similar to that had been obtained using conventional reflux method (about 70% to 80%), with reduction of time. The structures of synthesized N-alkylisatins and corresponding N-alkylisatin-β-thiocarbohydrazones were established on the basis of recorded spectral data from IR, GC-MS, ^{1}H NMR and ^{13}C NMR.*

Keywords— Microwave-assisted organic synthesis (MAOS), N-alkylisatin, N-alkylisatin-β-thiocarbohydrazone.

I. INTRODUCTION

Discovery of small molecules (MW < 1500 Da) play an essential role in medicinal chemistry. Some of these organic compounds derived from natural products and are endogenous, such as isatin (indoline-2,3-dione) identified in human, mammalians and plants [1, 2]. Isatin was discovered by Erdmann and Laurent in 1840 as an oxidation product of indigo, and numerous of its derivatives have been synthetically obtained and characterized so far [3, 4].

Isatins are a group of organic compounds containing the heterocyclic indole nucleus, where the aryl ring (A) is mono, di-, or tri-substituted, as can be seen on Fig.1. Some of isatin analogues have been obtained by derivatization of the indole nitrogen and/or carbonyl moieties: lactam and keto group on C2 and C3, respectively.

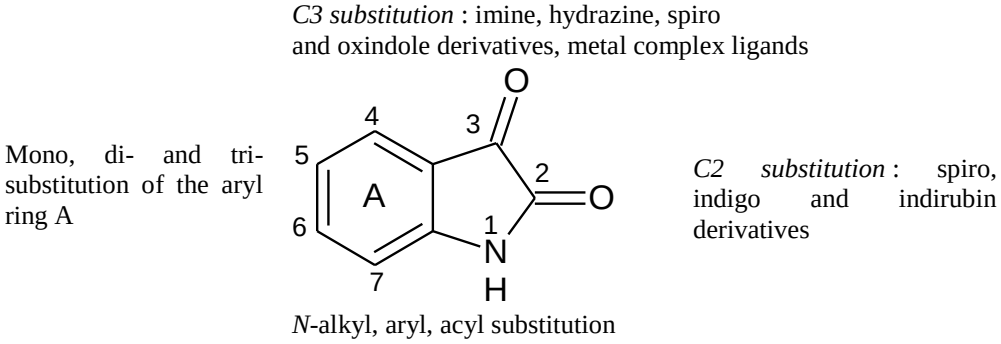

FIGURE 1. The various substitution types and patterns possible for the isatin scaffold

The literature reports information about the chemistry of isatin and its derivatives, their physicochemical properties [5] and biological activities [6, 7]. Isatin, at first was detected as monoamine oxidase (MAO) and identified as tribulin, but also possess anticonvulsant, sedative and anxiogenic properties [8]. Its derivatives exhibit a wide spectrum of pharmacological actions such as antiviral, antibacterial, antifungal, anticonvulsant, and anti-inflammatory, analgesic, anticancer, anti-HIV, herbicidal, hypotensive and enzymatic inhibition [9-12]. Therefore, synthesis and investigation of novel isatin derivatives is an active area of research and has the potential for the development of pharmacologically active molecules.

Antimicrobial activity studies revealed that the presence of strong electron-donating thiocarbohydrazone group enhances biological activity in respect to the parent molecule and is consistent to proposed pharmacophoric requirements in the molecules [6, 13]. This observation encouraged us to study the reaction of some substituted isatin heterocycles with thiocarbohydrazide and synthesized new derivatives with potential biological activity.

Recently, there has been a dramatic upsurge in the use of microwave heating within the pharmaceutical industry to facilitate the chemical synthesis of new chemical entities, and some *N*-alkylisatin derivatives have been obtained [14, 15]. Microwave-

assisted organic synthesis (MAOS) has been shown to be an invaluable tool for medicinal chemistry and drug discovery applications since it often dramatically reduces reaction times, minimizes secondary reactions and improves yield. These advantages of microwave-assisted chemistry over conventional approaches motivated us to evaluate this approach for synthesis of thiocarbohydrazones of *N*-methyl and *N*-ethylisatins, where the incorporated alkyl groups are increasing the lipophilicity of the molecules.

II. EXPERIMENTAL

2.1 General

Microwave-assisted reactions were carried out on CEM, MARS X 300W.ATR-FTIR Perkin-Elmer 2000 was used for recording IR spectra, directly from the solid samples. The mass spectra were recorded on GC-MS Schimadzu, DI-EI (70 eV). NMR spectra were recorded on Bruker-250 NMR Spectrometer determined in DMSO-d_6 as solvent and using tetramethylsilane as internal standard. Melting points were determined using Koffler apparatus and were uncorrected.

All chemicals used for synthesis and purification were of p.a. grade (Merck). Commercial isatin was recrystallized twice from ethanol. Preparative flash chromatography was performed using Merck silica gel 60 (230–400 mesh) and thin layer chromatography (TLC) was carried out on aluminum sheets with silica gel with fluorescent indicator (254 nm), obtained from Sigma-Aldrich. Spots were visualized using either UV-lamp at 254 nm or iodine.

2.2 Preparation Procedures

2.2.1 General synthesis of *N*-alkylisatins (1)

Isatin (1.0 mmol) was dissolved in DMF (5 ml), and K_2CO_3 (1.3 mmol) was added. The mixture was stirred under room temperature until isatin anion was obtained and hydrogen was removed. Alkyl halide (CH_3I or C_2H_5I, respectively) (4.0 mmol) was added to the reaction mixture. The reaction under reflux on 70 °C was completed after 1.5-2 hour, while the reaction time for the same reaction under microwave irradiation was 15 minutes, at 300 W and pressure 200 psi. Then the reaction mixtures were cooled overnight and the precipitates were formed in ice water. Further it was purified by recrystallization by ethanol or column chromatography (silica gel, petroleum ether / ethyl acetate = 20:1).

N-methylisatin (**1a**), melting point 133-134 °C (lit 130-134 [90]), yield 82 %

IR:cm^{-1}υ(CH aromatic) 3061, υ(CH aliphatic) 2923,υ(C=O) 1717, υ(C=O, lactam) 1603

GS-MS: molecular ion *m*/*z* =161, base peak at *m*/*z* = 104, fragments at *m*/*z* 146, 133 and 78.

^{1}H-NMR (600 MHz, DMSO-d_6): δ/ppm 7.12 – 7.67 (m, 4H, Ar-H), 3.12 (s,3 H, CH_3).

^{13}C-NMR (150,90 MHz, DMSO-*d6*): *δ*/ppm 183.47 (C=O, lactam), 158.63 (C=O), 110.57 (C_{Ar}), 117.37 (C_{Ar}) 123.21 (C_{Ar}), 124.25 (C_{Ar}), 138.19 (C_{Ar}), 151.37 (C_{Ar}), 26.02 (CH_3)

N-ethylisatin (**1b**), melting point 95-96 °C (lit 96) 90, yield 79 %

IR: cm^{-1} υ(CH aromatic) 3061, υ(CH aliphatic) 2989, υ(C=O) 1723, υ(C=O, lactam) 1607

GS-MS: molecular ion *m*/*z* = 175, base peak at *m*/*z* = 104, fragments at *m*/*z* 161, 147, 132 and 78.

^{1}H- NMR (600 MHz, DMSO-*d*6): *δ*/ppm 7.10 - 7.66 (m, 4H, Ar-H), 3.70 (q, 2H, CH_2), 1.79 (t, 3H, CH_3)

^{13}C-NMR (150,90 MHz, DMSO-*d6*): *δ*/ppm 183.66 (C=O, lactam), 157.76 (C=O), 110.62 (C_{Ar}), 117.50 (C_{Ar}) 123.10 (C_{Ar}), 124.51 (C_{Ar}), 138.21 (C_{Ar}), 150.39 (C_{Ar}), 34.3 (CH_2), 12.39 (CH_3).

2.2.2 General synthesis of *N*-alkylisatin-β-thiocarbohydrazones (**2**)

N-alkyl substituted isatin (1.0 mmol) and thiocarbohydrazide (3.0mmol) were dissolved in 5 ml hot water acidified with HCl to pH 1.5. The mixture was refluxed for an one hour with constant stirring, while the reaction under microwave irradiation at 300 W and pressure 200 psi was completed for 10 minutes. The obtained precipitates were collected by vacuum filtration, washed with hot water and air dried. The obtained solid products were recrystallized by ethanol.

N-methylisatin-*β*-thiocarbohydrazone (**2a**), melting point 205-207 ^{o}C, yield 83 %

IR: cm^{-1} υ(NH) 3207, υ(CH aromatic) 3051, υ(CH aliphatic) 2987, υ(C=N) 1677, υ(C=O, lactam) 1613

GS-MS: molecular ion *m*/*z* = 249, base peak at *m*/*z* =75, fragments at *m*/*z* 221, 175, 159, 146, 131, 104 and 91.

^{1}H- NMR (600 MHz, DMSO-*d*6): *δ*/ppm 12.36 (s, 1H, NH, C=NNH(CS)N-**H**), 9.99 (s, 1H, NH, C=NN-**H**), 5.12 (s, 2H, C=NNH(CS)NH-N**H$_2$**), 7.09 - 7.69 (m, 4H, Ar-**H**), 3.20 (s, 3H, C**H$_3$**)

^{13}C-NMR (150,90 MHz, DMSO-*d6*): *δ*/ppm 180.11 (**C**=S), 174.33 (**C**=O, lactam), 160.74 (**C**=N), 109.70 (C_{Ar}), 119.34(C_{Ar}), 122.81 (C_{Ar}), 130.82 (C_{Ar}), 134.71 (C_{Ar}), 143.23 (C_{Ar}), 25.63 (CH_3)

N-ethylisatin-*β*-thiocarbohydrazone (**2b**), melting point 190-191^{o}C, yield 80 %

IR: cm^{-1} υ(NH) 3213, υ(CH aromatic) 3052, υ(CH aliphatic) 2977, υ(C=N) 1668, υ(C=O, lactam) 1611

GS-MS: molecular ion *m*/*z* = 263, base peak at *m*/*z* =146, fragments at *m*/*z* 221, 175, 159, 146, 131, 104 and 91.

^{1}H-NMR (600 MHz, DMSO-*d*6): 12.39 (s, 1H, NH, C=NNH(CS)N-**H**), 9.99 (s, 1H, NH, C=NN-**H**), 5.20 (s, 2H, C=NNH(CS)NH-N**H$_2$**), 7.12 - 7.72 (m, 4H, Ar-**H**), 3.78 (q, 2H, C**H$_2$**), 1.11 (t, 3H, C**H$_3$**)

^{13}C-NMR (150,90 MHz, DMSO-*d6*): *δ*/ppm 180.10 (**C**=S), 174.26 (**C**=O, lactam), 160.39 (**C**=N), 109.76 (C_{Ar}), 119.52 (C_{Ar}) 122.74 (C_{Ar}), 130.87 (C_{Ar}), 134.75 (C_{Ar}), 142.23 (C_{Ar}), 33.96 (CH_2), 12.63 (CH_3)

III. RESULTS AND DISCUSSION

To develop more effective small molecules with potential biological activity, the title compounds were synthesized by two step reaction as shown in Scheme 1. The first step involved *N*-substitution of isatin to obtain the corresponding *N*-alkyl derivatives. Afterward, in the carbonyl-amine condensation of the *N*-alkyl substituted isatin with TCH, *N*-alkylisatin-*β*-thiocarbohydrazones were obtained. Microwave synthesis and traditional conductive heating methods were used in both reactions.

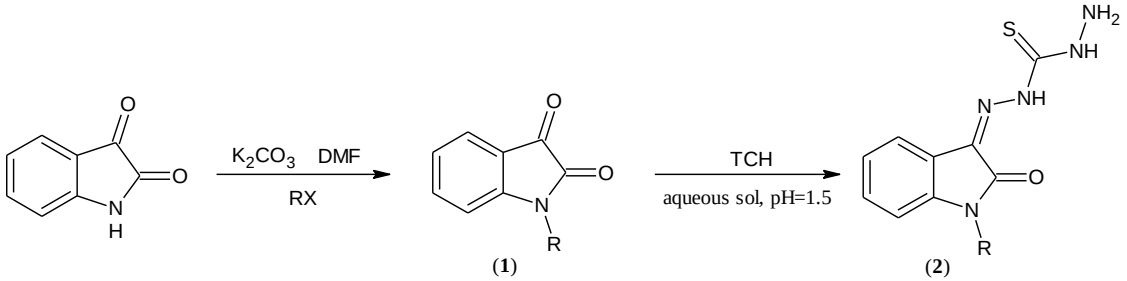

SCHEME 1. Synthesis of *N*-alkylisatin-*β*-thiocarbohidrazones (2) from corresponding *N*-alkylisatins (1) (RX is: CH_3I or C_2H_5I)

A variety of methods have been demonstrated for the *N*-alkylation of isatins [16]. *N*-alkyl derivatives of isatin are commonly synthesized from the reaction of the sodium salt of isatin with alkyl halides or sulphates. Some of the more general methods include the use of NaH, either in toluene under reflux or DMF (25-80 °C) or THF (-20 °C to room temperature), as well as CaH_2, (40-50 ^{o}C). Other methods involve the use of potassium carbonate in DMF or in acetone. An alternative method for preparing *N*-alkylisatins consists of the reaction between isatin and alkyl halides in benzene - chloroform / 50% aq. KOH biphasic system; utilize tetrabutyl-ammonium hydrogensulfate as the phase transfer catalyst.

In this work, the reaction of *N*-alkylation of isatin was carried out in the catalytic presence of K_2CO_3, using DMF as solvent. In this reaction of substitution, the isatin anion is the nucleophilic reactant to the alkyl halide. Higher solvent polarity that exhibits DMF can promote the proton-transfer equilibrium and leads to the higher yields. The typical yields of obtained products after recrystallizations from ethanol, using either microwave assisted synthesis or conventional heating methods are presented in Table 1.

TABLE 1
COMPARISON BETWEEN REACTION TIME AND YIELD OF OBTAINED ISATIN DERIVATIVES BY MICROWAVE SYNTHESIS AND CONVENTIONAL HEATING

Compound	Reagents		Catalyst	Solvent	Microwave synthesis		Conventional heating	
					Reaction time	Yield	Reaction time	Yield
1a	Isatin	CH_3I	K_2CO_3	DMF	15 min	82 %	1.5 h	75 %
1b	Isatin	C_2H_5I	K_2CO_3	DMF	15 min	79 %	2 h	68 %
2a	**1a**	TCH	HCl	H_2O	10 min	83 %	1 h	74 %
2b	**1b**	TCH	HCl	H_2O	10 min	80 %	1 h	70 %

The structures of *N*-methylisatin (**1a**) and *N*-ethylisatin (**1b**) were confirmed using ATR-FTIR, GC-MS, ^{1}H- NMR and ^{13}C-NMR. In the IR spectra of synthesized *N*-alkylisatins, the band at around 2900 cm^{-1} can be attributed with great certainty to υ(CH aliphatic). The most prominent bands are the ones due to the carbonyl stretching υ(C=O) of keto and lactam group at 1720 cm^{-1} and 1605 cm^{-1}, respectively. The method of direct sample injection into to ion source, without using gas chromatograph, was used. The mass spectra obtained by electron ionization mode demonstrated molecular ions at *m*/*z* 161 (**1a**) and 175 (**1b**), that represents molecular ion radicals with formula $C_9H_7NO_2$ and $C_{10}H_9NO_2$, respectively. The base peaks were observed at *m*/*z* 104 for both compounds and they due to a loss of an alkyl group and NCO fragment, which occurs in amides and lactams.

The ^{1}H-NMR spectra of (**1a**) and (**1b**) displayed characteristic multiplet at δ7.1 to 7.7 due to aromatic protons. The singlet at 3.12 ppm (**1a**) is attributed to protons from *N*-methyl group, while quadruplet at δ 3.70and triplet at δ 1.79 (**1b**) are from *N*-ethyl group CH_2 and CH_3 protons, respectively.

The^{13}C-NMR spectrum of (**1a**) exhibits 9 signals, while (**1b**) 10 signals. Six signals belong to the aromatic carbons (δ 110 to 152 ppm). There are two more signals in ^{13}C-NMR spectra from carbons of two chemically distinct carbonyl groups, lactam and keto, at 183 and 158 ppm, respectively. The presence of *N*-methyl and *N*-ethyl group in ^{13}C-NMR spectra is confirmed by corresponding signals at 26 ppm (**1a**), and at δ 34 and 12 ppm (**1b**).

In addition, we investigated the carbonyl-aminereaction of the *N*-alkyl isatin derivatives (**1a** and **1b**) with TCH. Thiocarbohydrazide condenses easily with two molecules of carbonyl compounds on the terminated hydrazineamino groups to produce the centrosymmetric dimmer. Here in, we report the optimal conditions for synthesis of monoth iocarbohydrazones, which may react with another carbonyl compound and gave new Schiff base.

In order to improve the yield of *N*-alkylisatin-β-thiocarbohydrazones (**2**), the effect of molar ratio of reactants and electing of solvent system were investigated. It was found that the condensation of isatin derivative (**1**) with excess of TCH (molar ratio of TCH and *N*-alkylisatin was 3:1) in water as solvent, acidified with HCl to pH 1.5, yield thiocarbohydrazone (**2**), rather than tetrazepine (**3**), triazine (**4**) or spyro system (**5**). Structures (**3**) and (**4**) were excluded based on appearing the lactam C=O, band in the IR spectra (1611 cm^{-1}). In ethanol with catalytic amount of acetic acid either in acetonitrile as solvents, nucleophilic addition at position C3 was followed by a spiro-annelation. The presence of this product (**5**) in a reaction mixture was confirmed by ^{13}C-NMR, since the chemical shift at 63.11 ppm is a result of sp^3 hybridized carbon in isatin moiety.

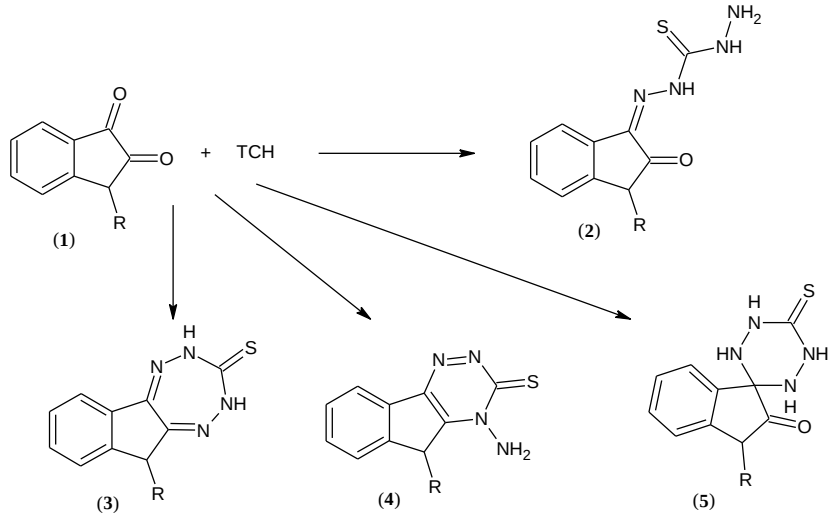

FIGURE 2. Possible isatin derivatives from the reaction of *N*-alkylisatin (1) with TCH under microwave irradiation

Structures of synthesized isatin derivatives (**2**) were determined by spectroscopic methods. Complex bands dominate in the 3500-2800 cm^{-1} spectral region of synthesized *N*-alkyl-*β*-thiocarbohydrazones. The band around 3207 cm^{-1} can be attributed with great certainty to υ(NH). The absence of carbonyl (C=O) peak at around 1750 cm^{-1} characteristic for the keto group on C3 in (1) could explain the formation of a thiocarbohydrazone derivative of isatin. The obtained DI-EI mass spectra of synthesized thiocarbohydrazones demonstrated molecular ions at *m*/*z* 249 (**2a**) and *m*/*z* 263 (**2b**), which represent molecular formulas $C_{10}H_{11}N_5OS$ and $C_{11}H_{13}N_5OS$, correspondingly. The base peak in MS of **2a** was observed at *m*/*z* 75 and arrived from the $–CSNHNH_2$ thiocarbohydrazide part of molecule, while the base peak of **2b** at *m*/*z* 146 resulted from cleavage of the

–CSNHNH$_2$ and loss of ethyl group with NCO fragment, characteristic for lactams. The further fragmentation involve the sequential loss of a same parts of isatin-*β*-thiocarbohydrazone structure.

The ^{1}H-NMR spectra of (**2**) displayed three separate singlets at 12.36, 9.99 and 5.15 ppm, which according of the chemical shifts and signal intensities can be attributed to protons from thiocarbohydrazyde moiety C=NNH(CS)N-**H**, C=NN-**H** and C=NNH(CS)NH-N**H$_2$**, respectively. The other peaks are the same as the corresponding *N*-alkylisatin (**1**).

The ^{13}C-NMR spectrum of **2a** exhibit 10 signals, while in spectrum of **2b** there are 11 signals, respectively. Of these signals, 6 belong to the aromatic carbons, (chemical shift at 109 to 143 ppm). The C2 and C3 atoms from isatin moiety and the C atom as a part of thicarbohydrazide were assigned on the basis of their chemical shifts at 174 ppm (C=O, lactam), 160 ppm (C=N) and 180 ppm (C=S). Other signals in the spectra belong to carbons from alkyl groups.

IV. CONCLUSION

N-alkylisatins (**1**) and *N*-alkylisatin-*β*-thiocarbohydrazones (**2**), where alkyl group is methyl or ethyl, have been prepared by two-step reaction pathway including (i) nucleophilic substitution of alkyl halide with isatin anion and (ii) subsequent carbonyl-amine condensation of *N*-alkylisatin with TCH. Reactions were performed using conventional heating technique and microwave-assisted synthesis. *N*-alkylisatins (1) and title compounds (2) were obtained by microwave irradiation for 10 to 15 minutes, so one of the advantages over conventional heating is reducing the reaction time. Investigation of the effect of the mole ratio of reactants and elected solvent indicated that the monothiocarbohydrazone derivatives of isatin were predominantly obtained in acidic media in water as solvent and triple molar excess of TCH. In ethanol and acetonitrile solutions, spyro compounds were detected. Synthesized compounds were characterized using GC-MS, ^{1}H-NMR and ^{13}C-NMR. *N*-ethylisatin-*β*-thiocarbohydrazone has cytostatic activity towards malignant melanoma cells.

REFERENCES

[1] P.Pakravan, S.Kashanian, M.M.Khodaei, and J.F. Harding, "Biochemical and pharmacological characterization of isatin and its derivatives: from structure to activity," Pharm. Rep., vol.65, pp. 313-335, 2013.

[2] M.Premanathan, S.Radhakrishnan, and K. Kathiresan,"Antioxidant & anticancer activities of isatin (1H-indole-2,3-dione), isolated from the flowers of Couroupita guianensis Aubl," Indian J. Med. Res., vol. 136(5), pp. 822-826, 2012.

[3] J.F.M. Da Silva, S.J. Garden, and A.C. Pinto, "The Chemistry of isatins: a review from 1975 to 1999," J. Braz. Chem. Soc., vol. 12(3), pp. 273-324, 2001.

[4] K. L.Vine, L.Matesic, J. M.Locke, M.Ranson, and D., Skropeta, "Cytotoxic and Anticancer Activities of Isatin and Its Derivatives: A Comprehensive Review from 2000-2008," Anti-Cancer Agents in Medicinal Chemistry, vol.9, pp. 397-414, 2009.

[5] P.Naumov, and F. Anastasova, "Experimental and theoretical vibrational study of isatin, its 5-(NO2, F, Cl, Br, I, CH3) analogues and the isatinato anion," Spectrochim. Acta A Mol. Biomol. Spectrosc., vol. 57, pp. 469–481, 2001.

[6] S. N.Pandeya, S.Smitha, M.Jyoti, and K.S.Sridhar, "Biological Activities of Isatin and its Derivatives,"Acta. Pharm., vol. 55, pp. 27-46, 2005.

[7] G.Chen, Y.Wang, X.Hao, and S.Mu, "Simple isatin derivatives as free radical scavengers: Synthesis, biological evaluation and structure-activity relationship," Chemistry Central Journal, pp. 5-37, 2011.

[8] A. E.Medvedev, and V. Glover, "Tribulin and endogenous MAO-inhibitory regulation in vivo,"Neurotoxicology, vol. 25(1-2), pp. 185-192, 2004.

[9] Z.Juranić, F.Anastasova, I.Juranić, T,Stanojković, S.Radulović, and N.Vuletić, "Antiproliferative action of isatine-β-thiocarbohydrazone and N-ethylisatine-β-thiocarbohydrazone on human PBMC and on two neoplastic cell lines," J. Exp. Clin. Cancer Res. Vol. 18(3), pp. 317-324, 1999.

[10] H.Pervez, M.Ramzan, M.Yaqub, and K.M. Khan, "Synthesis, cytotoxic and phytotoxic effects of some new N^4-aryl substituted isatin-3-thiosemicarbazones," Lett. Drug. Des. Discov., vol. 8, pp. 452-458, 2011.

[11] G.Mathur, and S. Nain,"Recent Advancement in Synthesis of Isatin as Anticonvulsant Agents: A Review,"Med. Chem., vol. 4(4), pp. 417-427, 2014.

[12] L. Matesic, J.M. Locke,J. B.Bremner, S.G. Pyne,D, Skropeta,M.Ranson, and K. L.Vine,"N-phenethyl and N-naphtylmetyl isatins and analogues as in vitro cytotoxic agents,"Bioorg.Med. Chem., vol. 16, pp. 3118-3124, 2008.

[13] N.Ristovska, F.Anastasova, and M.Stefova, "*N*"-[(3*Z*)-1-Acetyl-5-chloro-2-oxo-1,2-dihydro-3*H*-indol-3-ylidene] thiocarbonohydrazide," Molbank, vol. 2, pp 798-804, 2013.

[14] A.I.Perilo, M.S. Shmidt, A.M.Reverdito, L. Kremenchuzky, and M.M. Blanco "Simple and Efficient Microwave Assisted N-Alkylation of Isatin," Molecules, vol. 13, pp. 831-840, 2008.

[15] G.Kiran,T. Maneshwar,Y. Rajeshwar, and M.Sarangapani, "Microwave Assisted Synthesis, Characterization, Antimicrobial and Antioxidant Activity of Some New Isatin Derivatives,"Journal of Chemistry, vol. 2013, Article ID 192039, 7 pages

[16] M.C.Clay, H. M. Abdallah, C. Jordan, K. Knisley, and D. M. Ketcha,"*N*-Alkylation of isatins utilizing KF/alumina,"ARKIVOC vol. 6, pp. 317-325, 2012.

Dry solid feeding characteristics by computational particle-fluid dynamics simulation at high pressure

Woo Chang Sung[1], Seok Woo Chung[2], SungKyu Lee[3], Jong Sun Jung[4], Dong Hyun Lee[5]*

[1,5]School of Chemical Engineering, Sungkyunkwan University, Suwon, Republic of Korea
[2,3]Institute for advanced engineering, Youngin, Republic of Korea
[4]Seintec Corporation, Hwaseong, Republic of Korea

Abstract— *The parameters affecting particle injection in a high pressure powder fuel injection system were verified by using computational particle fluid dynamics (CPFD). The particles were coal ($\bar{d}_p$=175 μm, ρ_s = 1350 kg/m^3), and the simulation was performed by changing the clearance between the roller and the hose and by changing the total pressure drop. Also, the wall erosion of the hose was confirmed by changing the clearance. As the clearance decreases from 10 mm to 1 mm when the total pressure difference is 10 bar, it is confirmed that the injection of the particles is increased two-fold, but the power of the motor should be increased to 1.45 times. When the clearance is 5mm, as the total pressure drop is increased from 10 bar to 30 bar, the particle injection rate decreases 0.33-fold, but the motor power must be increased 3-fold. Also, it was confirmed that the wall erosion of the hose was large when the clearance was 7 mm or more*.

Keywords— Dry solid feeding, high pressure, simulation, Clearance, Backflow.

I. INTRODUCTION

Many devices in the chemical process operate at high pressure rather than atmospheric pressure**.** In the case of the gas phase reaction, a high pressure induces large gas density. Therefore, a greater amount of gas can be added, which leads to an increase in the production amount. Recently, the Integrated Gasification Combined Cycle (IGCC), which has been attracting attention due to its low carbon policy, has shown high efficiency as well as low SOx, NOx, and CO2 emissions compared to coal-fired power generation. However, the disadvantage of IGCC is its high cost compared to existing coal-fired power plants. Coal injection contributes about 43%-45% of the high cost of IGCC [1]. In the IGCC, it is necessary to inject coal from atmospheric pressure to high pressure; however, a general injection device cannot inject particles from atmospheric pressure to high pressure. This is due to the difficulty of injecting particles from atmospheric pressure to high pressure because the gas flows from a high pressure to a low pressure. In order to solve the problem of the backflow of gas, a lock hopper method is generally used when injecting particles from atmospheric pressure to high pressure. The advantage of the lock hopper method is that it can overcome a large pressure difference and can transfer the particles. However, the lock hopper method has disadvantages, since it is difficult to continuously inject particles because the pressurization and decompression must be repeatedly performed. Also, the lock hopper method requires equipment that is considerably large and relatively expensive in terms of construction and operating costs [2-5]**.** For example, in Shell's IGCC plant in Buggenum, which the existing lock hopper method is used, the cost of the coal injection part is estimated to be about 0.1 billion dollar [1]. Accordingly, a high-pressure powder fuel injection device has been developed to replace the lock hopper method injection device [1]. Stamet and Rocketdyne are developing the posimetric pump and the dry solid pump, respectively [1].

In this study, the experiment was carried out for the case of an atmospheric pressure condition, and the total pressure drop is 10 bar. However, it is difficult to find the variables that may affect the higher pressures and injection rate. In addition, to check the wall erosion of the hose, the hose must be operated for a long time; therefore, the wall erosion needs to be predicted for validity analysis. Therefore, in this study, we predicted the solid transfer characteristics of a high-pressure powder injector by using computational particle fluid dynamics (CPFD) method using the multi-phase particle-in-cell (MP-PIC) method.

II. EXPERIMENT AND SIMULATION

2.1 Experimental

Experiments were conducted using coal for verification of the simulation data. The specifications of the experimental apparatus are shown in **Figure 1**. A compression roller is installed in the chain, and the rotational force of the electric motor

is transmitted to the chain to rotate the compression roller. The upper hopper is filled with coal and the lower roller is compressed. At the same time, the high-pressure hose is pressed to transfer the coal in the high pressure hose to the lower hopper by the pushing force of the compression roller. The clearance between the hose and the roller was 10 mm. The speed of the roller was changed to 0 - 0.12 m / s using a motor inverter and the pressure of the lower hopper was changed to 10 bar at atmospheric pressure.

The injected rate was calculated using the mass value of the sample measured, using a load cell for 10 minutes under each condition.

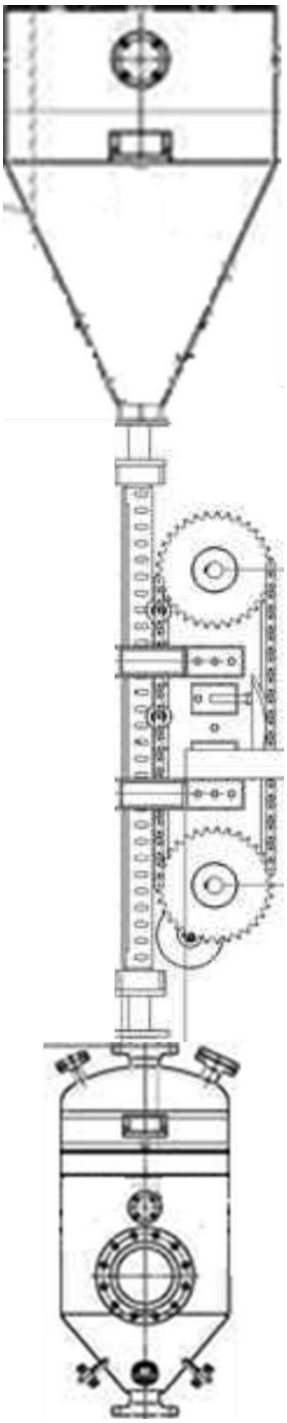

FIGURE 1.SCHEMATIC DIAGRAM OF EXPERIMENT

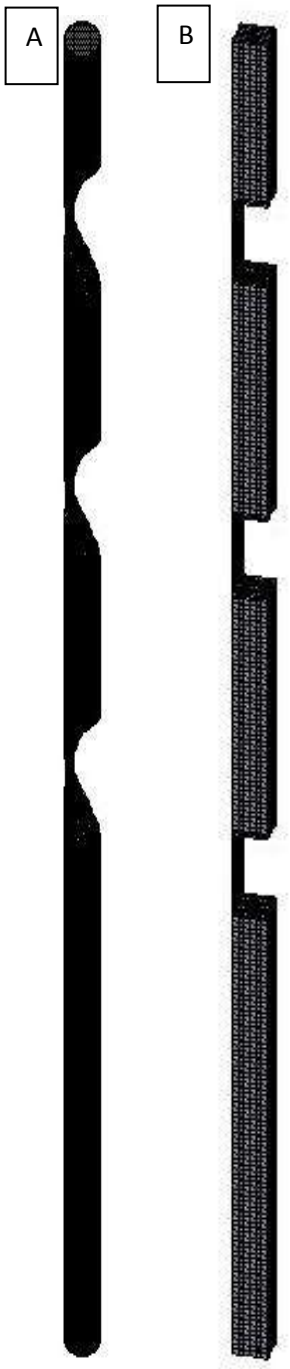

FIGURE 2. 3D DIMENSION OF HOSES THAT ARE PUSHED BY ROLLER. (A): REALIZATION MODEL, (B): SIMPLIFICATION MODEL

2.2 Governing equation

The CPFD method calculates the momentum of particles and fluids in three dimensions. The fluid is calculated using the Navier-Stokes equation and the particle is calculated using the MP-PIC numerical method. The phases of the fluid and the solid are considered together by calculating the drag force between the phases. The phase of the fluid is solved by the governing equations.

$$\frac{\partial}{\partial t}\left(\rho_f \theta_f\right) + \nabla \cdot \left(\rho_f \theta_f v_f\right) = S_f \tag{1}$$

For incompressible fluids, the momentum equation is expressed as (2).

$$\frac{\partial}{\partial t}(\rho_f \theta_f u_f) + \nabla \cdot \left(\rho_f \theta_f v_f v_f\right) = -\nabla p - F + \rho_f \theta_f g + \nabla \theta_f \tau_f \tag{2}$$

where ρ_f is the fluid density, θ_f is the volume fraction, v_f is the fluid velocity, and S_f is related to the fluid mass. τ_f is the fluid stress tensor, g is the gravity acceleration, and F is the ratio of momentum exchange in solid and fluid. F is calculated using equation (3).

$$F = \iiint f V_p \rho_p \left[D_p\left(v_f - v_p\right) - \frac{1}{\rho}\nabla p\right] dV_p d\rho_p dv_p \tag{3}$$

where v_p is the particle velocity, ρ_p is the particle density, D_p is the drag function depending on the particle position, and f is a probability density function calculated using the Liouville equation. The particle acceleration is calculated using the Largrangian method.

$$\frac{dv_p}{dt} = D_p\left(v_f - v_p\right) - \frac{1}{\rho_p}\nabla P + g - \frac{1}{\theta_p \rho_p}\nabla \tau_p \tag{4}$$

In equation (4), the value of D_p is calculated using the drag model. The Wen-Yu Ergun model of Gidaspow is used, which combines the Wen and Yu model, known to be well suited for the dilute system. Also, the Ergun model is used, which is known to fit well in the packing system. Equation (5) represents the expression of the drag model.

$$D = \begin{cases} D_1\,, & \theta_P < 0.75\theta_{CP} \\ (D_2 - D_1)\left(\frac{\theta_P - 0.75\theta_{CP}}{0.85\theta_{CP} - 0.75\theta_{CP}}\right) + D_1\,, & 0.75\theta_{CP} \le \theta_P \le 0.85\theta_{CP} \\ D_2 & \theta_P > 0.85\theta_{CP} \end{cases} \tag{5}$$

where θ_p is the particle volume fraction and θ_{cp} is the volume fraction when the particles are packed at maximum. D_1 is calculated using the Wen and Yu drag model.

$$D_1 = \frac{3}{8} C_d \frac{\rho_f |u_f - u_p|}{\rho_p r_p} \tag{6}$$

where C_d is the drag coefficient and is calculated using equation (7).

$$C_d = \begin{cases} \frac{24}{Re}\theta_f^{-2.65} & Re < 0.5 \\ \frac{24}{Re}\theta_f^{-2.65}(1 + 0.15Re^{0.687}) & 0.5 \le Re \le 1000 \\ 0.44\theta_f^{-2.65} & Re > 1000 \end{cases} \tag{7}$$

The Ergun equation is expressed as equation (8).

$$D_2 = 0.5\left(\frac{C_1 \theta_p}{\theta_f Re} + C_2\right)\frac{\rho_f |u_f - u_p|}{\rho_p r_p} \tag{8}$$

2.3 Modeling of apparatus

A schematic diagram of the 3D dimension for simulating the experimental setup used in this study with CPFD is shown in **Figure2**. The diameter of the hose is 0.04 m, the height is 1.45 m, and the thickness is 0.0125 m. The diameter of the roller pressing the hose is 0.16 m, and the distances between the first roller and the next roller are arranged at 0.3 m intervals. Based on the above information, a realization model is used when the roller presses the hose, and a simplification model is used that simplifies the cylindrical hose to a rectangular parallelepiped**.** In the case of the simplification model, the horizontal and vertical lengths of the rectangular parallelepiped are adjusted. As a result, the parallelepiped was simplified to a hose with a width of 0.035 m, a length of 0.035 m, and a height of 1.45 m.

2.4 Simulation condition

The average particle size of the particles used in the simulation was 175 μm, the density was 1350 kg/m^3, and air was used as the gas. The volume fraction of the particles was set at 0.6. The variables considered to be significant in the simulation are the clearance and total pressure difference between the inlet and outlet. The clearance was changed to 1-10 mm and the pressure drop was changed to 10-30 bar.

III. RESULTS AND DISCUSSION

3.1 Experiment result

When the clearance between the hose and the roller is 10 mm using coal, the injection rate according to the roller speed is confirmed when the total pressure difference is 0 bar and 10 bar. As shown in **Figure 3**, the injection rate increases linearly with the roller speed at each pressure condition. However, it was confirmed that the injection rate decreased more when the total pressure drop was 10 bar than when the pressure drop was 0 bar. This is considered to be because, as the pressure at the lower end increases, the gas at the lower end is forced to flow backward due to the pressure difference, and the particles must descend to overcome the force.

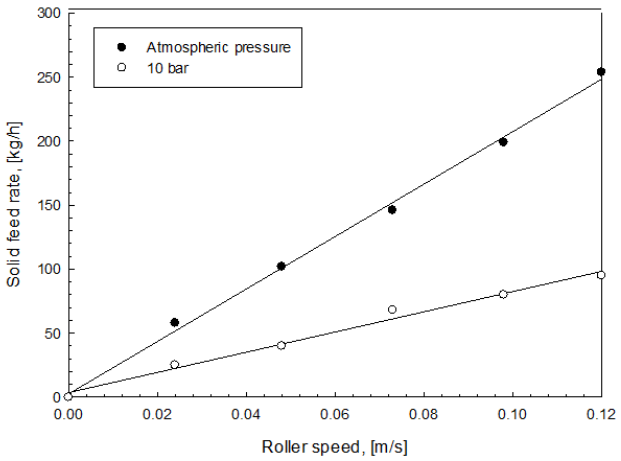

FIGURE 3. ROLLER SPEED VERSUS SOLID FEED RATE

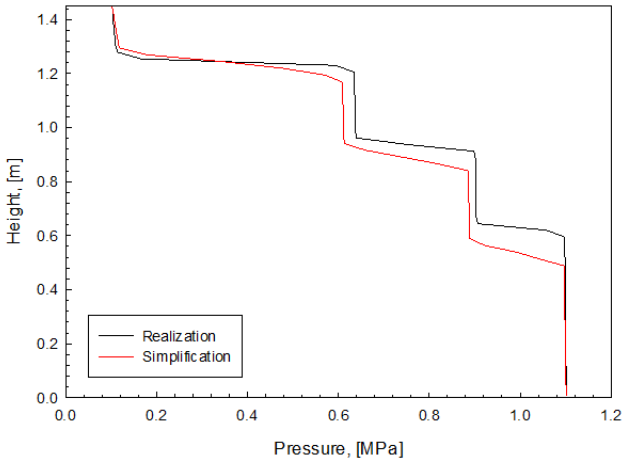

FIGURE 4. PRESSURE PROFILE OF REALIZATION AND SIMPLIFICATION

3.2 Comparison of realization and simplified model

In order to verify the validity of the simplified model, a simulation of the realization model is shown in **Figure 4**. By comparing the pressure drops among the rollers, an error of about 7% was found in the first roller at the bottom, 3% in the second roller, and 13% in the third roller. Although the contact areas of the rollers are the same, because the cylindrical roller is simplified into a rectangular parallelepiped, the difference is caused by the difference in height among the rollers. In addition, unlike the simplified model, the rubber hose is not pressed radially; rather, the pressure drop among the rollers differs from the actual model because the roller hose is gradually depressed according to the height of the roller. Likewise, the rubber hose is simplified to a rectangular parallelepiped in a simplified model, but the actual model is a cylinder. In the simplified model, the area pressed by the roller is constant, but in the actual model, the section which becomes extremely thin is generated. Therefore, in the simplified model, the pressure drop applied to the pressed part is constant according to the height, but in the actual model, the pressure drop according to the height increases in the narrower part. Increasing the pressure drop at the narrower part means that the force applied to the narrower part increases and eventually the entire the roller is not subjected to the same force but the part where the hose is pressed deeply under goes a larger force. However, the main purpose of this study is not to confirm the absolute value of the pressure drop, but to observe the change of the pressure drop according to the clearance or the tendency to change according to the total pressure. In addition, because the difference among the values is within 13% maximum, it can be confirmed that the simplified model can explain relation pressure drop and clearance. Consequently, the simulations were carried out using a simplified model.

3.3 Pressure profile according to clearance

Figure 5 shows the simulation results according to clearance and total pressure drop. Clearance refers to the distance between the roller and the hose at the roller contact distance. As can be seen in the graph, as the clearance is decreased, the

difference in pressure between the lower part and the upper part of the roller increases. On the other hand, the difference in pressure at the portion where the roller is not pressed decreased as the clearance decreased. When the clearance was 1mm, the pressure drop from the lower end of the hose to the lower end of the first roller at the lower end was 4.8 kPa and the pressure drop at the first lower roller was 207.7 kPa. When the clearance was 10 mm, the pressure drop from the lower end hose to the lower part of the first roller at the lower end was 71.4 kPa and the pressure drop at the first lower roller was 150.9 kPa. As the pressure drop at the portion where the roller is not pressed is increased, the possibility that the high-pressure gas at the lower end flows backward increases. As the width of the clearance is reduced, the stable particle injection becomes more advantageous, but as the width of the clearance is reduced, the pressure drop on the roller increases. The pushing force of the roller is proportional to the pressure drop applied to the roller, which is 1.38 times greater than 1 mm when the clearance is 10 mm. In other words, when the clearance is 10 mm, the force applied to the roller is greater as the pressure drop is larger at 10 mm than the 1 mm clearance; therefore, a greater force is required to drive the roller. By comparing the pressure drops applied to roller when clearance is 1 mm, it was confirmed that a high pressure drop was applied when position of roller goes up, 207.7 KPa in the lower part, 272.7 KPa in the middle part, and 490.9 KPa in the upper part. That is, the upper roller receives more force because of the relationship between the volume and the pressure of the gas. The volume of the gas increases as the pressure decreases, and the velocity of the gas increases due to the increased volume. As the velocity of the gas increases, the energy of the gas increases and it is confirmed that the upper roller undergoes a greater pressure drop. Comparing the pressure drop of the roller due to the pressure drop between the upper and lower parts, the sum of the pressure drop across the three rollers is 9.7 bar when the total pressure drop is 10 bar and clearance is 1 mm, and is 29.3 bar when the total pressure drop is 30 bar and the clearance is 1 mm. The roller pressure was3.02 times. For a total pressure drop of10 bar and a clearance of 10 mm, a pressure differential of 3.08 times greater was loaded to the roller. As the clearance increases, the pressure drop increase of the roller decreases as the total pressure increases. On the other hand, when the clearance is 1 mm, the pressure drop increases 2.43 times, while it increases 2.83 times at 10 mm. As the total pressure drop increases, the possibility of backflow of the gas increases, but if the clearance is narrow, the rate of increase of the pressure drop at the portion where the roller is not pressed is reduced. Therefore, when the clearance is narrow, it is relatively easy to inject particles at high pressure.

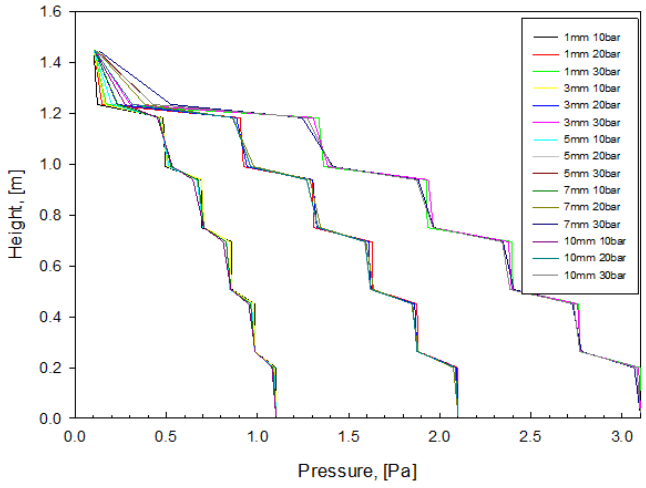

FIGURE 5. PRESSURE PROFILE WITH VARIED CLEARANCE AND TOTAL PRESSURE DROP

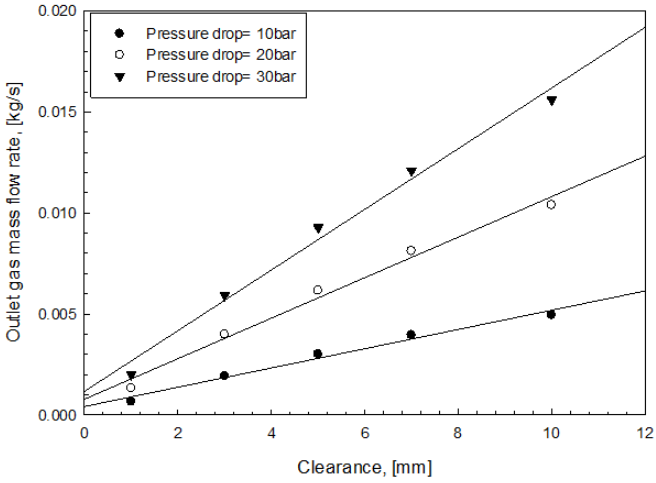

FIGURE 6. REVERSE GAS FLOW RATE WITH CHANGING CLEARANCE AND TOTAL PRESSURE

3.4 Backflow of gas

Figure 6shows the amount of backflow of gas at the top of the high-pressure powder fuel injector according to the clearance and total pressure.

The gas backflow rate increased with increasing clearance and total pressure drop. The data of the gas backflow amount is plotted with the differential pressure data from the hose where the roller is not pressed.

$$\text{Outlet gas mass flow rate}\left[\frac{\text{kg}}{\text{s}}\right] = 0.0166\left[\frac{kg}{s*MPa}\right] * Pressure\ drop(MPa) - 0.001 \quad (9)$$

That is, it can be seen that as the pressure drop of the portion of the hose where the roller is not pressed increases, the gas backflow increases. The differential pressure of the hose part where the roller is not pressed can be calculated by equation (9).

$$\text{Pressure drop}[MPa] = \text{Total pressure}[\text{MPa}] * (0.0322 * \text{Clearance}[\text{mm}] - 0.0188) + 0.1224 \quad (10)$$

It can be seen that the pressure drop increases when the clearance increases or when the total pressure drop increases. As the back flow of the gas increases, the mass flux of the downward flow of the solid particles must be increased in order to prevent the back flow of the gas under the actual operating conditions. Determining the solid mass flux is related to the speed of the roller. As the speed of the roller increases, the amount of dragging and dropping of particles during the same time increases, and the solid mass flux value increases; this can prevent gas backflow.

3.5 Wall erosion of hose

The above sections describe the power and speed of the motor according to clearance and the total pressure. This section discusses the wall erosion of the hose. If a problem arises when the erosion of the hose becomes serious, shutdown then must be frequently performed while operating the process, which results in increasing costs. Therefore, it is very important to know the conditions that cause the erosion. Equation (11) is used to calculate the wall erosion and is based on the default value provided by CPFD.

$$\text{Wall erosion} = \text{f}(\theta) * {m_s}^{1.5} * {v_p}^{3.5} \quad (11)$$

Where m is the mass of the particle, v is the velocity of the particle, and f(θ) is the value dependent on the angle. The wall erosion value is arelative value used to analyze the location of the wall erosion and the conditions under which further wall erosion would occur. **Figure 7** shows the wall erosion profile versus height, changing the clearance. In all cases, the wall erosion of the hose occurred at the part where the roller was pressed. At the point where the roller begins to be pressed, the velocity of the gas increases, and the velocity of the particle increases, causing considerable wall erosion. Also, at the end of the roller, the accelerated particles dispersed and caused erosion on the hose. On the other hand, the wall erosion value was very large when the clearance was 7 mm or more. As can be seen in **Figure 8**, when the clearance is greater than 7 mm, the movement of the particles in the x-direction is freer and the particle x velocity value is increased compared to when the clearance is narrow. The increase in particle x velocity resulted in more erosion effects than with particle z velocity; this caused a greater amount of erosion with a clearance greater than 7 mm.

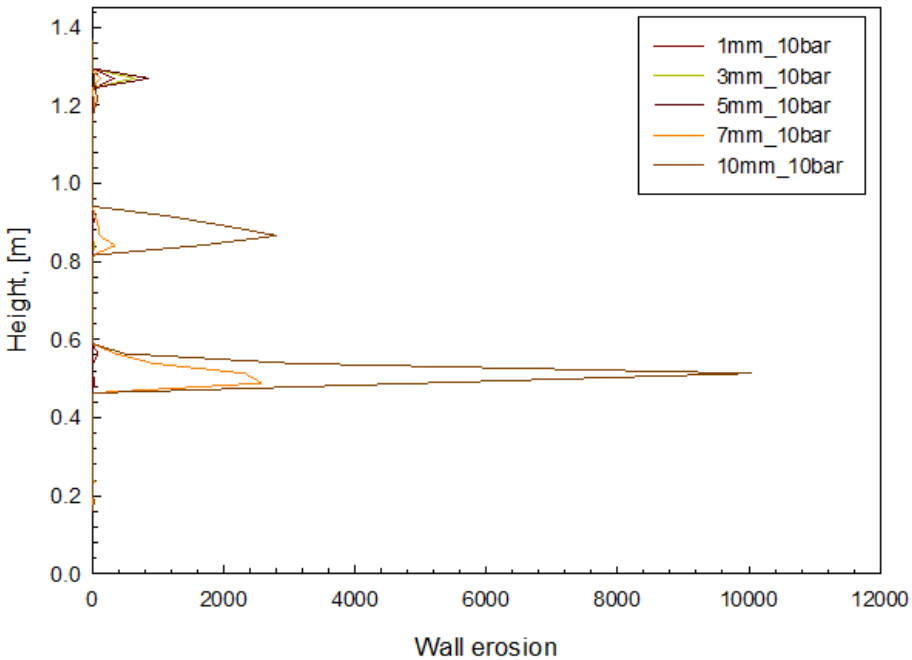

FIGURE 7.WALL EROSION VERSUS AXIAL HEIGHT WITH CHANGING CLEARANCE

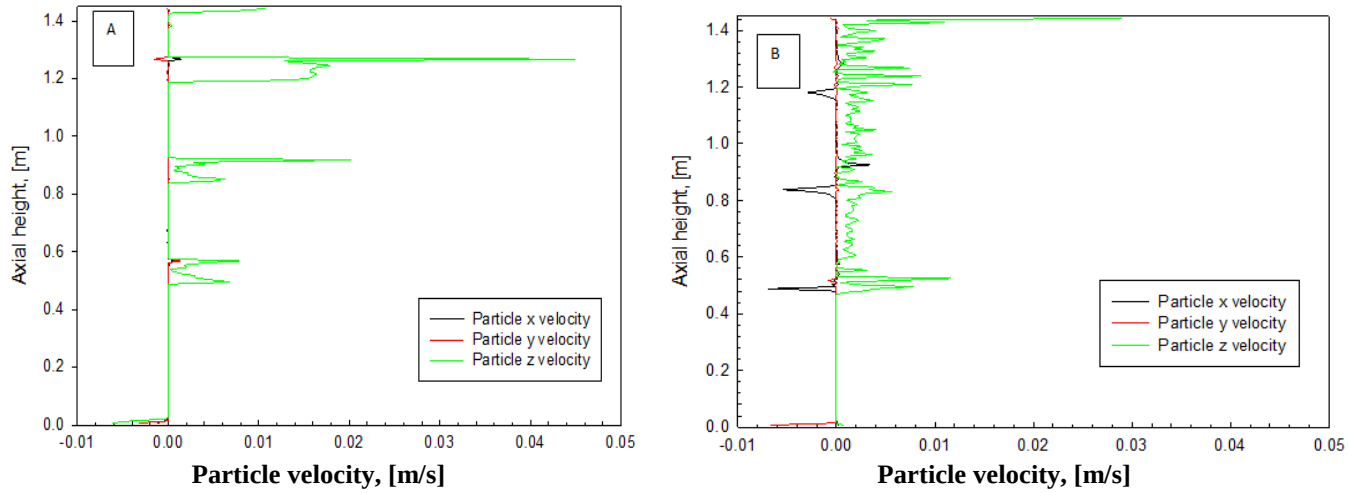

FIGURE 8.PARTICLE VELOCITY VERSUS AXIAL HEIGHT

3.6 Prediction of high pressure powder fuel injection system using CPFD

Simulation shows the effect of clearance and total pressure difference. In the experiment mentioned in Section 3-1, the injection amount ($\dot{m}_s$) of the particles according to the speed (0024-0.12 m/s) of the roller at the atmospheric pressure is expressed by equation (13) at equation (12) and 10 bar.

$$\text{Solid mass flow rate}((\dot{m}_s)\left[\frac{\text{kg}}{\text{s}}\right] = 2049.3\left[\frac{\text{kg}}{\text{m}}\right] \times \text{Roller speed}\left[\frac{\text{m}}{\text{s}}\right] + 2.5168 \quad (12)$$

$$\text{Solid mass flow rate}((\dot{m}_{s,10bar})\left[\frac{\text{kg}}{\text{s}}\right] = 789.15\left[\frac{kg}{m}\right] \times Roller\ speed\ \left[\frac{m}{s}\right] + 3.5896 \quad (13)$$

The slopes of equation (13), i.e., the weights of the particles per unit length, were compared using data obtained from CPFD to experiment. Assuming that the gas backflow is zero at normal pressure, the weight of particles per unit length is 2049.3 kg/m and the weight of particles per unit weight is 789.15 kg/m when the backflow is 0.4256 kg/s. Based on this data, **Table 1** shows the predicted motor force based on the predicted value of clearance and the particle weight per unit weight for the total pressure drop and the pressure drop on the roller, with 10 bar and clearance 10 mm as references. If the roller is operated at 20 bar at intervals of 10 mm, then it is not operating normally because it has a value of -0.108.6 kg/m. It can be seen that it is possible to reduce the gap to 5 mm or less in order to obtain a similar injection amount. However, the decrease in clearance increases the pressure drop of the roller, which means that the power of the motor increases. For example, if the clearance is 5 mm at 20 bar, the motor power needs to increase 2.53 times more than the reference.

TABLE 1
PREDICTED VALUE OF MASS PER UNIT LENGTH AND POWER RATIO

Pressure, [MPa]	Clearance, [mm]	Mass per unit length, [kg/m]	power ratio , [-]
0	10	2049.3	
1	10	789.1	1.00
1	7	1075.2	1.14
1	5	1265.8	1.25
1	3	1456.5	1.35
1	1	1647.2	1.45
2	10	-108.6	2.05
2	7	463.4	2.32
2	5	844.8	2.53
2	3	1226.2	2.72
2	1	1607.5	2.91
3	10	-1006.3	3.08
3	7	-148.3	3.53
3	5	423.8	3.82
3	3	995.8	4.10
3	1	1567.9	4.37

IV. CONCLUSION

CPFD simulations were carried out to identify the variables affecting the operation of the high-pressure powder fuel injection system and to understand the effect of the variables. It was found that as the clearance increased, the backflow of the gas also increased. However, as the clearance increased, the pressure drop on the roller decreased, so the load on the motor was reduced. On the other hand, CPFD simulation predicted that a clearance of 5mm or less should be maintained for the wall erosion of the hose, since a clearance of 7mm or more is expected to cause significant erosion.

ACKNOWLEDGMENT

This work was supported by a grant from the Korea Institute of Energy Technology Evaluation and Planning (KETEP), funded by the Ministry of Trade, Industry and Energy (MTIE) of the Korea government (No. 20163010050070).

NOMENCLATURE

$\bar{d}_p$	Sauter mean diameter [□ m]	m_s	Mass of solid [kg]
ρ_s	Solid density [kg/m^3]	θ	Angle of collision [°]
ρ_p	Particle density [kg/m^3]	S_f	Interpolation operator [-]
ρ_f	Fluid density [kg/m^3]	τ_f	Stress tensor of fluid [Pa]
θ_p	Particle volume fraction [-]	g	Gravitational acceleration [m/s^2]
θ_{cp}	Close pack particle volume fraction [-]	F	Momentum exchange rate per volume between the fluid and solid phases [Pa*s/m]
θ_f	Fluid volume fraction [-]	D_p	Interphase drag coefficient [m/s^2]
v_f	Fluid velocity [m/s]	f	Particle distribution function [-]
v_p	Particle velocity [m/s]	C_d	Drag coefficient [-]
$\dot{m}_s$	Solid mass flow rate [kg/s]		

REFERENCES

[1] Amin, S. M., & Wollenberg, B. F. (2005). Toward a smart grid: power delivery for the 21st century. *IEEE power and energy magazine*, *3*(5), 34-41.

[2] Anthony, E. J. (1995). Fluidized bed combustion of alternative solid fuels; status, successes and problems of the technology. *Progress in Energy and Combustion Science*, *21*(3), 239-268.

[3] Li, X. T., Grace, J. R., Lim, C. J., Watkinson, A. P., Chen, H. P., & Kim, J. R. (2004). Biomass gasification in a circulating fluidized bed. *Biomass and bioenergy*, *26*(2), 171-193.

[4] Marcus, R. D. (2012). *Pneumatic conveying of solids*. Springer Science & Business Media.

[5] Dai, J., Cui, H., & Grace, J. R. (2012). Biomass feeding for thermochemical reactors. *Progress in Energy and Combustion Science*, *38*(5), 716-736.

[6] Wen, CY (1966) Mechanics of fluidization. In *Chem. Eng. Prog. Symp. Ser.* (Vol. 62, pp. 100-111).

[7] Ergun, S. (1952). Fluid flow through packed columns. *Chem. Eng. Prog.*, *48*, 89-94.

[8] Gidaspow, D. (1994). *Multiphase flow and fluidization: continuum and kinetic theory descriptions*. Academic press

AD Publications
Sector-3, MP Nagar, Bikaner,
Rajasthan, India
www.adpublications.org, info@adpublications.org